ISSN 2071-4726
2071-0305

Инженерно-строительный журнал

НАУЧНОЕ ИЗДАНИЕ

№6(66) 2016

МАТЕРИАЛЫ

РАСЧЕТЫ

АНАЛИЗ

МЕТОДЫ

Picture 1. IR-spectra of PCR and modified samples

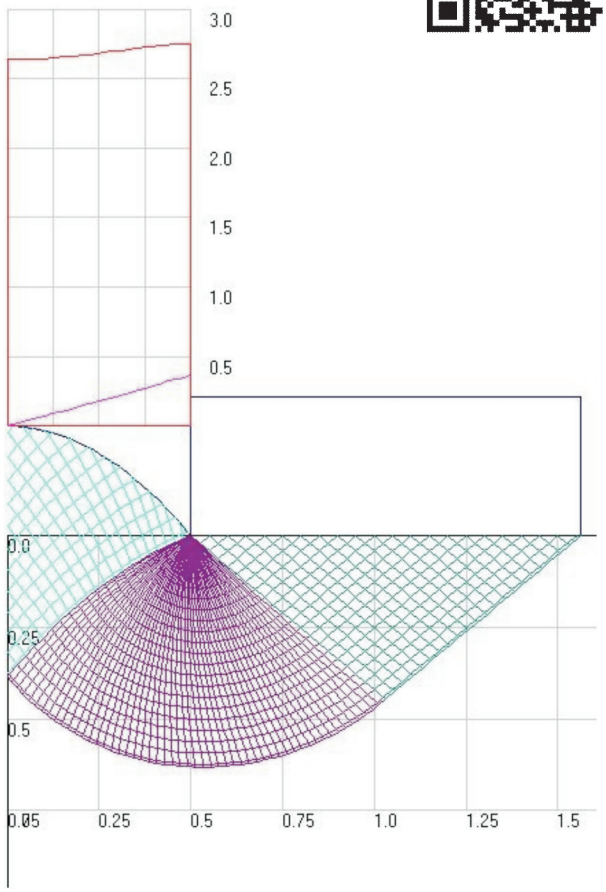

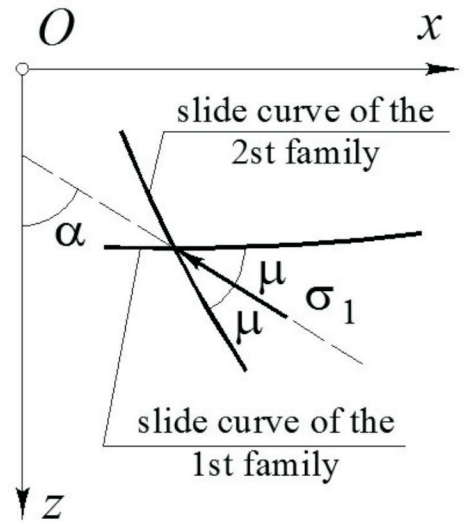

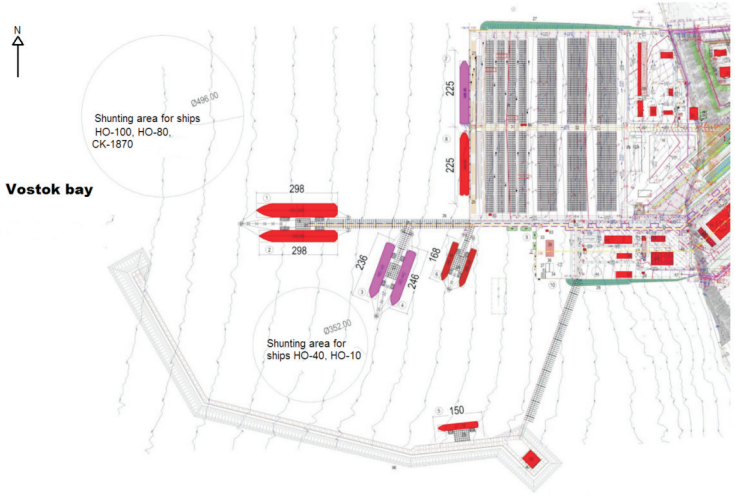

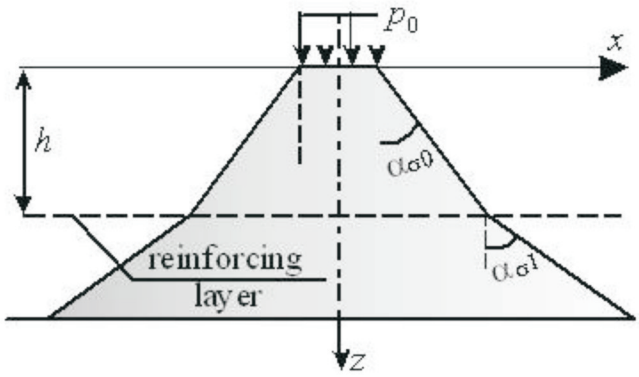

Федеральное государственное автономное образовательное учреждение высшего образования
Санкт-Петербургский политехнический университет Петра Великого

ПОЛИТЕХ
Санкт-Петербургский политехнический университет Петра Великого

Инженерно-строительный институт
Центр дополнительных профессиональных программ

195251, г. Санкт-Петербург, Политехническая ул., 29,
тел/факс: 552-94-60, www.stroikursi.spbstu.ru,
stroikursi@mail.ru

Приглашает специалистов организаций, вступающих в СРО, на курсы повышения квалификации (72 часа)

Код	Наименование программы	Виды работ*
Курсы по строительству		
БС-01-04	«Безопасность и качество выполнения общестроительных работ»	**п.1,2, 3, 5, 6, 7, 9, 10, 11, 12, 13, 14**
БС-01	«Безопасность и качество выполнения геодезических, подготовительных и земляных работ, устройства оснований и фундаментов»	**1,2,3,5**
БС-02	«Безопасность и качество возведения бетонных и железобетонных конструкций»	**6,7**
БС-03	«Безопасность и качество возведения металлических, каменных и деревянных конструкций»	**9,10,11**
БС-04	«Безопасность и качество выполнения фасадных работ, устройства кровель, защиты строительных конструкций, трубопроводов и оборудования»	**12,13,14**
БС-05	«Безопасность и качество устройства инженерных сетей и систем»	**15,16,17,18,19**
БС-06	«Безопасность и качество устройства электрических сетей и линий связи»	**20,21**
БС-08	«Безопасность и качество выполнения монтажных и пусконаладочных работ»	**23,24**
БС-12	«Безопасность и качество устройства мостов, эстакад и путепроводов»	**29**
БС-13	«Безопасность и качество выполнения гидротехнических, водолазных работ»	**30**
БС-14	«Безопасность и качество устройства промышленных печей и дымовых труб»	**31**
БС-15	«Осуществление строительного контроля»	**32**
БС-16	«Организация строительства, реконструкции и капитального ремонта. Выполнение функций технического заказчика и генерального подрядчика»	**33**
Курсы по проектированию		
БП-01	«Разработка схемы планировочной организации земельного участка, архитектурных решений, мероприятий по обеспечению доступа маломобильных групп населения»	**1,2,11**
БП-02	«Разработка конструктивных и объемно-планировочных решений зданий и сооружений»	**3**
БП-03	«Проектирование внутренних сетей инженерно-технического обеспечения»	**4**
БП-04	«Проектирование наружных сетей инженерно-технического обеспечения»	**5**
БП-05	«Разработка технологических решений при проектировании зданий и сооружений»	**6**
БП-06	«Разработка специальных разделов проектной документации»	**7**
БП-07	«Разработка проектов организации строительства»	**8**
БП-08	«Проектные решения по охране окружающей среды»	**9**
БП-09	«Проектные решения по обеспечению пожарной безопасности»	**10**
БП-10	«Обследование строительных конструкций и грунтов основания зданий и сооружений»	**12**
БП-11	«Организация проектных работ. Выполнение функций генерального проектировщика»	**13**
Э-01	«Проведение энергетических обследований с целью повышения энергетической эффективности и энергосбережения»	
Курсы по инженерным изысканиям		
И-01	«Инженерно-геодезические изыскания в строительстве»	**1**
И-02	«Инженерно-геологические изыскания в строительстве»	**2,5**
И-03	«Инженерно-гидрометеорологические изыскания в строительстве»	**3**
И-04	«Инженерно-экологические изыскания в строительстве»	**4**
И-05	«Организация работ по инженерным изысканиям»	**7**

***(согласно приказам Минрегионразвития РФ N 624 от 30 декабря 2009 г.)**

По окончании курса слушателю выдается удостоверение о краткосрочном повышении квалификации установленного образца (72 ак. часа)

Для регистрации на курс необходимо выслать заявку на участие, и копию диплома об образовании по телефону/факсу: 8(812) 552-94-60, 535-79-92, , e-mail: stroikursi@mail.ru.

Http://www.engstroy.spbstu.ru – полнотекстовая версия журнала в сети Интернет.
Бесплатный доступ, обновление с каждым новым выпуском

Инженерно-строительный журнал
НАУЧНОЕ ИЗДАНИЕ

ISSN 2071-4726

Свидетельство о государственной регистрации: ПИ №ФС77-38070, выдано Роскомнадзором

Специализированный научный журнал. Выходит с 09.2008.

Включен в Перечень ведущих периодических изданий ВАК РФ

Периодичность: 8 раз в год

Учредитель и издатель:

Санкт-Петербургский политехнический университет Петра Великого

Адрес редакции:

195251, СПб, ул. Политехническая, д. 29, Гидрокорпус-2, ауд. 227А

Главный редактор:
Вера Михайловна Якубсон

Научный редактор:
Николай Иванович Ватин

Выпускающий редактор:
Екатерина Александровна Линник

Технический редактор:
Ксения Дмитриевна Борщева

Редакционная коллегия:
д.т.н., проф. В.В. Бабков;
д.т.н., проф. М.И. Бальзанников;
к.т.н., проф. А.И. Боровков;
д.т.н., проф. Н.И. Ватин;
PhD, professor M. Вельжкович;
д.т.н., проф. А.Д. Гиргидов;
д.т.н., проф. Э.К. Завадскас;
д.ф.-м.н., проф. М.Н. Кирсанов;
D.Sc., professor M. Кнежевич;
д.т.н., проф. В.В. Лалин;
д.т.н., проф. Б.Е. Мельников;
д.т.н., проф. Ф. Неправишта;
д.т.н., проф. Р.Б. Орлович;
Dr. Sc. Ing., professor
Л. Пакрастиньш;
Dr.-Ing. Habil., professor
Х. Пастернак;
д.т.н., проф. А.В. Перельмутер;
к.т.н. А.Н. Пономарев;
д.ф.-м.н., проф. М.Х. Стрелец;
д.т.н., проф. О.В. Тараканов.

Содержание

© ФГАОУ ВО СПбПУ, 2016

На обложке: иллюстрации авторов к статьям номера

Установочный тираж 1000 экз.
Подписано в печать 16.01.2017. Формат 60x84/8, усл. печ. л. 8,5. Заказ № 43.
Отпечатано в типографии СПбПУ. СПб, ул. Политехническая, д. 29

Контакты:
Тел. +7(812)535-52-47 E-mail: mce@ice.spbstu.ru
Web: http://www.engstroy.spbstu.ru

Http://www.engstroy.spbstu.ru – full-text open-access version in Internet. It is updated immediately with each new issue.

Magazine of Civil Engineering
SCHOLAR JOURNAL

ISSN 2071-4726
Peer-reviewed scientific journal
Start date: 2008/09
8 issues per year

Publisher:
Peter the Great St. Petersburg Polytechnic University

Indexing:
Scopus, Russian Science Citation Index (WoS), Compendex, DOAJ, EBSCO, Google Academia, Index Copernicus, ProQuest, Ulrich's Serials Analysis System

Corresponding address:
227a Hydro Building, 29 Polytechnicheskaya st., Saint-Petersburg, 195251, Russia

Editor-in-chief:
Vera M. Yakubson

Science editor:
Nikolay I. Vatin

Executive editor:
Ekaterina A. Linnik

Technical editor:
Ksenia D. Borshcheva

Editorial board:
V.V. Babkov, D.Sc., professor
M.I. Balzannikov, D.Sc., professor
A.I. Borovkov, PhD, professor
M. Veljkovic, PhD, professor
E.K. Zavadskas, D.Sc., professor
M.N. Kirsanov, D.Sc., professor
M. Knezevic, D.Sc., professor
V.V. Lalin, D.Sc., professor
B.E. Melnikov, D.Sc., professor
F. Nepravishta, D.Sc., assoc. professor
R.B. Orlovich, D.Sc., professor
L. Pakrastinsh, Dr.Sc.Ing., professor
H. Pasternak, Dr.-Ing.habil., professor
A.V. Perelmuter, D.Sc., professor
A.N. Ponomarev, PhD, professor
M.Kh. Strelets, D.Sc., professor
O.V. Tarakanov, D.Sc., professor

Contents

© Peter the Great St. Petersburg Polytechnic University. All rights reserved.

On the cover: authors' illustrations

+7(812) 535-52-47
E-mail: mce@ice.spbstu.ru
Web: Http://www.engstroy.spbstu.ru/eng/index.html

doi: 10.5862/MCE.66.1

Structure-forming processes of cement composites, modified by sucrose additions

Процессы структурообразования цементных композиций, модифицированных добавками сахарозы

T.S. Shepelenko,
U.S. Sarkisov,
N.P. Gorlenko,
N.A. Tsvetkov,
O.A. Zubkova,
Tomsk State University of Architecture and Building, Tomsk, Russia

Канд. хим. наук, доцент Т.С. Шепеленко,
д-р техн. наук, профессор Ю.С. Саркисов,
д-р техн. наук, профессор Н.П. Горленко,
д-р техн. наук, профессор Н.А. Цветков,
канд. техн. наук, доцент О.А. Зубкова,
Томский государственный архитектурно-строительный университет, г. Томск, Россия

Key words: cement; sucrose; products of sucrose corrosion of cement; addition agent; density

Ключевые слова: цемент, сахароза, продукты сахарной коррозии цемента, добавка, прочность

Abstract. The effect of sucrose on the kinetics of cement hardening has been studied. The study was carried out in two comparative ways, one of which had the organic modifier introduced into cement as gauging liquid (“water – 2% sucrose solution”), the other – as suspensions “cement – water – 2% sucrose solution”. The products of sucrose corrosion, synthesized in suspensions, were used as addition agents in the “cement – water” system. Suspension-based approach is interesting because of cement modification by introducing the corrosion products of the same cement, which provides setting acceleration and higher composite density.The structurization role of addition agents, containing products of sucrose corrosion of cement, is provided by synergetic influence of several factors: intensive growth of ettringite crystal nuclei – the main reinforcement component of a cement system, reduction of Ca(OH)2 in solid phase of a rock, CSH-gel densifying and plasticizing. The use of sucrose as gauging liquid results in adverse effect for isolation of cement particles by adsorption layers, impeding the hydration, growth and possible coalescence of crystal – the destructurization of the setting system: the rocks, available from cement gauging with 2 % sucrose solution were not set during the whole trial period. The results were interpreted by means of physic-chemical approaches: X-ray phase analysis, IR-spectroscopy, differential thermal analysis.

Аннотация. Изучено влияние сахарозы на кинетику твердения цемента. Исследование проведено в двух сравнительных вариантах, в одном из которых органический модификатор вводился в цемент в качестве жидкости затворения («вода–2%-й раствор сахарозы»), в другом – в виде суспензий «цемент–вода–2%-й раствор сахарозы». Продукты сахарной коррозии, синтезированные в суспензиях, применялись как добавки в систему «цемент–вода». Научный подход, основанный на использовании суспензий интересен тем, что цемент модифицируется введением продуктов коррозии этого же цемента и обеспечивает значительное ускорение схватывания и увеличение прочности композитов. Структурообразующая роль добавок, содержащих продукты сахарной коррозии цемента, обеспечивается благодаря синергетическому влиянию нескольких факторов: интенсивному росту зародышей кристаллов эттрингита – главного армирующего компонента цементной системы, уменьшению количества Ca(OH)2 в твердой фазе камня, уплотнению CSH-геля и пластифицирующему действию. Применение сахарозы в качестве жидкости затворения приводит к отрицательному эффекту изолирования частиц цемента адсорбционными оболочками, затрудняющими гидратацию, рост и возможность срастания кристаллов – наблюдается деструктуризация вяжущей системы: камни, полученные затворением цемента 2%-м раствором сахарозы, не обнаружили схватывания в течение всего испытательного срока. Интерпретация результатов проведена с помощью физико-химических методов: РФА, ИК-спектроскопии, ДТА.

Шепеленко Т.С., Саркисов Ю.С., Горленко Н. П., Цветков Н.А., Зубкова О.А. Процессы структурообразования цементных композиций, модифицированных добавками сахарозы // Инженерно-строительный журнал. 2016. № 6(66). С. 3–11.

Introduction

Cement concrete is the main construction material in the world, therefore modification of its properties is under constant consideration of both Russian and foreign scientists. Cement is modified in the first place, as it is the binding agent that specifies the technological and operational features of concrete mixtures. P.-C. Aitchin, the author of HPC (High Performance Concrete) conception – provided rationalization for functional unity of cement and concrete, gaining density with effective addition agents [1]. In 2014 Russia produced 68424 ths. tons of cement, 48 % of which is Portland cement with addition agents [2]. A particular value is assigned to organomineral addition agents, effecting rheological and physic-mechanical properties of cement and concrete [3–7].

In [8] it is shown that structurization processes of cement systems are regulated by introducing sucrose-containing addition agents. The influence of organic modifier upon kinetics of binding agent hardening has been studied in two comparative ways, one of which had the sucrose introduced into cement as a "water–sucrose solution" gauging liquid, the other – as "cement–water–sucrose" suspensions ("CWS"). Sucrose solutions, aggressive to cement, worked as a corrosive environment. The products of corrosion, synthesized in suspensions, were used as addition agents in the "cement–water" system, similarly to [9]. Depending on means of sucrose introduction, solution concentration and the quantity of addition agent the modification result varies from no setting of cement paste at all to sufficient acceleration of setting and hardening of cement composite materials.

The present work attempts to explain and prove the results of [8] on the example of modified samples MS2-0.1 and MS2, which have the polar opposite compression resistance values (Table 1). The comparison is interesting because of the same concentration of organic modifier in both instances – 2 %, but different means of sucrose introduction. Thus, rock MS2-0.1 was produced by introduction of an agent into cement paste, which was synthesized in "cement–water–2% sucrose solution" suspension (M – modified sample; 2 – concentration of sucrose solution, %; 0.1 – amount of addition agent, wt. %). MS2-0.1 during the whole period of hardening is distinguished by considerable increase in density compared to plain cement rock (PCR). The rock MS2, produced by gauging of the binding agent with 2 % solution of sucrose, was not set throughout the whole trial period.

Methods

Plain cement rocks and modified cement rocks (MCR) were produced of topkinsky cement of PC400 D20 brand, shaped as cubes measuring 2 cm on edge, within normal hardening conditions; water-cement ratio is 0,34.

MCR were produced in the following ways:

– MS2 was produced by means of gauging the base cement with 2 % sucrose solution;

– MS2-0.1 was produced by means of introducing the "CWS" addition agent into the "cement-water" system in proportion 0.1 % to the mass of the dry cement.

The "CWS" addition agent was synthesized through the following procedure:

1. A sample of the base gauging liquid was matured in a 2 % sucrose solution in liquid/solid proportion 1:5 for 24 hours after thorough mixing of the suspension produced;
2. After the exposure period the solid and liquid parts of the suspension were separated by means of 2-hour filtering;
3. The solid residue was transferred quantitatively from the paper filter onto the Petri dish, stirred thoroughly, distributed evenly with a spreading rod, and dried in the air for 3 hours;
4. Thus prepared addition agent was ground in a porcelain mortar, passed through the strainer 008 according to the National State Standard 6613 and dried in a baker until it reached a constant weight at the temperature of (110 ± 5)° C according to the National State Standard 5382-91.

Table 1 shows the means of modifying the cement systems, as well as the compression resistance values (R, MPa) and density growth of MS2-0.1 compared to PCR (ΔR, %).

Compression resistance values of the rocks in the set terms of cement hardening (1–3–7–28) were determined following 6 separate measurements of every test point. The average density was calculated on the basis of three closest values, providing a margin of error not more than 5.6 %.

Table 1 PCR and MCR specification

CR	Composition of CR	Period of hardening, days			
		1	3	7	28
		R, Mpa/Δ*R* (versus PCR), %			
PCR	(cement + H_2O)	6.6	21.1	38.9	46.2
MS2-0.1	(cement +H_2O) + addition agent “CWS”	13.2 100	25.7 22	42.0 8	61.9 34
MS2	(cement + 2% sucrose solution)	–	–	–	–

The physiochemical analysis was carried out on the 28-day samples. The rocks were prepared for testing immediately after the density test. The samples, broken by the press, were ground in a planetary mill MP/0.5-4. The dispersion degree was checked by the powder measuring machine PSH-10a up to the specific surface value of 200 m^2/kg. There have been no measures taken to stop the hydration processes, as the period of time from the grade strength evaluation to the physiochemical analysis lasted not more than 2 hours for all the cement systems under consideration.

Table 2 shows the results of X-ray phase analysis. Figure 1 shows IR-spectra of the samples in question, Figure 2 – the results of differential thermal analysis.

IR-specters of the samples were registered with Fourier spectrometer Varian Excalibur HE 3600 within the frequency range 400–4000 cm^{-1}; quality of neoformations composition was measured by X-ray diffraction meter of Shimadzu XRD-7000 with copper anode in range 5–90 deg. Differential thermal analysis was carried out by means of derivatograph NETZSCH STA 449 F3A–0010–M.

Results and Discussion

X-ray of MS2, produced by means of gauging a binding agent with 2 % sucrose solution, shows that the reflex intensity of C_3S on 2θ scale at angles 29.280 ^{0} and 34.155 ^{0} versus unhydrated cement is only 5 % and 8 % lower respectively, of C_2S (32.172 ^{0}) – 20 % lower (Table 2).

IR-specter MS2 has the typical for unhydrated cement adsorption bands – 920 and 516 cm^{-1} (stretching and deformation vibrations of Si–O–Ca) – preserved and highly intensive (Figure 1). Given results are proved by reduction of portlandite reflection height in XPA patterns of MS2 versus PCR: 58 to 100 % in the most important reflexes of this phase (Table 2).

According to DTA dehydration endoeffect area of $Ca(OH)_2$ at 451 ^{0}C on the MS2 thermograph is 4 times reduced versus PCR (Figure 2); adsorption in the IR-specter area with 3640 cm^{-1} max is also reduced. Low-level consumption of C_3S и C_2S and sharp reduction of portlandite quantity show that the use of sucrose as gauging liquid suppresses the hydration of cement silicate phases, similarly to [10–12].

Hydration of C_3A и C_4AF in MS2 is hindered as well – that is implied by 3 of 4 adsorption bands of unhydrated cement preserved in IR-specter in the area 600–700 cm^{-1} (deformation vibrations of $(AlO_4)^-$ tetrahedral in aluminates and alumoferrites, with stretching vibrations 1000–1150 $см^{-1}$). The authors [10–12] also registered the “aluminates accumulation” in cement composites, modified with sucrose.

Typical for MS2 is exothermic effect, peaking in 333.7 ^{0}C (Figure 2), corresponding to oxidation of organic compositions, allegedly antacidins [11, 13] – products of sucrose reaction to $Ca(OH)_2$.

It is noted in reference literature that small additions of sucrose slow down the hydration and hardening of cement. Sucrose, with the properties of hydrophilic SAS, peptizes cement particles and heightens early solubility of a binding agent. However the following “adsorption of sucrose on the surfaces of initial and metastable hydrate phases, as well as formation and adsorption of complex composites” [14] contributes to formation of membranes, screening the cement nuclei and hindering the hydration, growth and possible coalescence of crystals. Modifying effect of sucrose works on both aluminic and silicate phases of cement and comes from the capacity of OH-groups of organic addition agent to form hydrogen-bonds [7, 10–19]. Primary stage of C_3A hydration is accelerated due to aluminates involved in complex formation. The following slowdown of hydration is determined by hexagonal phases stabilization and hindering of their transformation into cubic phase by means of

sucrose adsorption on the hydrate surfaces and formation of protective membranes. Data concerning surface complexes with hexagonal phases is obtained by means of DTA [14].

Table 2 X-ray phase analysis results

Reflex intensity of primary crystalline phases of PCR and MCR versus unhydrated cement, %				
Phases	2θ,^{0}	PCR	MS2	MS2-0.1
C_3S	34.155	–36.0	–8.0	–32.0
	29.280	–47.4	–5.3	–21.1
C_2S	32.172	–54.2	–20.8	–25.0
Reflex intensity of new crystalline phases of MCR versus PCR, %				
Phases	2θ,^{0}	MS2	MS2-0.1	
Ettringite	9.016	PCR level	+40	
	15.530		+67	
	22.962		+25	
Portlandite	17.978	–73	–50	
	34.061	–58	–37	
	50.976	–100	–33	

Y.E. Young [20, 21] stated that sucrose molecules change the morphology of ettringite and stabilize it, which conforms to ideas of sugars slowing the transformation of hydrated calcium sulfoaluminate into monosulfoaluminate [14, 22].

The slowdown effect of organic modifier was related to stabilization of the surface complex, including surfaces of alite hydration products – CH and CSH, sucrose and water, while complex stabilization is the higher, the higher is sucrose concentration in gauging liquid [12, 14, 15, 23]. It has been discovered that sucrose adsorption changes the CSH-phase sufficiently and prevents its nucleation. X-ray phase analysis has proved that introduction of wt. 0.3 % sucrose causes the deformation of CSH structure. Disaccaride molecules are adsorbed horizontally on the surfaces of hydrosilicates, creating steric hindrance during their crystallization and raising inhomogenity of calcium hydrosulfate phases [10].

It is noted that the dosage of sucrose higher than 0.7 wt. % [10] has “catastrophic effect on cement systems” due to higher role of adsorption membranes [10, 11, 13], hindering the intensity of hydrolized hydration. In [3] it was shown that with use of 1 % sucrose solution as gauging liquid the binding agent does not set during 7 days; at the 28th day modified cement rocks show compression strength of 2.6 Mpa. Raising sucrose concentration in gauging liquid to 2 % spikes the negative effect of disaccharide: cement system does not set during 28 days (Table 1).

In [8] it was confirmed that aggressive effect of sucrose is diminished if the means of introduction into “cement-water” system is changed: use of sucrose in addition agent, synthesized in “CWS” suspension, raises the 1-day density of modified rock MS2-0.1 to 100 % versus PCR, 28-day density – to 34 % (Table 1).

XRD results show that the reflex intensity of hydrated calcium sulfoaluminate in MS2-0.1 at reflex angles 22.962 ^{0}, 9.016 ^{0} и 15.530 ^{0} on 2θ scale versus PCR is higher in 25 %, 40 % and 67 % accordingly (Table 2). That may be considered a progressive factor, responsible for intensive

development of reinforcement net of structural skeleton, forming the density of cement composite [24, 25].

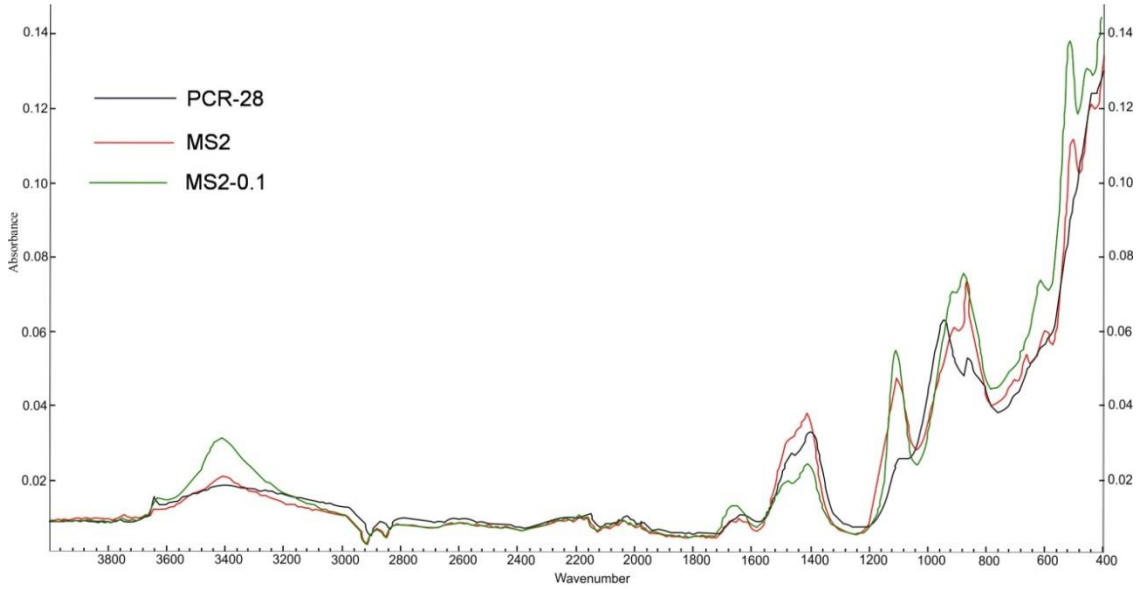

Figure 1. IR-spectra of PCR and modified samples

One more key factor, contributing to the development of more homogeneous and dense structure of MS2-0.1 rock versus PCR is a sufficient reduction of portlandite amount – the less stable component of a cement rock. The reduction of reflex intensity in the crucial reflexes of the given crystal line on 2θ scale is 33 % (50.976 ^{0}), 37 % (3.061 ^{0}) and 50 % (17.978 ^{0}).

IR-specter of MS2-0.1 is specified by sufficiently higher adsorption in every area, typical for cement systems, except for maximum 1475 cm^{-1} band, responsible for water molecules vibrations in interlayer structure of calcium hydrosulphates. Higher adsorption at 3411 cm^{-1} is explained by vibrations of water molecules in crystallohydrates, as well as OH-groups of sucrose (3150–3600 cm^{-1}). More remarkable changes take place in the area with the peak of 1080 cm^{-1}, responsible for the formation of lowly crystallized phases of tobleromorite-like structured calcium hydrosulphate: if considering PCR a dependent blurred shoulder peak to 953 cm^{-1} band is observed, MS2-0.1 specter shows a sharp peak, higher in 112 % (Pic. 1). In the wavenumbers interval 600–700 cm^{-1} specter MS2-0.1 has only one peak with 613 cm^{-1} left out of the adsorption bands of unhydrated cement (596, 614, 677, and 727 cm^{-1}), which proves the hydration of C_3A and C_4F, different from MS2, modified by sucrose solution.

It is known, that up to 70 % of solid phase of completely hydrated cement consists of CSH-gel, with high density of adhesive bonding with other hydration products, which specifies crucial operative features of cement rock: density, volume stability, permeability, plastic flow and shrinking properties. Contemporary approaches of colloid system studies describe CSH-phase as a cluster of particles about 5 nm, on the higher level grouping into units of 30–100 nm. Every base particle consists of united submicrocrystals of banded structure [26–30]. It is considered, that “real CSH is a banded hybrid of natural equivalent minerals – 1.4 nm of tobermorite $Ca_4Si_5O_6 \cdot 2.7H_2O$ and jennite $Ca_9Si_6O_{18} \cdot 6.8H_2O$” [28, 31].

The quality of gel – density, homogeneity, adaptability, adhesion capability – is specified by the quantity and distribution properties of water in calcium hydrosulphate. A significant amount of water is concentrated “between interlayer sheets, dividing them slightly wider than one water molecule”. Quantum-mechanic calculations proved the energy of binding superplastifier C3 sulpho-group with alite to be 540 kJ/mol, which is 2.8 times higher than similar value for water molecule (190 kJ/mol). That means that C-3 molecules are stronger bound to alite surface and can push water out of interlayer space, contributing to binding of particles or layers. Every monomerous link of C-3 supplaces up to 30 H_2O molecules, providing the plasticization of the cement system [32].

Hardening effect of plasticizers on the structure of a binding agent in concrete, apart from plasticization procedure, is shown in their influence on the dispersive-crystallite structure of a cement rock. Real crystal is a coagulate of smaller irregular-shaped crystals – microcrystals (grains). A grain is

comprised of mosaic blocks, which have their atomic levels, wedged from one another at a small angle of several minutes [33]. It is proved that C_3S hydration with 1 % (wt.) C-3 is followed by higher amount of CSH (I) and lower amount of CSH (II); the size of mosaic blocks is reduced from 20–33 to 15–17 nm. Such changes lead to sufficient raise in hardening structure density.

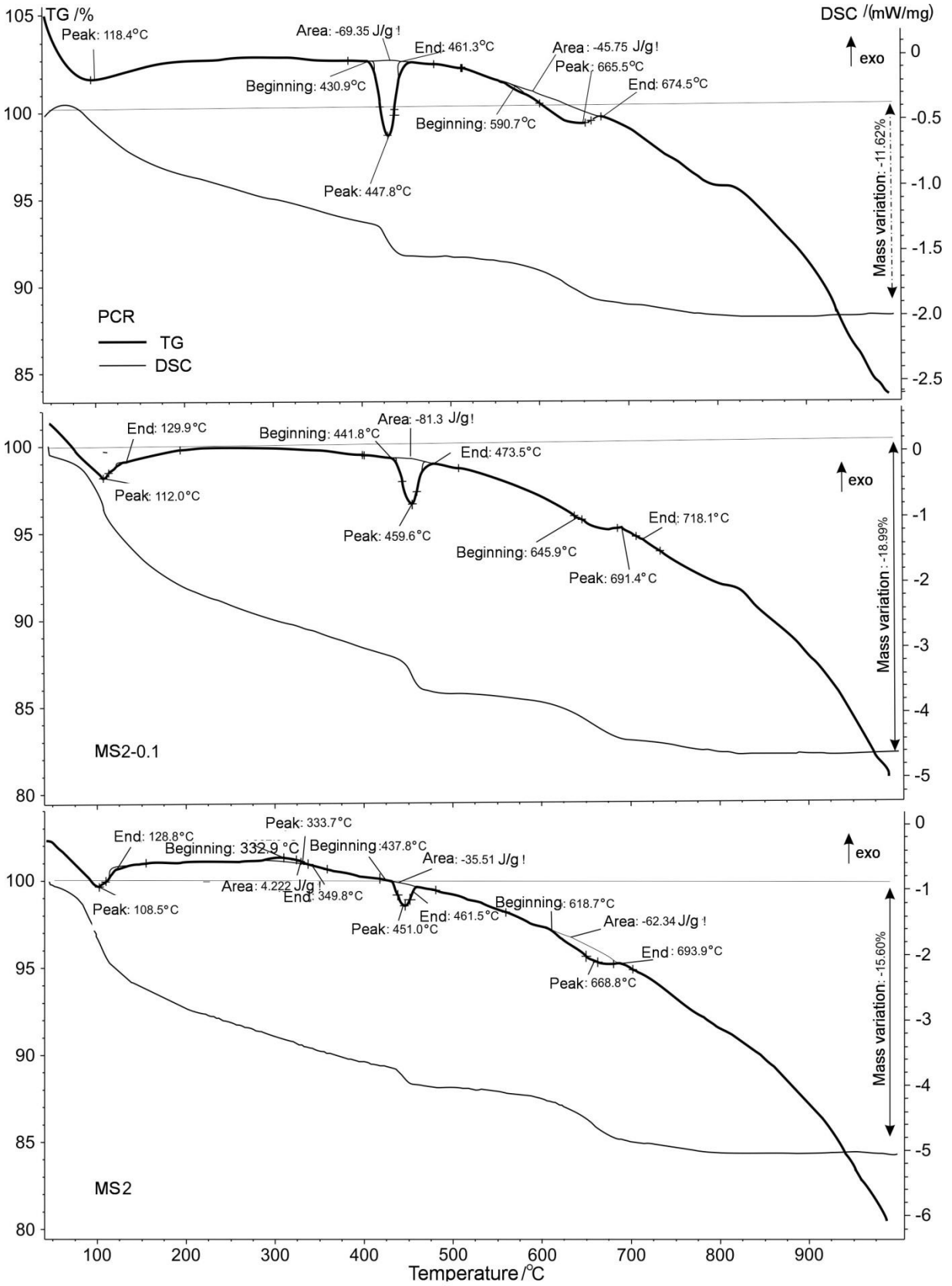

Figure 2. Derivatograms of PCR and modified samples

Shepelenko T.S., Sarkisov U.S., Gorlenko N.P., Tsvetkov N.A., Zubkova O.A. Structure-forming processes of cement composites, modified by sucrose additions. *Magazine of Civil Engineering.* 2016. No. 6. Pp. 3–11. doi: 10.5862/MCE.66.1

The effect of sucrose on cement as a plasticizing agent, while shown sufficiently lower due to lesser size of disaccharide molecules and lower amount of functional groups, in general is similar to C-3 effect. It is circumstantially proved by abovementioned reduction of adsorption intensity in IR-specter of the MS2-0.1 rock in 1475 cm^{-1} area, specifying the vibrations of interlayer water – 42 % versus PCR and 58 % versus MS2. However the discovered phenomenon calls for more solid experimental evidence.

One can suppose that the products of sucrose corrosion of cement, synthesized in "CWS" suspensions – microcrystals of ettringite, other crystal phases and neoformations of organomineral nature (hybrid composites, cognate to both cement and sucrose), being introduced into "water–cement" system work as active centers of structure development. The addition agent, enriched with cement corrosion products, according to Le Chatelier principle, inhibits the activity of early destruction of clinker minerals and catalyses the development of skeletal matrix of a cement rock, realizing the known principle of self-reinforcing [24], also positively affecting the properties of cement gel and heightening its density.

Conclusions

The conducted studies and interpretation of the results, offered in the article, allow to draw the following conclusions:

1. Acceleration of setting and hardening of the cement composite MS2-0.1 is realized due to synergic effect of several factors: intensive growth of ettringite crystal nuclei – the main reinforcing component of the cement system, reduction of $Ca(OH)_2$ amount in the solid phase of a cement rock, densifying of CSH-gel and plasticizing effect.

2. The use of sucrose as gauging liquid causes the adverse effect: cement particles are isolated by adsorption membranes, hydration processes are hindered, destructurization of the binding system takes place.

Thus the addition of "CWS" suspension carries out the structurization function onto the "water–cement" system and can be recommended to improve the operational properties of cement composites.

References

1. Aitchin P.-C. Cements of yesterday and today: concrete of tomorrow. *Cement and concrete research*. 2000. Vol. 3. No. 9. Pp. 1349–1359.
2. Zharko V.I., Guz' V.A., Afanas'ev A.F. Proizvodstvo i rynok tsementa v Rossii v 2014 godu [Prodaction and market of cement in Russia 2014]. *Tsement i ego primenenie*. 2015. No. 1. Pp. 18–21. (rus)
3. Gussoni M., Greco F., Bonazzi F., et al. 1H NMR spin-spin relaxation and imaging in porous systems: an application to the morphological study of white portland cement in the presence of organic. *Magn Reson Imag.* 2004. No. 22(6). Pp. 877-879.
4. Kuo W.-Y., Huang J.-S., Lin C.-H. Effects of organo-modified montmorillonite on strengths and permeability of cement mortars. *Cem. Concr. Res.* 2006. Vol. 36. No. 5. Pp. 886–895.
5. Abalaka A.E. Effects of sugar on physical properties of ordinary portland cement paste and concrete. *AU J. T.* 2011. Vol. 14. No. 3. Pp. 225–228.
6. Tkach R.V., Rakhimov M.A., Toimbaeva V.M., Rakhimova V.M. Vliyanie organomineral'nogo modifikatora na fiziko-mekhanicheskie i deformativnye svoistva betona [The effect of the organic-mineral modifier on physical and mechanical deformation properties of the concrete]. *Fundamental'nye issledovaniya.* 2012. No. 3. Pp. 428–431. (rus)
7. Shoshin E.A., Bylinkina N.N. Uglevody, kak elementy upravleniya strukturoi nanofazy tsementnogo kamnya [Carbohydrates as a way to control the structure of cement stone nanofazy]. *Vestnik BGTU im. V.G. Shukhova*. 2015. No. 5. Pp. 53–57. (rus)
8. Shepelenko T., Sarkisov Y., Afanasyev D., Akimova N. Regulatorsh ardening, containing products of sugar. *Cambridge Journal of Education and Science.* 2015. No. 2(14). Pp. 585–592.

Литература

1. Aitchin P.-C. Cements of yesterday and today: concrete of tomorrow // Cement and concrete research. 2000. Vol. 3. № 9. Pp. 1349–1359.
2. Жарко В.И., Гузь В.А., Афанасьев А.Ф. Производство и рынок цемента в России в 2014 году // Цемент и его применение. 2015. № 1. С. 18–21.
3. Gussoni M., Greco F., Bonazzi F., et al. 1H NMR spin-spin relaxation and imaging in porous systems: an application to the morphological study of white portland cement in the presence of organic // Magn. Reson. Imag. 2004. № 22(6). Pp. 877–879.
4. Kuo W.-Y., Huang J.-S., Lin C.-H. Effects of organo-modified montmorillonite on strengths and permeability of cement mortars // Cem. Concr. Res. 2006. Vol. 36. № 5. Pp. 886–895.
5. Abalaka A.E. Effects of sugar on physical properties of ordinary portland cement paste and concrete // AU J. T. 2011. Vol. 14. № 3. Pp. 225–228.
6. Ткач Р.В., Рахимов М.А., Тоимбаева В.М., Рахимова В.М. Влияние органоминерального модификатора на физико-механические и деформативные свойства бетона // Фундаментальные исследования. 2012. № 3. С. 428–431.
7. Шошин Е.А., Былинкина Н.Н. Углеводы, как элементы управления структурой нанофазы цементного камня // Вестник БГТУ им. В.Г. Шухова. 2015. № 5. С. 53–57.
8. Shepelenko T., Sarkisov Y., Afanasyev D., Akimova N. Regulatorsh ardening, containing products of sugar // Cambridge Journal of Education and Science. 2015. № 2(14). Pp. 585–592.
9. Shepelenko T.S., Sarkisov Y.S. Corrosion products of cement, as effective modifiers increase the strength of cement systems // Australian Journal of Scientific Research. 2014. № 1(5). Pp. 374–381.

Шепеленко Т.С., Саркисов Ю.С., Горленко Н. П., Цветков Н.А., Зубкова О.А. Процессы структурообразования цементных композиций, модифицированных добавками сахарозы // Инженерно-строительный журнал. 2016. № 6(66). С. 3–11.

9. Shepelenko T.S., Sarkisov Y.S. Corrosion products of cement, as effective modifiers increase the strength of cement systems. *Australian Journal of Scientific Research*. 2014. No. 1(5). Pp. 374–381.
10. Tarakanov O.V.*Tsementnye materialy s dobavkami ug-levodov* [Cement materials with carbohydrate addives]. Penza: PGASA, 2003. 166 p. (rus)
11. Ivashchenko Yu.G., Kozlov N.A. Issledovanie vliyaniya or-ganomineral'nogo modifikatora na protsessy strukturoobrazovaniya i kinetiku nabora prochnosti tsementnykh kompozitsii [Research of influence of organic modifier on the processes of structure and kinetics of strength development in cement composites]. *Vestnik BGTU im. V.G. Shukhova. Seriya: Stroitel'stvo i arkhitektura.* 2011. No. 4(49). Pp. 15–18. (rus)
12. Smith B.J., Rawal A., Funkhouser G.P., et al. Origins of saccharide-dependent hydration at aluminate, silicate and aluminosilicate surfaces. *PNAS*. 2011. Vol. 108. No. 22. Pp. 8949–8954.
13. Kireev Yu.L., Nesterova N.N., Luchinina I.G. O vzaimodeistvii mineralov portlandtsementnogo klinkera s rastvorom sakhara [On the interaction of Portland cement clincer minerals with a sugar solution]. *Cement.* 1999. No. 4. Pp. 19–21. (rus)
14. Ramachandran V.S., Fel'dman R.F., Kollepardi M. *Dobavki v beton: spravochnoe posobie* [Additives in concrete: a handbook]. Moskva: Stroiizdat, 1988. 575 p.(rus)
15. Glekel' F.L., Kopp R. Z., Musaeva R. I. I dr. Zavisimost' effekta deistviya plastifikatora tsementnykh dispersii ot prirody gidratiruyushchikhsya faz [The dependence of effect of cement dispersions plasticizer on the nature of the hydrating phase]. *J. of Applied Books*. 1989. Vol. 62. No. 5. Pp. 1026–1028. (rus)
16. Thomas N.L., Birchall J.D. The retarding action of sugars on cement. *Cement and Concrete Research*. 1983. Vol. 13. No. 6. Pp. 830–842.
17. Juenger M.C. New insights into the effect of sugar on the hydration and microstructure of cement pastes. *Cement and Concrete Research*. 2002. Vol. 32. No. 3. Pp. 393–399.
18. Ivashchenko Yu.G. Modifitsiruyushchee deistvie organiche-skikh dobavok na tsementnye kompozitsionnye materialy [Modifying effect of organic additives on cement composites]. *Vestnik SGTU.* 2012. No. 4(68). Pp. 202–205. (rus)
19. Reschard A., Gorin A., Fredon E., et. al. Influence of polysaccharides on cement hydratation. *Key Engineering Materials*. 2004. Vol. 264. Rp. 2141–2144.
20. Young Y.E. Effect of organic compounds on the Interconversion of calcium Aluminate Hydrate. Hydratation of the Tricalcium Aluminate. *J. of the American Ceramic Society*. 1970. No. 53. Pp. 65–69.
21. Young Y.E. Reaction mechanism of Organic Admixtures with Hydrating Cement Compounds. *Transportation Research Record*. 1976. No. 564. Pp. 1–9.
22. Moore A. and Taylor H.F.W. Crystal structure of ettringite. *Nature.* 1968. Vol. 218. Pp. 1048–1049.
23. Shoshin Ye.A., Polyakov A.V., Burov A.M. Izmenenie nanostruktury model'noi silikatnoi sistemy v usloviyakh posledovatel'nogo izmeneniya kontsentratsii sakharozy [Changes in the nanostructure of a model silicate system in terms of sequenial changes in the concentration of sucrose]. *Vestnik BGTU im. V.G. Shukhova.* 2016. No. 3. Pp. 23–30. (rus)
24. Timashev V.V., Sycheva I.I., Nikonova N.S. *Struktura samoarmirovannogo tsementnogo kamnya. Izbrannye trudy. Sintez i gidratatsiya vyazhushchikh materialov* [Structure of self-reinforced cement rock. Selected works. Synthesis and hydration of cementitious materials]. Moskva: Nauka, 1986. Pp. 390–400. (rus).
25. Chernyshov E.M., Korotkikh D.N. Nanofibrerein for cement
10. Тараканов О.В.Цементные материалы с добавками углеводов. Пенза: ПГАСА, 2003. 166 с.
11. Иващенко Ю.Г., Козлов Н.А. Исследование влияния органоминерального модификатора на процессы структурообразования и кинетику набора прочности цементных композиций // Вестник БГТУ им. В.Г. Шухова. Серия: Строительство и архитектура. 2011. № 4(49). С. 15–18.
12. Smith B.J., Rawal A., Funkhouser G.P., et al. Origins of saccharide-dependent hydration at aluminate, silicate and aluminosilicate surfaces // PNAS. 2011. Vol. 108. № 22. Pp. 8949–8954.
13. Киреев Ю.Л., Нестерова Н.Н., Лучинина И.Г. О взаимодействии минералов портландцементного клинкера с раствором сахара // Цемент. 1999. № 4. С. 19–21.
14. Рамачандран В.С., Фельдман Р.Ф., Коллепарди М. Добавки в бетон: справочное пособие. М.: Стройиздат, 1988. 575 с.
15. Глекель Ф.Л., Копп Р. З., Мусаева Р. И. И др. Зависимость эффекта действия пластификатора цементных дисперсий от природы гидратирующихся фаз // Журнал прикладной химии. 1989. Vol. 62. № 5. С. 1026–1028.
16. Thomas N.L., Birchall J.D. The retarding action of sugars on cement // Cement and Concrete Research. 1983. Vol. 13. № 6. Pp. 830–842.
17. Juenger M.C. New insights into the effect of sugar on the hydration and microstructure of cement pastes // Cement and Concrete Research. 2002. Vol. 32. № 3. Pp. 393–399.
18. Иващенко Ю.Г. Модифицирующее действие органических добавок на цементные композиционные материалы // Вестник СГТУ. 2012. № 4(68). С. 202–205.
19. Reschard A., Gorin A., Fredon E., et. al. Influence of polysaccharides on cement hydratation // Key Engineering Materials. 2004. Vol. 264. Pp. 2141–2144.
20. Young Y.E. Effect of organic compounds on the Interconversion of calcium Aluminate Hydrate. Hydratation of the Tricalcium Aluminate // J. of the American Ceramic Society. 1970. № 53. Pp. 65–69.
21. Young Y.E. Reaction mechanism of Organic Admixtures with Hydrating Cement Compounds // Transportation Research Record. 1976. № 564. Pp. 1–9.
22. Moore A. and Taylor H.F.W. Crystal structure of ettringite // Nature. 1968. Vol. 218. Pp. 1048–1049.
23. Шошин Е.А., Поляков А.В., Буров А.М. Изменение наноструктуры модельной силикатной системы в условиях последовательного изменения концентрации сахарозы // Вестник БГТУ им. В.Г. Шухова. 2016. № 3. С. 23–30.
24. Тимашев В.В., Сычева И.И., Никонова Н.С. Структура самоармированного цементного камня. Избранные труды. Синтез и гидратация вяжущих материалов. М.: Наука, 1986. С. 390–400.
25. Chernyshov E.M., Korotkikh D.N. Nanofibrerein for cement of cement stone structures with help of crystals as a space of concrete fracture strength. // Scientific Israel Technological. 2009. Vol. 11. Pp. 23–28.
26. Manzano H., Agueva A., Dolado J.S. On the formation of cementitious C-S-H nanoparticles // J. Comp.-Aided Mater. Design. 2007. № 14. Pp. 45–51.
27. Richardson I.G. The calcium silicate hydrates // Cement and concrete research. 2008. Vol. 38. Pp. 137–158.
28. Pelleng R.J.-M. A realistic molecular model of cements hydrates // Proceedings of the national Academy of the Sciences. 2009. Vol. 106. № 38. Pp. 16102–16107.
29. Allen A.J., Tomas J.J. Analysis of C-S-H gel and cement paste by small-angle neutron scattering // Cem. Concr. Res. 2007. Vol. 37. № 3. Pp. 319–324.

Shepelenko T.S., Sarkisov U.S., Gorlenko N.P., Tsvetkov N.A., Zubkova O.A. Structure-forming processes of cement composites, modified by sucrose additions. *Magazine of Civil Engineering.* 2016. No. 6. Pp. 3–11. doi: 10.5862/MCE.66.1

of cement stone structures with help of crystals as a space of concrete fracture strength. *Scientific Israel Technological*. 2009. Vol. 11. Pp. 23–28.

26. Manzano H., Agueva A., Dolado J.S. On the formation of cementitious C-S-H nanoparticles. *J. Comp.-Aided Mater*. Design. 2007. No. 14. Pp. 45–51.
27. Richardson I.G. The calcium silicate hydrates. *Cement and concrete research*. 2008. Vol. 38. Pp. 137–158.
28. Pelleng R.J.-M. A realistic molecular model of cements hydrates. *Proceedings of the national Academy of the Sciences*. 2009. Vol. 106. No. 38. Rp. 16102–16107.
29. Allen A.J., Tomas J.J. Analysis of C-S-H gel and cement paste by small-angle neutron scattering. *Cem. Concr. Res.* 2007. Vol. 37. No. 3. Pp. 319–324.
30. Beaudoin J.J., Drame H., Raki L. Alizadeh R. Formation and properties of C-S-H – HDTMA. *J. Mater. Res.* 2008. Vol. 23. No. 10. Pp. 2804–2815.
31. Bonaccorsi E., Merlino S., Taylor H.F.W. The crystal structure of jennite, $Ca_9Si_6O_{18}(OH)6\text{-}8H_2O$. *Cem. Concr. Res.* 2004. No. 34. Pp. 1481–1488.
32. Yuhnevsky P.I., Zelenkovskii V.M., Soldatov V.S. O modeli struktury gidrosilikatnogo gelya i vliyanii khimicheskikh dobavok-plastifikatorov. [On a model of the hydrosilicate gel structure and the effect of the chemical plasticizing additives]. *Nauka – proizvodstvu*. 2013. No.1. Pp. 25–29. (rus)
33. Yuhnevsky P.I., Zelenkovskii V.M., Soldatov V.S. Kvantovo-khimicheskoe modelirovanie vzaimodeistviya polimetilennaftalinsul'fonatov natriya (dobavka C-3) s gidratirovannoi poverkhnost'yu alita S_3S. [Quantum-chemical modeling of the interaction of sodium polymethylenenaphtalenesulfonate (additive C-3) with a surface hydrated alite C_3S]. *Tekhnologiya betonov*. 2010. No. 5–6. Pp. 31–33. (rus)

30. Beaudoin J.J., Drame H.,Raki L. Alizadeh R. Formation and properties of C-S-H – HDTMA // J. Mater. Res. 2008. Vol. 23. № 10. Pp. 2804–2815.
31. Bonaccorsi E., Merlino S., Taylor H.F.W. The crystal structure of jennite, Ca9Si6O18(OH)6-8H2O // Cem. Concr. Res. 2004. № 34. Pp. 1481–1488.
32. Юхневский П.И., Зеленковский В.М., Солдатов В.С. О модели структуры гидросиликатного геля и влиянии химических добавок-пластификаторов // Наука – производству. 2013. № 1. С. 25–29.
33. Юхневский П.И., Зеленковский В.М., Солдатов В.С. Квантово-химическое моделирование взаимодействия полиметиленнафталинсульфонатов натрия (добавка С-3) с гидратированной поверхностью алита C_3S // Технология бетонов. 2010. № 5–6. С. 31–33.

Tatiana Shepelenko,
+7(382)642445; shepta72@mail.ru

Yuri Sarkisov,
+7(3822)640907; sarkisov@tsuab.ru

Nicholas Gorlenko,
+7(3822)640907; Gorlen52@mail.ru

Nicholas Tsvetkov,
+7(3822)654281; nac.tsuab@yandex.ru

Olga Zubkova,
+7(3822)642445; zubkova0506@mail.ru

Татьяна Станиславовна Шепеленко,
+7(382)642445; эл. почта: shepta72@mail.ru

Юрий Сергеевич Саркисов,
+7(3822)640907; эл. почта: sarkisov@tsuab.ru

Николай Петрович Горленко,
+7(3822)640907; эл. почта: Gorlen52@mail.ru

Николай Александрович Цветков,
+7(3822)654281;
эл. почта: nac.tsuab@yandex.ru

Ольга Александровна Зубкова,
+7(3822)642445;
эл. почта: zubkova0506@mail.ru

© Shepelenko T.S., Sarkisov U.S., Gorlenko N.P., Tsvetkov N.A., Zubkova O.A., 2016

Шепеленко Т.С., Саркисов Ю.С., Горленко Н. П., Цветков Н.А., Зубкова О.А. Процессы структурообразования цементных композиций, модифицированных добавками сахарозы // Инженерно-строительный журнал. 2016. № 6(66). С. 3–11.

doi: 10.5862/MCE.66.2

Compatibility of portland cement and polycarboxylate-based superplasticizers in high-strength concrete for precast constructions

Совместимость портландцемента и суперпластификаторов на поликарбоксилатной основе для получения высокопрочного бетона сборных конструкций

O.M. Smirnova,
Petersburg State Transport University,
St. Petersburg, Russia

Канд. техн. наук, доцент О.М. Смирнова,
Петербургский государственный университет путей сообщения Императора Александра I,
г. Санкт-Петербург, Россия

Key words: building materials; construction; precast concrete; heat-steaming treatment; polycarboxylate-based superplasticizer; stiff fresh concrete

Ключевые слова: строительство; строительные материалы; сборный бетон; тепловлажностная обработка; суперпластификатор на поликарбоксилатной основе; жесткая бетонная смесь

Abstract. Application of polycarboxylate-based superplasticizers can contribute to the increase of concrete early strength. It makes possible to obtain the concrete of the required strength after heat-steaming treatment with decreasing the isothermal temperature and the Portland cement quantity compared to the concrete without admixtures. Reducing of water-cement ratio and lack of accelerated high-temperature of heat-steaming treatment raises the durability of precast concrete. The use of low heat-steaming treatment must not lead to an increase of the duration of treatment and reduction of productivity of plant with double turnover of moulds per day. It is necessary to take into account the compatibility of Portland cement and polycarboxylate-based superplasticizers to obtain the high concrete strength after heat-steaming treatment. The problem of the compatibility of Portland cement and polycarboxylate-based superplasticizers in precast concrete production contains the following items: the influence of chemical and mineralogical compositions of Portland cement on the water-reducing effect of polycarboxylate-based superplasticizers, on the retention of workability of fresh concrete as well as on the growth of early concrete strength. Most of the published papers contain the results received when investigating the cement paste. However, the effect of polycarboxylate-based superplasticizers in stiff fresh concrete has not yet been fully investigated. The optimal dosages of polycarboxylate-based superplasticizers, requirements to the granulometric and chemical-mineralogical compositions of Portland cements with the purpose of reducing the cement consumption and providing the required concrete strength after the heat-steaming treatment at 40 °C have been defined.

Аннотация. Применение поликарбоксилатных суперпластификаторов позволяет получать высокопрочный бетон и может способствовать повышению ранней прочности бетона. Это дает возможность получать бетон с требуемой прочностью после тепловлажностной обработки (ТВО) при снижении температуры изотермической выдержки и расхода портландцемента по сравнению с бетоном без добавок. При этом необходимо учитывать совместимость портландцемента и поликарбоксилатного суперпластификатора. В области производства сборного бетона и железобетона под вопросом совместимости портландцементов с суперпластификаторами следует понимать влияние химико-минералогического состава портландцемента на водоредуцирующее действие добавок, исключение быстрой потери подвижности бетонной смеси, почасовую кинетику набора ранней прочности бетона с суперпластификатором. Большая часть работ отражает результаты, полученные на цементном тесте. Однако эти вопросы не исследованы для жестких бетонных смесей. Установлены оптимальные расходы суперпластификаторов, требования к гранулометрическому и химико-минералогическому составу портландцементов с целью снижения расхода цемента и обеспечения требуемой прочности бетонов после ТВО продолжительностью 12

часов при температуре изотермической выдержки 40 °С. Получены зависимости прочности бетона после ТВО от расхода портландцемента и поликарбоксилатных суперпластификаторов.

Introduction

Application of polycarboxylate-based superplasticizers can contribute to the increase of concrete early strength. It makes possible to obtain the concrete of the required strength after heat-steaming treatment with decreasing the isothermal temperature and the Portland cement quantity compared to the concrete without admixtures. Steaming at high temperatures reduces a number of technical characteristics of concrete such as strength at age of 28 days and frost resistance [1]. Reducing of water-cement ratio and the lack of accelerated high-temperature of heat-steaming treatment raises durability of precast concrete due to the improvement of the concrete structure [2–6]. The use of low heat-steaming treatment must not lead to an increase of the duration of treatment and reduction of productivity of plant.

It is necessary to take into account the incompatibility of Portland cement and polycarboxylate-based superplasticizers to obtain the high concrete strength after heat-steaming treatment. Such concrete should provide the required transfer strength (strength at the moment of release tension bars) in a relatively short time 10–12 hours. For example, with double turnover moulds per day at the plant the concrete strength of class B40 should be not less than 35 MPa at the age of 10–12 hours and 44 MPa – for concrete strength of class B50.

Considering the problem of the incompatibility of Portland cement and polycarboxylate-based superplasticizers in precast concrete production it is necessary to take into account the influence of chemical and mineralogical compositions of Portland cement on the water-reducing effect of polycarboxylate-based superplasticizers, on the retention of workability of fresh concrete as well as on the growth of early concrete strength.

Considerable decrease of water quantity in fresh concrete mixes of equal workability by means of introducting small dosages of polycarboxylate-based superplasticizer accelerates the Portland cement hydration. On the other hand, the increased dosages of polycarboxylate-based superplasticizer slow down the Portland cement hydration in spite of their high water-reducing effect.

The authors [7, 8] highlight the role of a soluble alkali and C_3A in the retention of workability of fresh cement paste.

The papers published on incompatibility theme can be classified into the following subjects depending on the factor studied: chemical and mineralogical compositions of Portland cement (quantity of C_3A, Na_2O_{equiv}, SO_3) and its fineness [9–10]; fineness and quantity of mineral fillers [11–15]; quantity of admixture [12, 16]; chemical base of admixture, structure of its molecule [17], speed of polycarboxylate-based superplasticizer adsorption on the cement particles being hydrated [18–23].

The mineral additions in Portland cement impact rheology of cement paste and affect the interaction between superplasticizers and cements. The results of paper [11] show that cement-superplasticizers compatibility is altered by the physical (specific surface) and chemical (surface charge) characteristics of the mineral additions (limestone, fly ash and silica fume). In paper [14] it has investigated the incompatibility of Blended cement and polycarboxylate-based superplasticizers in range from 0.7 to 1.2 %. The delay of admixtures on cement hydration intensifies with rising PCE dosage. This admixture-mediated retarding effect was also observed to vary depending on the nature of the addition, and was most intense in slag-blended cement.

Most of the published papers contain the results received when investigating the cement paste. However, the effect of polycarboxylate-based superplasticizer in stiff fresh concrete has not yet been fully investigated. It is necessary to specify to what changes in admixture dosage or water quantity as well as in concrete strength development the changing Portland cement properties can lead to. The results of the research can be used in the production of precast prestressed reinforced concrete with polycarboxylate-based superplasticizers on the existing technological lines of plants with double turnover of moulds per 24 hours.

Materials and methods of research

For research it was selected the domestic Portland cements PC500-D0-N of six manufacturers corresponding to Russian Standard GOST 30515-97 “Cements. General technical conditions” and CEM I 42.5N from two factories corresponding to Russian Standard GOST 31108-2003 “Cements. Technical conditions”. Chemical and mineralogical compositions of Portland cements are presented in

Tables 1 and 2. Most of Portland cements had the content of C_3S within 60 % and the content of C_3A – 6–9 %. Such Portland cements are the most effective in the precast concrete production under conditions of heat-steaming treatment at temperature 80 °C. As polycarboxylate-based superplasticizers it was selected those, which due to their certain molecule structure are able to increase the concrete early strength. These are: Glenium ACE 430, Sika Viscocrete 20 Gold. The sand and crushed stone aggregates were according to Russian Standards GOST 8736-93 and GOST 8267-93. The control sample was prepared from the concrete mix (Portland cement 470 kg/m^3) used in the production of precast prestressed reinforced concrete with the double turnover of moulds every 24 hours and heat-steaming treatment at the isothermal temperature of 80 °C. The workability of fresh concrete was 18–20 seconds.

Table 1. Chemical compositions of Portland cements

No of sample	Cement	CaO	SiO_2	Al_2O_3	Fe_2O_3	MgO	SO_3	K_2O	Na_2O	Na_2O_{eqv}	$CaO_{св}$	L.O.I.
1	CEM I 42.5N	63.80	21.20	4.90	3.90	1.00	2.80	0.60	0.13	0.52	0.30	1.10
2	PC500-D0-N	63.90	21.00	4.88	4.12	0.92	2.77	0.58	0.17	0.55	0.25	1.00
3	CEM I 42.5N	66.20	21.60	5.77	4.12	1.09	2.50	0.57	0.30	0.68	-	1.06
4	PC500-D0-N	65.97	21.41	5.67	5.12	0.80	2.57	0.68	0.31	0.76	-	0.86
5	PC500-D0-N	63.79	21.26	3.67	3.54	1.75	2.76	0.59	0.76	1.15	-	1.17
6	PC500-D0-N	65.74	21.50	4.96	5.32	1.32	2.60	0.57	0.32	0.69	0.07	0.33
7	PC500-D0-N	63.56	20.56	5.21	4.13	1.41	2.82	0.65	0.36	0.79	-	0.94
8	PC500-D0-N	61.90	19.70	4.92	3.30	3.90	3.12	0.67	0.71	1.15	-	-

The following methods were used: analysis of the particle size distribution (the laser particle size distribution analyzer – MicroSizer 201), termokinetic analysis (Calvet-type calorimeter), scanning electron microscopy (Supra55VP-3249 Zeiss). The kinetics of the plastic strength growth of the cement paste was investigated using a cone plastometer following the methodology of academician P.A. Rebinder [24]. The tests were conducted at intervals of cone immersing, equal to 30 minutes. As the criterion were used the value of the plastic strength in MPa, which was determined from the expression:

$$P_m = K \cdot \frac{F \cdot g}{100000 \cdot h^2},$$

where F – the load in g;

h – depth of cone immersion in cm, h = 1 cm;

K – coefficient depending on the angle of the cone at the top, at 45° K = 0.656.

The results of defining the plastic strength are expressed graphically in the form of plastograms, on which one can distinguish specific periods: the initial period (induction period) and that of rapid growth plastic strength.

Table 2. Mineralogical compositions of Portland cements

No of sample	C_3S	C_2S	C_3A	C_4AF
1	63.0	14.7	6.5	13.0
2	63.1	14.6	6.3	13.5
3	64.4	14.3	9.9	11.0
4	59.1	17.0	6.2	15.5
5	66.4	14.6	4.2	10.7
6	63.9	13.0	4.1	16.0
7	65.0	9.4	6.4	12.4
8	62.1	10.4	6.9	11.3

Results and discussion

Comparison of particle size distribution of the selected Portland cements showed that there are fewer particles having the grains size less than 2, 3, 5 and 10 μm in Portland cements No. 1, 2, 3, 4 than in the other Portland cements (Table 3).

Table 3. The particle size distribution of Portland cements

No of sample	Содержание зерен размером менее, %					
	2 мкм	3 мкм	5 мкм	10 мкм	16 мкм	32 мкм
1	7.2	9.9	15.9	25.7	37.8	59.6
2	6.3	8.6	14.1	23.7	48.8	68.9
3	9.7	13.6	20.2	33.8	44.2	71.6
4	9.0	12.5	19.8	36.7	47.1	72.6
5	14.8	20.8	28.7	42.9	51.3	70.7
6	11.6	16.6	23.7	38.6	49.2	75.2
7	6.6	11.5	24.0	38.9	45.8	71.0
8	13.9	19.7	27.4	42.2	51.8	73.8

Setting time can be estimated on cement pastes through the Vicat needle method. A recent study [25, 26] suggested improving the Vicat test by using a static method that allows monitoring of the evolution of the setting starting immediately from the mixing time. Based on ultrasound techniques, a new testing device is suggested to analyze setting and hardening of concrete materials. In this paper the cone plastometer of academician P.A. Rebinder are proposed. This method allows also monitoring of the evolution of the setting starting immediately from the mixing time [27].

By comparing the kinetics of the plastic strength development it was found out that Portland cements, which have a shorter initial period (induction period) of hardening and more intensive plastic strength development in the second period of hardening, contained the increased number of grains of size less than 10 μm, which was 36–42 % (Figure 1). The application of such Portland cements allows reducing the duration of curing before heat-steaming treatment of concrete.

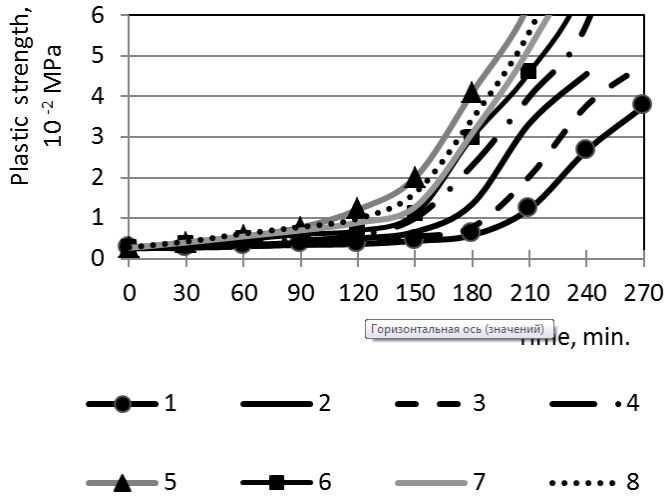

Figure 1. Influence of Portland cements on plastic strength development cement paste of equal fluidity

It was stated that the required strength of concrete of class B40 (34.9 MPa) after the heat-steaming treatment duration of 12 hours at isothermal temperature of 40 °C, can be obtained on Portland cements with the content of grains of size less than 3 μm within 17–21 % (Figure 2).

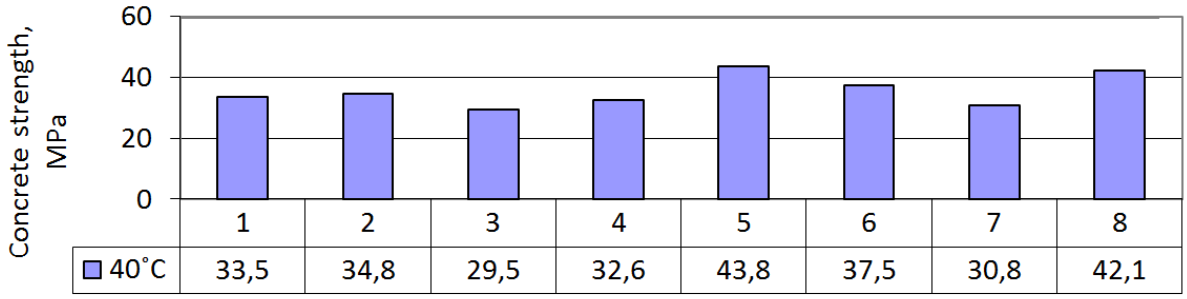

	1	2	3	4	5	6	7	8
40°C	33,5	34,8	29,5	32,6	43,8	37,5	30,8	42,1

Figure 2. Concrete strength after the heat-steaming treatment duration of 12 hours at isothermal temperature of 40 °C

However, not always the high value of early concrete strength on Portland cements, containing the defined number of fine particles is a characteristic that guarantees the high early strength of concrete on these Portland cements with polycarboxylate-based superplasticizers.

The water-reducing effect of polycarboxylate-based superplasticizers depends on the chemical and mineralogical compositions of cement (Figures 3–4). It is established that the increasing of C_3A in Portland cement results in the decreasing of the water-reducing effect of polycarboxylate-based superplasticizers. This was also confirmed in fresh concrete mixes of equal workability when comparing the water-reducing effect of Sika Viscocrete 20 Gold and Glenium ACE 430 (Figure 5). The content of SO_3 and alkaline metals in Portland cement No. 1, 2, 3 was almost the same, so their influence on the plasticizing action of admixtures can be neglected. Reduction of water consumption within the limits of 16 % was received in concrete mixtures on Portland cement containing C_3A about 6.5 % with the introduction of 0.4 % of polycarboxylate-based superplasticizers and 0.8 % of polycarboxylate-based superplasticizers – on Portland cement containing C_3A about 9.9 %. With the increase of dosage of polycarboxylate-based superplasticizers the difference between their water-reducing effects in fresh concrete on these Portland cements is decreased.

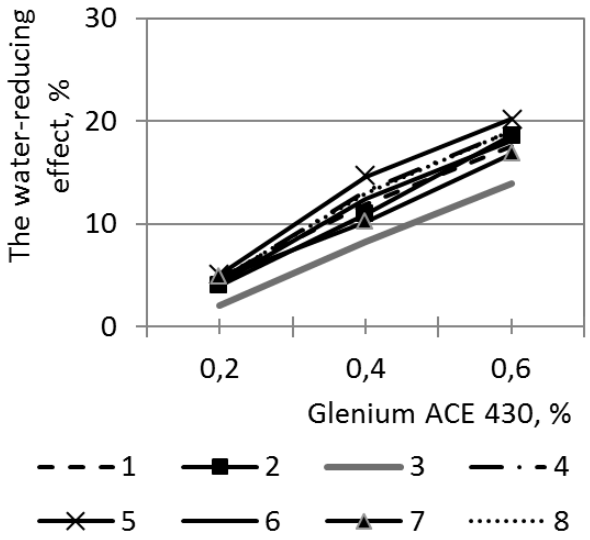

Figure 3. The water-reducing effect of Glenium ACE 430 depending on cement

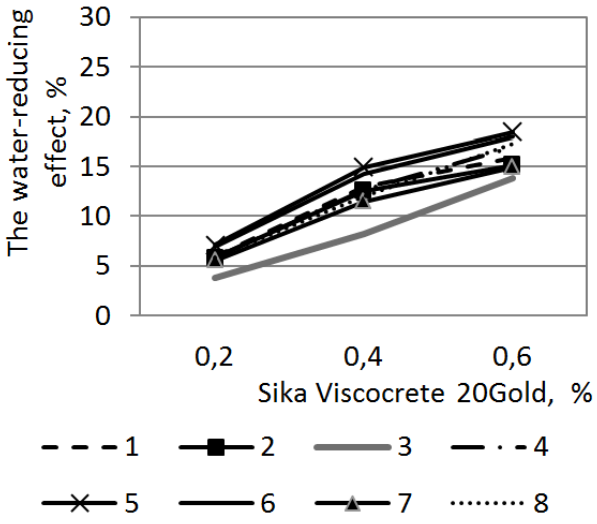

Figure 4. The water-reducing effect of Sika Viscocrete 20 Gold depending on cement

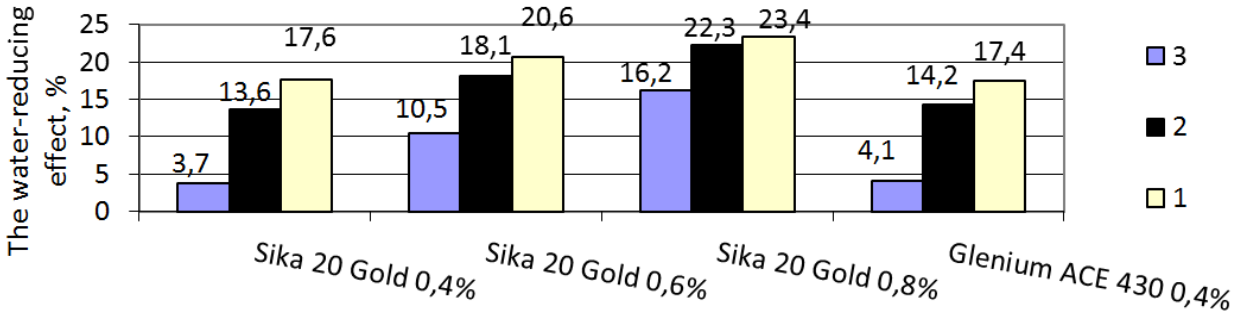

Figure 5. The water-reducing effect of polycarboxylate-based superplasticizers in the stiff fresh concrete mixes depending on cement

In fresh concrete containing polycarboxylate-based superplasticizers and Portland cements with a high content of alkali metals in 8–15 minutes from the moment of water addition there was observed the rapid loss of workability. This agrees with the data obtained by calorimetric measurements on cement pastes with polycarboxylate-based superplasticizers (Figures 6–9). The influence of alkali metal content in cement on the value of first peak of heat flow curve was shown. In the cement paste on Portland cement No. 2 (Na_2O_{equiv} = 0.55) the first peak appears in 3–5 minutes, i.e. actually in the period of preparation of fresh concrete mix. When increasing the alkali metal content in cement to Na_2O_{equiv} = 1.15 the first peak appears in 8–12 minutes. According to G. Verbek [28] the value of heat flow is proportional to the number of hydrate phases, therefore, in case of Portland cements with high content of alkali metals there occurs the intensive growth of hydrate phases and the fast loss of workability of fresh concrete mix. The second peak of heat flow curve was noted on Portland cements No. 5 and 8 earlier than on the others, which agrees with the data of more high strength concrete on these cements at the age of 12 hours.

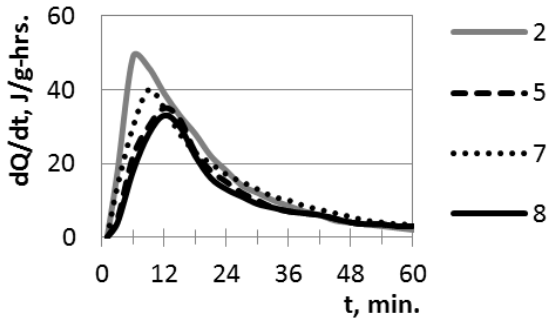

Figure 6. Heat rate of Portland cements with Sika Viscocrete 20 Gold 0.4 % during first hour of hydration

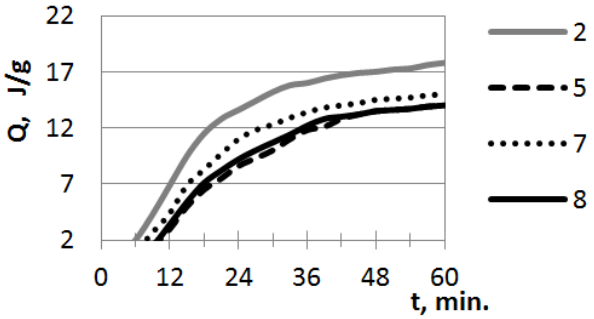

Figure 7. Cumulative heat of Portland cements with Sika Viscocrete 20 Gold 0.4 % during first hour of hydration

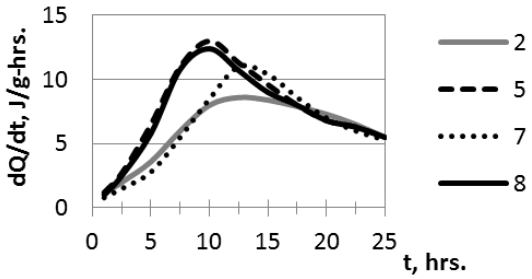

Figure 8. Heat rate of Portland cements with Sika Viscocrete 20 Gold 0.4 % during 25 hours of hydration

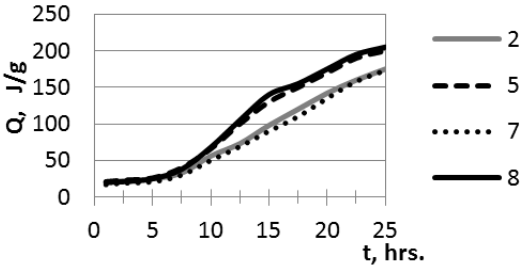

Figure 9. Cumulative heat of Portland cements with Sika Viscocrete 20 Gold 0.4 % during 25 hours of hydration

In order to avoid the loss of workability of fresh concrete with polycarboxylate-based superplasticizers on Portland cements, containing increased quantity of alkaline metals, it is necessary to add the mixing water in two stages. The polycarboxylate-based superplasticizers should be added with the second part of mixing water or it is necessary to increase the duration of mixing up to 1–2 minutes. In the absence of the possibility of adding the mixing water in the two stages it is necessary to increase the total quantity of the mixing water up to 5–7 %. However, the increase of mixing water leads to the reducing the early concrete strength and does not allow to receive the significant saving of Portland cement.

According to the results of studies of eight Portland cements it turned out that to ensure the high water-reducing effect of polycarboxylate-based superplasticizers and to eliminate the rapid loss of workability of fresh concrete, the recommended content of the C_3A, SO_3, Na_2O_{equiv} in Portland cements should be within 4.0–7.0 %; 2.57–2.82 %; 0.52–0.79 % respectively.

When comparing the effectiveness of admixtures such as Sika Viscocrete 20 Gold and Glenium ACE 430 in the studied Portland cements in order to ensure the necessary strength of concrete (class B40) after the heat-steaming treatment at the isothermal temperature of 40 °C and the duration of 12 hours, it was established that the maximum reduction of Portland cement consumption can be obtained with the Portland cement, with the content of cement grains of size less than 3 μm with 17 % and content of C_3A, SO_3, Na_2O_{equiv} within the limits mentioned above (Figure 10).

	1	2	3	4	5	6	7	8
Sika 20 Gold 0.4%	5	30	5	35	47	75	65	50
Glenium ACE 430 0.4%	5	30	5	29	38	70	60	45

Figure 10. Saving of Portland cement after the heat-steaming treatment at 40 °C and the duration of 12 hours

Smirnova O.M. Compatibility of portland cement and polycarboxylate-based superplasticizers in high-strength concrete for precast constructions. *Magazine of Civil Engineering*. 2016. No. 6. Pp. 12–22. doi: 10.5862/MCE.66.2

The dependences of concrete strength after the heat-steaming treatment at temperature 40 °C and the duration of 12 hours on the Portland cement consumption and admixture dosage were obtained. Regression equations were calculated, which allows to choose the concrete compositions depending on the required concrete strength at the age of 12 hours. Variable factors were: admixture dosage – X1 (%) and Portland cement consumption – X2 (kg). The regression equations, obtained as a result of statistical data processing are the following:

1. $R = 38.837 + 3.158X1 + 13.1X2 + 0.303X1^2 + 6.428X2^2 – 2.150X1X2$,

where X1 – dosage of Sika 20 Gold.

2. $R = 40.676 + 0.713X1 + 3.970X2 – 3.098X1^2 – 2.048X2^2 – 2.070X1X2$,

where X1 – dosage of Glenium ACE 430.

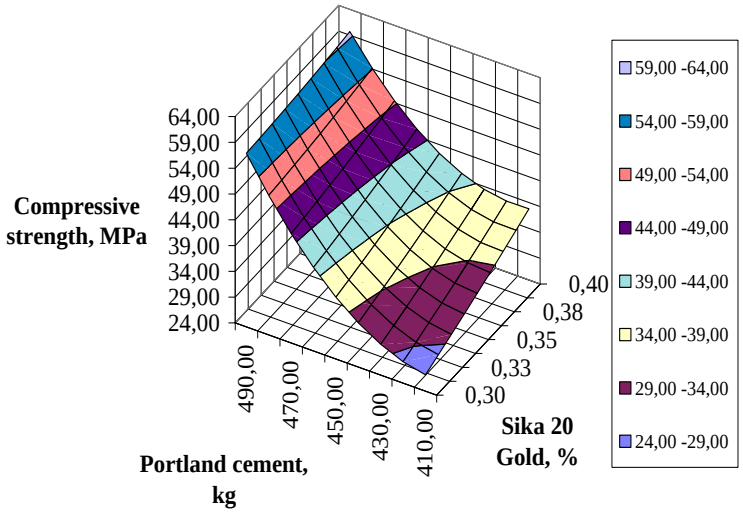

Figure 11. The dependence of concrete strength after the heat-steaming treatment at 40 °C and the duration of 12 hours on the cement consumption and admixture dosage

Checking adequacy according to the criterion of the Fisher in the level of reliability of 0.95 showed the suitability of mathematical models for the description of the investigated dependencies. In Figures 11 and 12 one can see the graphical representation of mathematical models. The use of admixtures in optimal quantity: Sika Viscocrete 20 Gold of 0.38 %, Glenium ACE 430 – 0.4 % made it possible to reduce Portland cement consumption by 15 % and the isothermal temperature of heat-steaming treatment from 80 °C to 40 °C. The concrete strength of samples with admixtures at the age of 28 and 360 days was actually equal to the samples without admixtures.

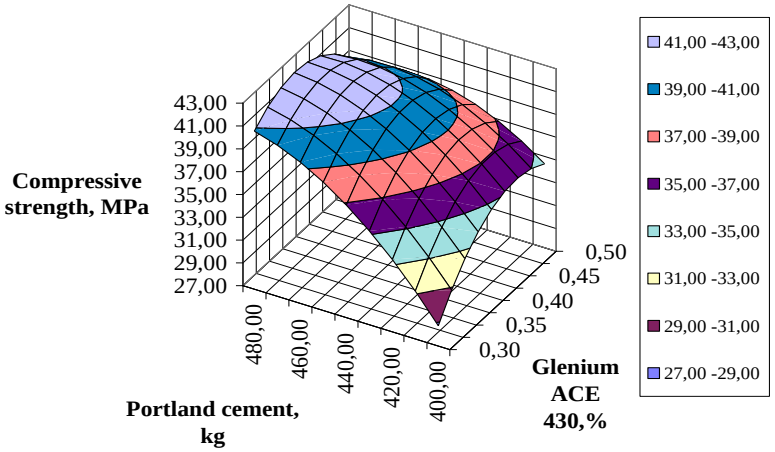

Figure 12. The dependence of concrete strength after the heat-steaming treatment at 40 °C and the duration of 12 hours on the cement consumption and admixture dosage

Смирнова О.М. Совместимость портландцемента и суперпластификаторов на поликарбоксилатной основе для получения высокопрочного бетона сборных конструкций // Инженерно-строительный журнал. 2016. № 6(66). С. 12–22.

When comparing the shape and size of C-S-H phases by means of scanning electron microscopy it could be seen that the samples of the cement stone at the age of 12 hours with the admixture of Sika Viscocrete 20 Gold (0.4 %) are much finer and the structure of C-S-H phases is much denser (Figures 13–14), which increases the number of contacts between C-S-H phases and helps to increase the strength of cement stone.

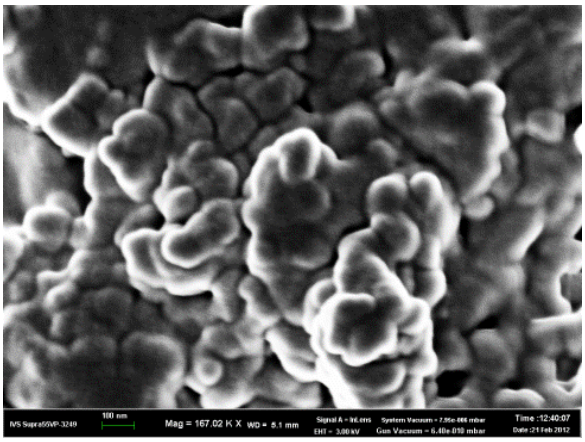

Figure 13. The structure of C-S-H phases in sample without admixture after the heat-steaming treatment at 40 °C and the duration of 12 hours

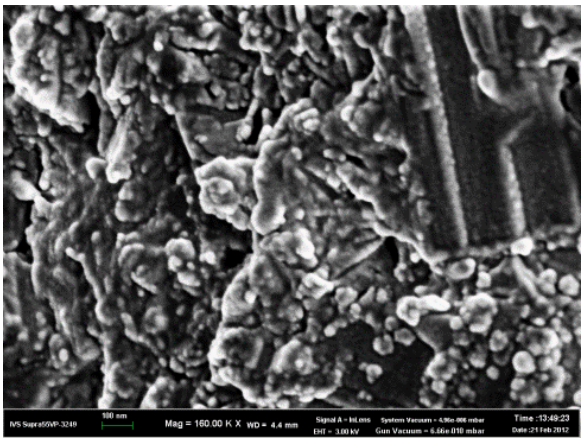

Figure 14. The structure of C-S-H phases in sample with admixture after the heat-steaming treatment at 40 °C and the duration of 12 hours

The C–S–H that forms in the hydration of Portland cement has variable stoichiometry depending on the water to cement ratio, curing conditions and use of supplementary cementitious materials [29, 30]. According [31] there are two types of C–S–H in hydrated Portland cement: low density and high density. The low-density C–S–H phase has a mean stiffness of about 22 GPa while the mean stiffness is about 29 GPa for high-density C–S–H.

Conclusions

1. The results of the research can be used in the production of precast prestressed reinforced concrete with polycarboxylate-based superplasticizers on the existing technological lines of plants with double turnover of moulds per day. The influence of chemical and mineralogical compositions of Portland cements should be taken into account to ensure the high water-reducing effect of these admixtures with their small dosage.

2. The optimal dosages of polycarboxylate-based superplasticizers, requirements to the granulometric and chemical-mineralogical compositions of Portland cements with the purpose of reducing the cement consumption and providing the required concrete strength after the heat-steaming treatment at 40 °C have been defined.

3. According to the results of studies of eight Portland cements it turned out that to ensure the high water-reducing effect of polycarboxylate-based superplasticizers and to eliminate the rapid loss of workability of fresh concrete, the recommended content of the C_3A, SO_3, Na_2O_{equiv} in Portland cements should be within 4.0–7.0 %; 2.57–2.82 %; 0.52–0.79 % respectively.

4. It was stated that the required strength of concrete of class B40 (34.9 MPa) after the heat-steaming treatment duration of 12 hours at isothermal temperature of 40 °C, can be obtained on Portland cements with the content of grains of size less than 3 μm within 17–21 %.

5. The use of admixtures in quantity: Sika Viscocrete 20 Gold of 0.38 %, Glenium ACE 430 – 0.4 % made it possible to reduce Portland cement consumption by 15 % and the isothermal temperature of heat-steaming treatment from 80 °C to 40 °C with providing the required concrete strength after the heat-steaming treatment.

References

1. Serenko A.F., Petrova T.M. *Besproparochnaya tekhnologiya proizvodstva podrelsovykh konstruktsiy* [No-steaming technology of under-railway sleepers]. M.: FGBOU Uchebno-metodicheskiy tsentr po obrazovaniyu na zheleznodorozhnom transporte, 2012. 136 p. (rus)
2. Bazhenov Yu.M., Kalashnikov V.I., Demyanova V.S.

Литература

1. Серенко А.Ф., Петрова Т.М. Беспропарочная технология производства подрельсовых конструкций. М.: ФГБОУ Учебно-методический центр по образованию на железнодорожном транспорте, 2012. 136 с.
2. Баженов Ю.М., Калашников В.И., Демьянова В.С.

Smirnova O.M. Compatibility of portland cement and polycarboxylate-based superplasticizers in high-strength concrete for precast constructions. *Magazine of Civil Engineering*. 2016. No. 6. Pp. 12–22. doi: 10.5862/MCE.66.2

Vysokokachestvennyy beton [High-performance concrete]. M.:Izd-vo ASV, 2007. 555 p. (rus)
3. Petrova T.M., Smirnova O.M., Stasiuk I.A., Dzhashi N.A. Influence of Portland cement properties on the early strength of concrete with polycarboxylate-based superplasticizers. *Proceedings of 18. Internationale Baustofftagung.* IBAUSIL. Weimar, 2012. Pp. 660–667.
4. Calvo G.J.L. Performance of concrete in precast products due to heat curing. *Proceedings of XIII International Congress on the chemistry of cement*. Madrid, 2011. 183 p.
5. Ozbay E., Gesoglu M., Guneyisi E. Transport properties based multi-objective mix proportioning optimization of high performance concretes. *Materials and Structures*. 2011. Vol. 44. No. 1. Pp. 139–154.
6. Huang H., Qian C., Zhao F., Qu J., Guo J., Danzinger M. Improvement on microstructure of concrete by polycarboxylate superplasticizer (PCE) and its influence on durability of concrete. *Construction and Building Materials.* 2016. Vol. 110. Pp. 293–299.
7. Nkinamubanzi P.-C., Mantellato S., Flatt R.J. 16 – Superplasticizers in practice. *Science and Technology of Concrete Admixtures.* 2016. Pp. 353–377.
8. Gelardi G., Flatt R.J. 11 – Working mechanisms of water reducers and superplasticizers. *Science and Technology of Concrete Admixtures.* 2016. Pp. 257–278.
9. Xu L. Study on the relationship of narrow particle size fractions and properties of cement. *Proceedings of XIII International Congress on the chemistry of cement.* Madrid, 2011. 17 p.
10. Asghari A.A., Hernandez A.M.L., Feys D., De Schutter G. Which parameters, other than the water content, influence the robustness of cement paste with SCC consistency? *Construction and Building Materials.* 2016. Vol. 124. Pp. 95–103.
11. Burgos-Montes O., Palacios M., Rivilla P., Puertas F. Compatibility between superplasticizer admixtures and cements with mineral additions. *Construction and Building Materials.* 2012. Vol. 31. Pp. 300–309.
12. Smirnova O.M. *Vysokokachestvennyye betony dlya predvaritelno napryazhennykh zhelezobetonnykh konstruktsiy* [High performance concrete for precast prestressed concrete constructions]. Sankt-Peterburg: Izd-vo RGPU im.A.I.Gertsena, 2014. 67 p. (rus)
13. Petrova T.M., Smirnova O.M., Shabiev R.O. Some properties of plasticized compositions of Portland cement-granulated blast furnace slag. *Proceedings of XIII International Congress on the chemistry of cement*. Madrid, 2011. 135 p.
14. Alonso M.M., Palacios M., Puertas F. Compatibility between polycarboxylate-based admixtures and blended-cement pastes. *Cement and Concrete Composites.* 2013. Vol. 35. No. 1. Pp. 151–162.
15. Smirnova O.M. Ispolzovaniye mineralnogo mikronapolnitelya dlya povysheniya aktivnosti portlandtsementa [Use of mineral fillers to increase the Portland cement activity]. *Stroitelnyye materialy*. 2015. No. 3. Pp. 30–33. (rus)
16. Cheung J., Jeknavorian A., Roberts L., Silva D. Impact of admixtures on the hydration kinetics of Portland cement. *Cement and Concrete Research*. 2011. Vol. 41. No. 12. Pp. 1289–1309.
17. Janowska-Renkas E. The influence of the chemical structure of polycarboxylic superplasticizers on their effectiveness in cement pastes. *Procedia Engineering.* 2015. Vol. 108. Pp. 575–583.
18. Plank J., Hirsch C. Impact of zeta potential of early cement hydration phases on superplasticizer adsorption. *Cement and Concrete Research.* 2007. No. 37. Pp. 537–542.
19. Yu B., Zeng Z., Ren Q., Chen Y., Liang M., Zou H. Study on the performance of polycarboxylate-based superplasticizers synthesized by reversible addition–fragmentation chain transfer (RAFT) polymerization. *Journal of Molecular Structure*. 2016. Vol. 1120. Pp. 171–179.

Высококачественный бетон. М.: Изд-во АСВ, 2007. 555 с.
3. Petrova T.M., Smirnova O.M., Stasiuk I.A., Dzhashi N.A. Influence of Portland cement properties on the early strength of concrete with polycarboxylate-based superplasticizers // Proceedings of 18. Internationale Baustofftagung. Weimar: IBAUSIL, 2012. Pp. 660–667.
4. Calvo G.J.L. Performance of concrete in precast products due to heat curing // Proceedings of XIII International Congress on the chemistry of cement. Madrid, 2011. 183 p.
5. Ozbay E., Gesoglu M., Guneyisi E. Transport properties based multi-objective mix proportioning optimization of high performance concretes // Materials and Structures. 2011. Vol. 44. № 1. Pp. 139–154.
6. Huang H., Qian C., Zhao F., Qu J., Guo J., Danzinger M. Improvement on microstructure of concrete by polycarboxylate superplasticizer (PCE) and its influence on durability of concrete // Construction and Building Materials. 2016. Vol. 110. Pp. 293–299.
7. Nkinamubanzi P.-C., Mantellato S., Flatt R.J. 16 – Superplasticizers in practice // Science and Technology of Concrete Admixtures. 2016. Pp. 353–377.
8. Gelardi G., Flatt R.J. 11 – Working mechanisms of water reducers and superplasticizers // Science and Technology of Concrete Admixtures. 2016. Pp. 257–278
9. Xu L. Study on the relationship of narrow particle size fractions and properties of cement // Proceedings of XIII International Congress on the chemistry of cement. Madrid, 2011. 17 p.
10. Asghari A.A., Hernandez A.M.L., Feys D., De Schutter G. Which parameters, other than the water content, influence the robustness of cement paste with SCC consistency? // Construction and Building Materials. 2016. Vol. 124. Pp. 95–103.
11. Burgos-Montes O., Palacios M., Rivilla P., Puertas F. Compatibility between superplasticizer admixtures and cements with mineral additions // Construction and Building Materials. 2012. Vol. 31. Pp. 300–309.
12. Смирнова О.М. Высококачественные бетоны для предварительно напряженных железобетонных конструкций // СПб: Изд-во РГПУ им.А.И.Герцена. Санкт-Петербург, 2014. 67 с.
13. Petrova T.M., Smirnova O.M., Shabiev R.O. Some properties of plasticized compositions of Portland cement-granulated blast furnace slag // Proceedings of XIII International Congress on the chemistry of cement. Madrid, 2011. 135 p.
14. Alonso M.M., Palacios M., Puertas F. Compatibility between polycarboxylate-based admixtures and blended-cement pastes // Cement and Concrete Composites. 2013. Vol. 35. № 1. Pp. 151–162.
15. Смирнова О.М. Использование минерального микронаполнителя для повышения активности портландцемента // Строительные материалы. 2015. № 3. С. 30–33.
16. Cheung J., Jeknavorian A., Roberts L., Silva D. Impact of admixtures on the hydration kinetics of Portland cement // Cement and Concrete Research. 2011. Vol. 41. № 12. Pp. 1289–1309.
17. Janowska-Renkas E. The influence of the chemical structure of polycarboxylic superplasticizers on their effectiveness in cement pastes // Procedia Engineering. 2015. Vol. 108. Pp. 575–583.
18. Plank J., Hirsch C. Impact of zeta potential of early cement hydration phases on superplasticizer adsorption // Cement and Concrete Research. 2007. № 37. Pp. 537–542.
19. Yu B., Zeng Z., Ren Q., Chen Y., Liang M., Zou H. Study on the performance of polycarboxylate-based superplasticizers synthesized by reversible addition–

Смирнова О.М. Совместимость портландцемента и суперпластификаторов на поликарбоксилатной основе для получения высокопрочного бетона сборных конструкций // Инженерно-строительный журнал. 2016. № 6(66). С. 12–22.

20. Moratti F., Magarotto R., Mantellato S. Influence of polycarboxylate side chains length on cement hydration and strengths development. *Proceedings of XIII International Congress on the chemistry of cement*. Madrid, 2011. 248 p.
21. Gelardi G., Mantellato S., Marchon D., Palacios M., Eberhardt A.B., Flatt R.J. 9 – Chemistry of chemical admixtures. *Science and Technology of Concrete Admixtures.* 2016. Pp. 149–218.
22. Zeminian N., Magarotto R., Tucci I. Effect of the molecular weight of PCE-based superplasticizers on their interaction with different cements. *Proceedings of XIII International Congress on the chemistry of cement.* Madrid, 2011. 373 p.
23. Kong F.-R., Pan L.-S., Wang C.-M., Zhang D.-L., Xu N. Effects of polycarboxylate superplasticizers with different molecular structure on the hydration behavior of cement paste. *Construction and Building Materials.* 2016. Vol. 105. Pp. 545–553.
24. Rebinder P.A., Cemenenko N.A. O metode pogruzheniya konusa dlya kharakteristiki strukturno-mekhanicheskikh svoystv plastichno-vyazkikh tel [The method of dipping the cone to characterize structural and mechanical properties of the plastic-viscous bodies]. *Doklady Akademii Nauk SSSR* [Proceedings of the USSR Academy of Science]. 1949. Vol. LXIV, No. 6. Pp. 835–838. (rus)
25. Riad M.Y., Shoukry S., Sosa E., William G. Prediction of concrete initial setting time in field conditions through multivariate regression analysis. *Materials and Structures.* 2011. No. 6(44). Pp. 1063–1077.
26. Hassan S., Perrot A., Amziane S. A new look at the measurement of cementitious paste setting by Vicat test. *Cement Concrete Res.* 2010. No. 5(40). Pp. 681–686.
27. Smirnova O.M. Trebovaniya k granulometricheskomu sostavu portlandtsementov dlya proizvodstva sbornogo zhelezobetona po maloprogrevnoy tekhnologii [Requirements for particle size distribution of Portland cement for the manufacture of precast concrete with no-steaming technology]. *Cement and its applications.* 2012. No. 2. Pp. 205–207. (rus)
28. Verbek G. *Perevody IV mezhdunarodnogo kongressa po khimii tsementa* [Translations of the IV International Congress of cement chemistry]. Moscow: Stroyizdat, 1964. Pp. 335–343. (rus)
29. Taylor H.F.W. Cement chemistry. 2nd edn. Thomas Telford. London, 1997. 476 p.
30. Alizadeh R., Beaudoin J.J., Raki L. Mechanical properties of calcium silicate hydrates. *Materials and Structures*. 2011. No. 1(44). Pp. 13–28.
31. Constantinides G., Ulm F.-J. The effect of two types of C–S–H on the elasticity of cement-based materials: results from nanoindentation and micromechanical modeling. *Cem Concr Res.* 2004. No. 1(34). Pp. 67–80.

fragmentation chain transfer (RAFT) polymerization // Journal of Molecular Structure. 2016. Vol. 1120. Pp. 171–179.

20. Moratti F., Magarotto R., Mantellato S. Influence of polycarboxylate side chains length on cement hydration and strengths development // Proceedings of XIII International Congress on the chemistry of cement. Madrid, 2011. 248 p.
21. Gelardi G., Mantellato S., Marchon D., Palacios M., Eberhardt A.B., Flatt R.J. 9 – Chemistry of chemical admixtures // Science and Technology of Concrete Admixtures. 2016. Pp. 149–218.
22. Zeminian N., Magarotto R., Tucci I. Effect of the molecular weight of PCE-based superplasticizers on their interaction with different cements // Proceedings of XIII International Congress on the chemistry of cement. Madrid, 2011. 373 p.
23. Kong F.-R., Pan L.-S., Wang C.-M., Zhang D.-L., Xu N. Effects of polycarboxylate superplasticizers with different molecular structure on the hydration behavior of cement paste // Construction and Building Materials. 2016. Vol. 105. Pp. 545–553.
24. Ребиндер, П.А., Семененко, Н.А. О методе погружения конуса для характеристики структурно-механических свойств пластично-вязких тел // Доклады Академии Наук СССР. 1949. Т. LXIV, № 6, С. 835–838.
25. Riad M.Y., Shoukry S., Sosa E., William G. Prediction of concrete initial setting time in field conditions through multivariate regression analysis // Materials and Structures. 2011. № 6(44). Pp. 1063–1077.
26. Hassan S., Perrot A., Amziane S. A new look at the measurement of cementitious paste setting by Vicat test // Cement Concrete Res. 2010. № 5(40). Pp. 681–686.
27. Смирнова О.М. Требования к гранулометрическому составу портландцементов для производства сборного железобетона по малопрогревной технологии // Цемент и его применение. 2012. № 2. С. 205–207.
28. Вербек, Г. Переводы IV международного конгресса по химии цемента. М.: Стройиздат, 1964. С. 335–343.
29. Taylor H.F.W. Cement chemistry. 2nd edn. Thomas Telford. London, 1997. 476 p.
30. Alizadeh R., Beaudoin J.J., Raki L. Mechanical properties of calcium silicate hydrates // Materials and Structures. 2011. № 1(44). Pp. 13–28.
31. Constantinides G., Ulm F.-J. The effect of two types of C–S–H on the elasticity of cement-based materials: results from nanoindentation and micromechanical modeling // Cem Concr Res. 2004. № 1(34). Pp. 67–80.

Olga Smirnova,
+7(905)2826022; smirnovaolgam@rambler.ru

Ольга Михайловна Смирнова,
+7(905)2826022;
эл. почта: smirnovaolgam@rambler.ru

© Smirnova O.M., 2016

Smirnova O.M. Compatibility of portland cement and polycarboxylate-based superplasticizers in high-strength concrete for precast constructions. *Magazine of Civil Engineering*. 2016. No. 6. Pp. 12–22. doi: 10.5862/MCE.66.2

doi: 10.5862/MCE.66.3

Load-bearing capacity of soil loaded with strip-shell foundations

Несущая способность основания, нагруженного ленточно-оболочечными фундаментами

J.V. Naumkina,
Y.A. Pronozin,
L.R. Epifantseva,
Industrial University of Tyumen, Tyumen, Russia

Канд. техн. наук, доцент Ю.В. Наумкина,
канд. техн. наук, доцент Я.А. Пронозин,
канд. техн. наук, доцент Л.Р. Епифанцева,
Тюменский индустриальный университет, г. Тюмень, Россия

Key words: load-bearing capacity; strip foundations; compressible soils; shell

Ключевые слова: несущая способность; ленточные фундаменты; сжимаемые основания; оболочка

Abstract. The paper describes the special features of the calculation based on the load-bearing capacity of soil loaded with strip-shell foundations which offer high efficiency in construction of medium and high-rise buildings on strongly compressible soils. The necessity of this calculation is caused by the requirements of Building Regulations. Problem solution of load-bearing capacity of subsoil with a bent cylindric surface based on the known Prandtl Solution was considered. The new static solution to the Coulomb's wedge theory of load-bearing capacity of soil loaded with strip-shell foundations (SSF) indicating that taking into account a bent surface of the soil under the shell and the counterweight from strip foundations make it possible to reasonably increase the load-bearing capacity of soil.

Аннотация. В статье рассмотрены особенности расчета по несущей способности основания, нагруженного ленточно-оболочечными фундаментами, которые обладают высокой эффективностью при строительстве зданий средней и повышенной этажности на сильносжимаемых грунтовых основаниях. Необходимость разработки данного расчета обусловлена требованиями действующих норм. Рассмотрено решение задачи о несущей способности грунтового основания фундамента с криволинейной цилиндрической поверхностью на основе известного решения Прандтля. Получено новое статическое решение теории предельного равновесия грунтов для задачи о несущей способности грунтового основания ленточно-оболочечного фундаментама, показывающее, что учет криволинейной поверхности основания под оболочкой, с учетом пригруза от ленточных фундаментов, позволяют обоснованно увеличивать несущую способность основания.

Introduction

Strip-shell foundations (SSF) are widely used in construction of medium and high-rise buildings on strongly compressible soils; these are shallow foundations composed of cross sectional strip foundations joined by gently sloping shells formed on natural or artificial soils. These foundations are applicable due to their efficiency and lower calculations compared to traditional slab foundations. Earlier the authors described the analysis techniques for interaction of SSF and soil using the Winkler model [1]. The paper aims at setting forth the results on the soil-bed load-bearing capacity loaded across the curvilinear convex upwards surface and comparing them with load-bearing capacity of subsoil loaded with a flat footing – this is the main "core" solution presented in the Building Regulation 22.13330.2011 [2]. It is necessary to underline that as a special case, SSF composed of one shell may be used as a foundation for a single-aisle building.

Yet, it is necessary to complete the given techniques with analysis of the load-bearing capacity of soil loaded with SSF. This is due to the fact that the Building Regulation 22.13330.2011 [2] for soil analysis on both groups of ultimate limit states gives solutions for a single strip foundation. In case of other schematic views new solutions to the Coulomb's wedge theory (CWT) – the main theoretical basis for analysis of the load-bearing capacity should be found. For instance, many authors [3, 4, 5] including

the foreign ones [6, 7, 8] formulated the problem on the load-bearing capacity of soil for foundations placed closely to each other taking into account their mutual influence on ultimate pressure magnitude.

In addition, in accordance with the Building Regulation 22.13330.2011 [2] the analysis based on the load-bearing capacity is required for strongly compressible soils, e.g. the soils composed of slowly compacting water-saturated clays and therefore, the new solution of CWT is a necessary requirement of the Building Regulations [9, 10].

This solution gives a certain ultimate pressure magnitude allowing the settlements to be analyzed using the finite element analysis (FEA) not only in the stage of linearly deformable soil, but also beyond it using the nonlinear soil models [11, 12]. Numerical solutions to this class of problems using FEA are given in [13, 14, 15].

There is also a considerable amount of foreign works dealing with the problems of the soil load-bearing capacity in terms of the static method of CWT [16, 17]. The papers of C.M. Martin and E.C.J. Hazell [18, 19] where the classical solutions of CWT obtained earlier are adapted to water-saturated soils should be highlighted.

Methods

Earlier the authors [20] considered the problem solution of the soil bed load-bearing capacity with a bent cylindric surface. Let us reproduce the basic calculation of the solution in terms of the strict static method of CWT:

$$\frac{\partial \sigma_x}{\partial x}+\frac{\partial \tau_{xz}}{\partial z}=0,\ \frac{\partial \tau_{xz}}{\partial x}+\frac{\partial \sigma_z}{\partial z}=\gamma;$$

$$\sqrt{(\sigma_x-\sigma_z)^2+4\tau_{xz}^2}=(\sigma_x+\sigma_z+2c\cdot\mathrm{ctg}\varphi)\sin\varphi, \quad (1)$$

where γ, φ and c – specific gravity, internal friction angle and specific cohesion.

The system of equations (1) was transformed to an accepted form – the equations drawn up by the characteristic lines being in agreement with the slide curves (Figure 1):

$$dx=dz\cdot\mathrm{tg}(\alpha\pm\mu),$$

$$d\sigma\pm 2\sigma\mathrm{tg}\varphi\cdot d\alpha=\gamma(dz\mp dx\cdot tg\varphi), \quad (2)$$

where $\sigma=\frac{\sigma_x+\sigma_z}{2}+c\cdot\mathrm{ctg}\varphi$ – average reduced stress; α – angle between the direction of the first main stress σ_1 and axis Oz; $\mu=\pi/4-\varphi/2$ – angle between the direction σ_1 and slide curves.

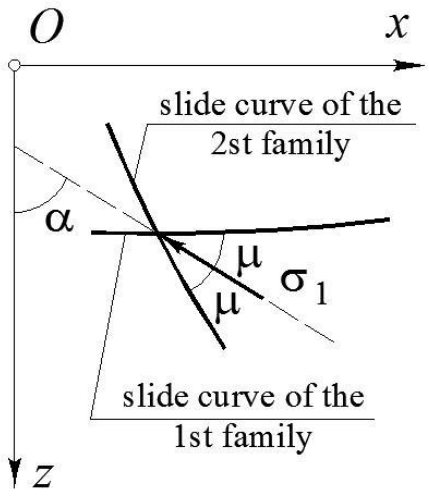

Figure 1. Relative orientation of the slide curves and direction σ_1

The solution for the specific schematic views was obtained by numerical integration of the accepted equations (2) by the method of finite differences using certain boundary value problems according to the algorithm given, e.g., in [21]. Components of the ultimate limit stresses were evaluated by the formulas:

$$\left.\begin{matrix}\sigma_x\\ \sigma_z\end{matrix}\right\} = \sigma(1 \mp \sin\varphi\cos 2\alpha) - c\cdot\operatorname{ctg}\varphi\,,\ \tau_{xz} = \sigma\sin\varphi\sin 2\alpha \qquad (3)$$

The schematic view of the given problem is shown in Figure 2.

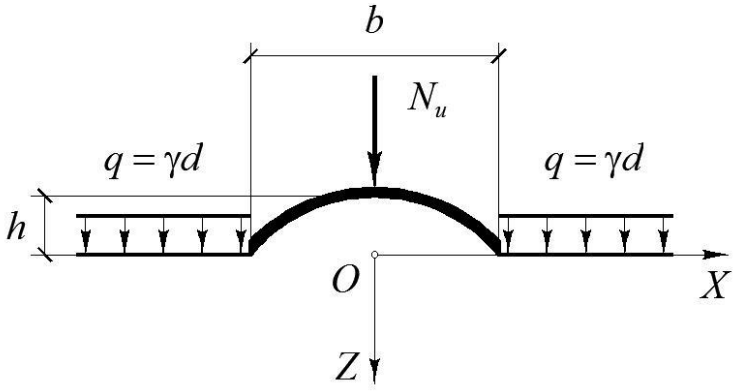

Figure 2. Schematic view (*d* – foundation depth)

The shell is of width *b* and height *h*. The equation of the bed is accepted as:

$$z = ax^2 - h\,,$$

where *a* – geometric parameter, 4*h*/*b* – for the given diagram.

Taking the contact pressure equal to the value of natural pressure at the level of the foundation depth is some simplification which on the one hand takes into account the counterweight from strip foundations though ill-defined, on the other hand makes it possible to reveal the significance of the principal factors affecting the bearing capacity of soil bed loaded across the bent surface against the "basic" solution given in the Building Regulation under identical operating conditions.

Let us solve the problem using the strict static method of the Coulomb's wedge theory. The basic equations for the static method and the necessary explanations are given above. The order of boundary value problems is shown in Figure 3.

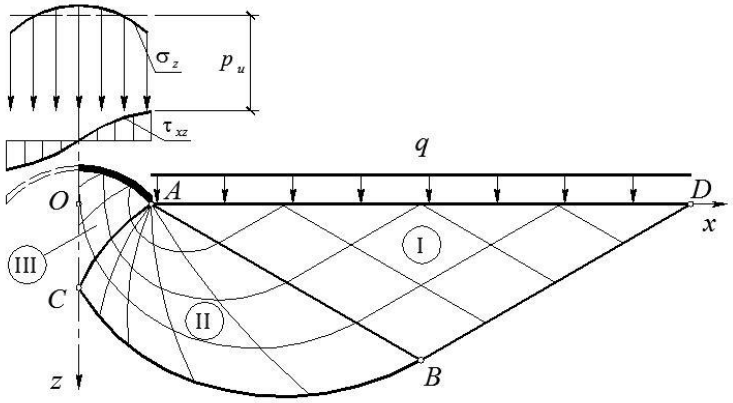

Figure 3. Grouping of boundary value problems (right half of the symmetrical schematic view)

In general, the solution agrees with the known Prandtl Solution [22, 23]. So let us describe the main details of the solution in short and the new features of it.

The ABD area is evaluated by the known integrals of the accepted equations of the static method (I boundary value problem):

$$\sigma = \frac{q + \gamma z + c \cdot \mathrm{ctg}\,\varphi}{1 - \sin\varphi},\ \alpha = \frac{\pi}{2}.$$

Let us remind that $\sigma = \frac{\sigma_x + \sigma_z}{2} + c \cdot \mathrm{ctg}\,\varphi$ – average reduced stress, α – angle between the direction σ_1 and axis *Oz*.

In the *ABC* radial sheaf one can solve the II boundary value problem with the known parameters of the accepted system of equations *x*, *z*, σ, α with *AB* characteristic line and conditions at the singular point *A*:

$$\sigma = \frac{q + c \cdot \mathrm{ctg}\,\varphi}{1 - \sin\varphi} e^{(\pi - 2\alpha)\mathrm{tg}\,\varphi}, \qquad \frac{\pi}{2} \geq \alpha \geq \alpha_F.$$

The boundary condition α_F and the length of the *AD* segment are sorted out on the assumption of meeting the conditions of symmetry at point *C*:

$$\alpha = 0, \quad x = 0,$$

i.e. the first main stress must be vertically oriented.

Here the value can't be lower than

$$\alpha_{F,\min} = -\frac{\pi}{2} + \mu - \mathrm{arctg}\left(\frac{dz}{dx}\right)_{x=b/2}.$$

The value $\alpha_{F,\min}$ means that the leftmost characteristic line (from the side of the foundation) can appear at the singular point *A* at a tangent to the bent surface (here $dz/dx = 2ax = 4h/b$) or appear "inside" the surface, i.e. below the level of the bed.

When the *ABC* area is completed, two ways to analyze the ultimate load can be chosen. Firstly, knowing all the parameters of the accepted system of equations on the *AC* characteristic line, the area limited by the *AC* line below and the shell at the top can be seen; taking the balance of the area, the vertical component of the ultimate press force can be analyzed. The soil located in this area may be both in the compressed state from a theoretical point of view (the so-called rigid core) and in the ultimate state. Secondly, it is possible to build up the *ACC* area on the *AC* characteristic line and the axis of symmetry *Oz* by solving the III boundary value problem (Figure 4). In this case, the soil under the shell formally "becomes" ultimately stressed, but this fact doesn't affect the value of the load-bearing capacity.

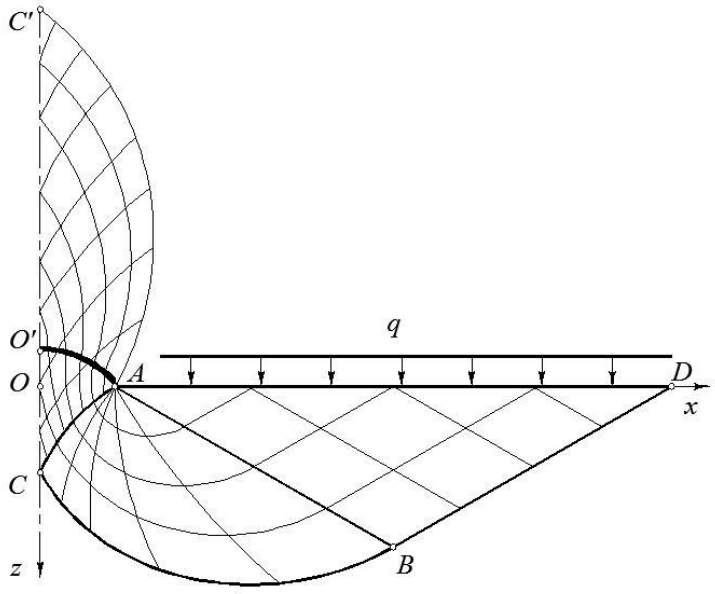

Figure 4. On building up the solution in the soil under the foundation bed

Naumkina J.V., Pronozin Y.A., Epifantseva L.R. Load-bearing capacity of soil loaded with strip-shell foundations. *Magazine of Civil Engineering*. 2016. No. 6. Pp. 23–34. doi: 10.5862/MCE.66.3

Soil conditions in the core under the foundation bed – conditionally “elastic” or ultimate – have been traditionally a matter of debate. When considering the strip-shell foundations there are more arguments for the "elastic" state. However, in this case it is much more difficult to obtain pressure diagram along the bed. In fact, this approach – ultimate limit state in the prism of a bulging area, radial sheaf and “elastic” state in the core under the foundation – was implemented by M.I. Gorbunov-Posadov. Due to considerable technical difficulties, this approach hasn’t widespread use, although in view of the availability of software systems that implement FEA, it seems possible to be implemented. The formal parameter of “elasticity” in the core can lead to the zones of destruction occurring in the stresses analyzed by the linear-deformable model, and hence it will lead to a new complication of the problem and new issues on compliance with the experimental data.

On the other part, ultimate limit stresses under the stamp make it possible to determine stress distribution diagrams along the bed; according to the numerous comparisons they agree with the experiments as to quality and quantity. Therefore, taking into account the conditionality of the ultimate limit state under the shell, let us integrate the accepted equations. Let us emphasize once again that the final result – the resultant ultimate limit pressure – is not affected, but allows determining the stresses along the bed.

Solution of the III boundary value problem, as discussed, will give the *ACC′* area which falls outside the limits of the soil surface (Figure 4). Let us do the following. The *AO′* line coinciding with the curvilinear foundation bed cuts off the “excess” part of *AO′C′*. The whole of the parameters of the accepted equations – *x*, *z*, σ, α are determined on this line, totally included in the *ACC ′* area. Thus, the contact vertical and horizontal stresses acting on the curvilinear shell can be analyzed using the known formulas:

$$\sigma_z = \sigma(1+\sin\varphi\cos 2\alpha) - c\cdot\operatorname{ctg}\varphi,\ \tau_{xz} = \sigma\sin\varphi\sin 2\alpha$$

This is the final problem solution.

Results

The results may be analyzed in relative variables: *b* – width unit, γb – stress unit. For added convenience, let us use the relative reduced stresses in the arguments. Thus, the relative counterweight and average ultimate limit pressure along the bed are as follows:

$$q' = \frac{q + c\cdot\operatorname{ctg}\varphi}{\gamma b},\ p'_u = \frac{p_u + c\cdot\operatorname{ctg}\varphi}{\gamma b}$$

Figures 5 and 6 illustrate examples of the slide curves mesh (characteristic lines), vertical and horizontal stress distribution diagrams along the bed and the lateral counterweight. An interesting feature is needed to be pointed out: if the shell height increases, the diagram of vertical stresses (convex for a flat stamp) progressively flattens and in certain values it can even take a convex shape with low curvature.

Tables 1–4 show the values of the relative reduced forces N_u' ultimate limit pressure for internal friction angles $\varphi = 10°, 20°, 30°, 40°$, reduced values of lateral counterweights $q' = 1, 2, 3, 5$ and 10 and relative shell heights $\bar{h} = 0, \ldots, 5$ with spacing of 0.05. The main conclusion is obvious – the ultimate load significantly increases if the shell height $\bar{h}$ increases.

Attention is drawn to some reduction in N_u' values in low-level heights $\bar{h}$ and small values of the lateral counterweight q'. It is easily understandable, since in the absence of the counterweight the convex surface, of course, will carry loading less than the horizontal one until considerable horizontal forces perform, which, are formed due to the curvilinear surface of loading and in turn, further compress the soil; this is manifested in some values of $\bar{h}$.

It should be noted that stiffness of the shell itself and primarily tensile stiffness EA affects redistribution of the load transmitted to the soil bed through shells and strips and distribution of contact “reactive” pressures directly under the shell. Influence of the contact pressure distribution law under the bent surface of the shell can affect the values of horizontal forces and load-bearing capacity of the bed in a certain manner; however, this issue is the subject-matter of further research.

For greater clarity, let us illustrate the dependencies of the relative increase of the ultimate press force by the coefficient:

$$k = \frac{N'_u}{N'_{u,\text{СП}}},$$

where N_u' – relative reduced ultimate press force of SSF on soil, $N'_{u,\text{СП}}$ – relative reduced ultimate press force of a flat strip foundation which can be analyzed after the Building Regulation [2] (in Tables 1–4 the values are given in $\bar{h} = 0$):

$$N'_u = N_\gamma + q'N_q,$$

where N_γ, N_q – coefficients of the load-bearing capacity.

Dependency graphs $k(\bar{h}, q')$ for $\varphi = 10°, 20°, 30°, 40°$ are shown in Figures 7, 8.

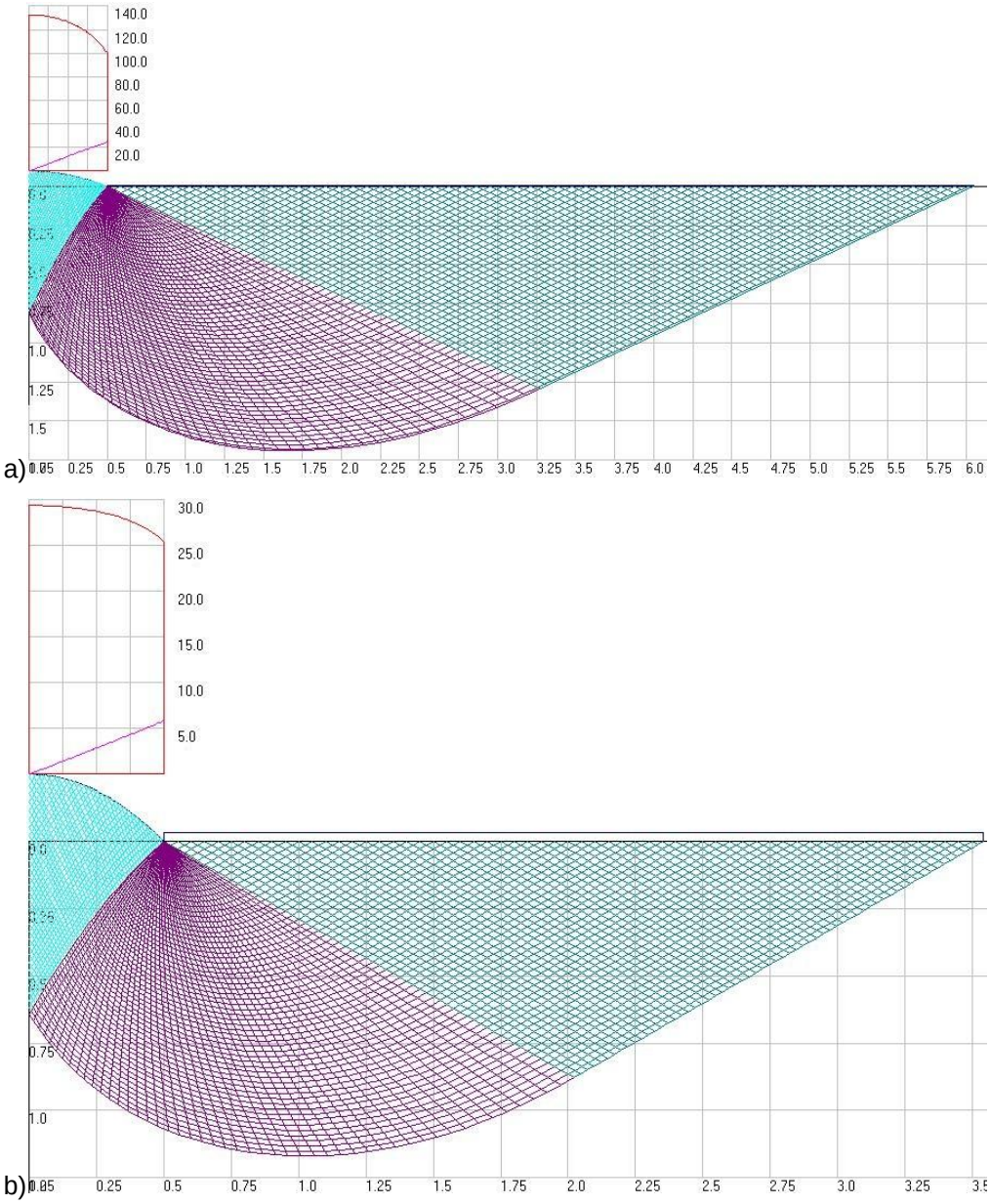

Figure 5. Examples of solution:
$\varphi = 40°$, $q' = 1$, $\bar{h} = 0.1$ (a); $\varphi = 30°$, $q' = 1$, $\bar{h} = 0.25$ (b)

Naumkina J.V., Pronozin Y.A., Epifantseva L.R. Load-bearing capacity of soil loaded with strip-shell foundations. *Magazine of Civil Engineering*. 2016. No. 6. Pp. 23–34. doi: 10.5862/MCE.66.3

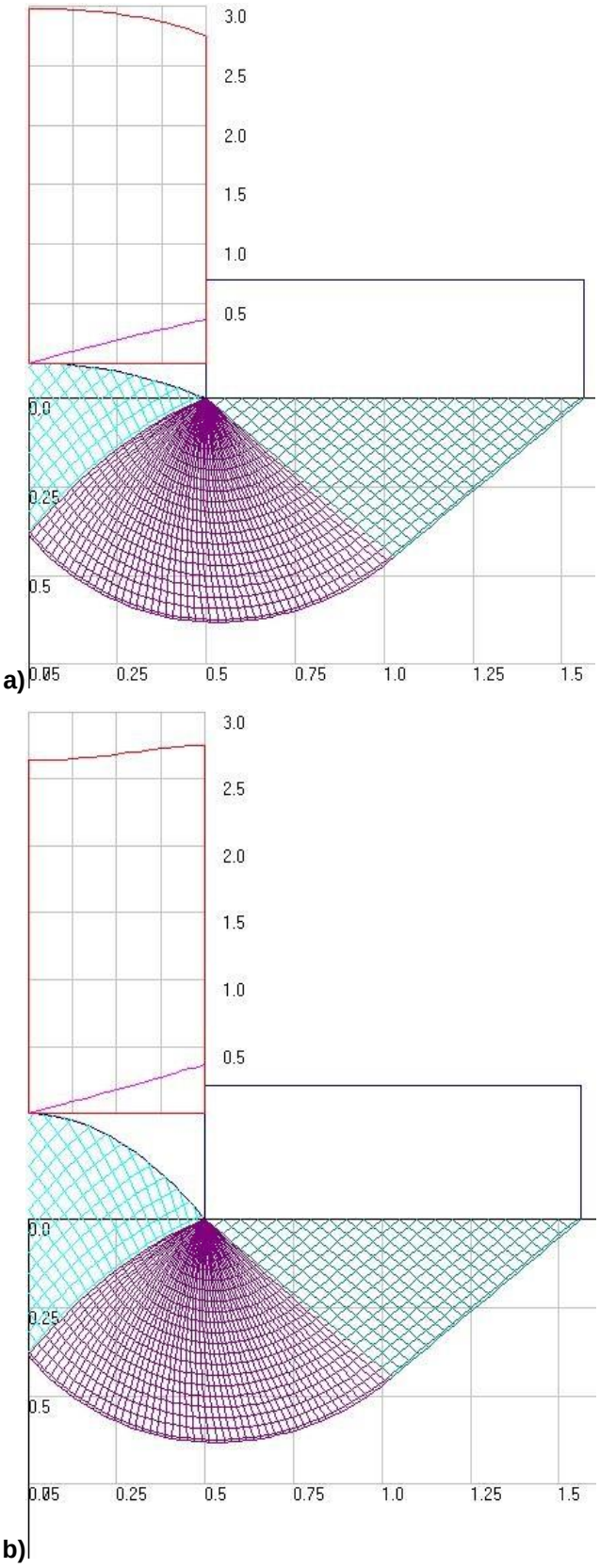

Figure 6. Examples of solution:
$\varphi = 10°$, $q' = 1$, $\bar{h} = 0.1$ (a); $\varphi = 10°$, $q' = 1$, $\bar{h} = 0.3$ (b)

The coefficients *k* do not considerably depend on the internal friction angle, but they significantly depend on the shell height and lateral counterweight.

Table 1. Relative reduced ultimate pressure forces for $\varphi = 10°$

$\bar{h}$	$q' = 1$	$q' = 2$	$q' = 3$	$q' = 5$	$q' = 10$
0	3.034	5.561	8.062	13.030	25.422
0.05	2.993	5.532	8.044	13.044	25.506
0.1	2.990	5.573	8.131	13.226	25.926
0.15	3.019	5.675	8.309	13.555	26.638
0.2	3.075	5.829	8.562	14.011	27.600
0.25	3.152	6.024	8.879	14.571	28.772
0.3	3.244	6.252	9.245	15.216	30.115
0.35	3.349	6.506	9.651	15.928	31.596
0.4	3.463	6.780	10.089	16.695	33.175
0.45	3.582	7.069	10.550	17.500	34.785
0.5	3.706	7.368	11.030	18.310	36.344

Table 2. Relative reduced ultimate pressure forces for $\varphi = 20°$

$\bar{h}$	$q' = 1$	$q' = 2$	$q' = 3$	$q' = 5$	$q' = 10$
0	9.159	15.812	22.329	35.282	67.502
0.05	9.049	15.714	22.271	35.275	67.599
0.1	9.075	15.852	22.527	35.775	68.716
0.15	9.197	16.163	23.033	36.675	70.606
0.2	9.400	16.620	23.750	37.915	73.160
0.25	9.668	17.197	24.641	39.439	76.269
0.3	9.987	17.869	25.672	41.192	79.830
0.35	10.346	18.616	26.814	43.129	83.760
0.4	10.734	19.421	28.044	45.214	87.990
0.45	11.144	20.270	29.342	47.417	92.454
0.5	11.570	21.153	30.693	49.711	97.036

Table 3. Relative reduced ultimate pressure forces for $\varphi = 30°$

$\bar{h}$	$q' = 1$	$q' = 2$	$q' = 3$	$q' = 5$	$q' = 10$
0	30.39	49.79	68.72	106.09	198.65
0.05	30.18	49.65	68.67	106.35	199.61
0.1	30.30	50.09	69.45	107.84	202.87
0.15	30.74	51.08	71.00	110.52	208.41
0.2	31.45	52.53	73.20	114.24	215.91
0.25	32.37	54.35	75.93	118.80	225.04
0.3	33.47	56.48	79.10	124.05	235.51
0.35	34.69	58.84	82.60	129.85	247.06
0.4	36.02	61.38	86.37	136.10	259.48
0.45	37.43	64.06	90.36	142.70	272.63
0.5	38.89	66.86	94.50	149.58	286.35

Table 4. Relative reduced ultimate pressure forces for $\varphi = 40°$

$\bar{h}$	q′ = 1	q′ = 2	q′ = 3	q′ = 5	q′ = 10
0	126.94	196.61	263.95	395.86	720.51
0.05	126.20	196.41	263.55	397.23	724.94
0.1	126.76	198.12	266.45	402.58	736.50
0.15	128.64	201.96	272.26	412.40	756.32
0.2	131.63	207.59	280.54	426.02	783.22
0.25	135.51	214.70	290.85	442.79	816.03
0.3	140.10	222.99	302.78	462.10	853.64
0.35	145.25	232.19	316.01	483.46	895.17
0.4	150.82	242.11	330.26	506.45	939.85
0.45	156.71	252.59	345.30	530.73	987.09
0.5	162.83	263.48	360.96	556.05	1036.41

.

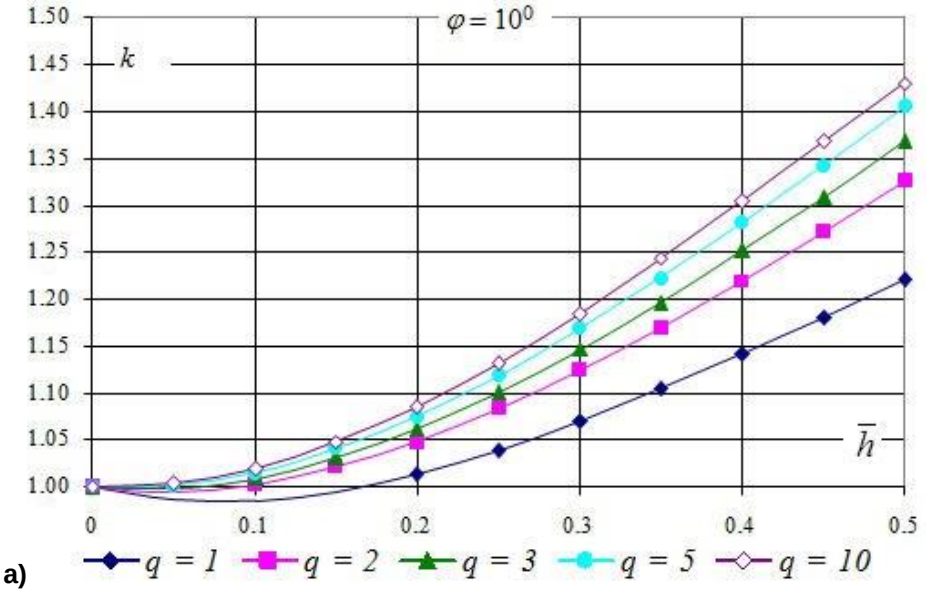

a)

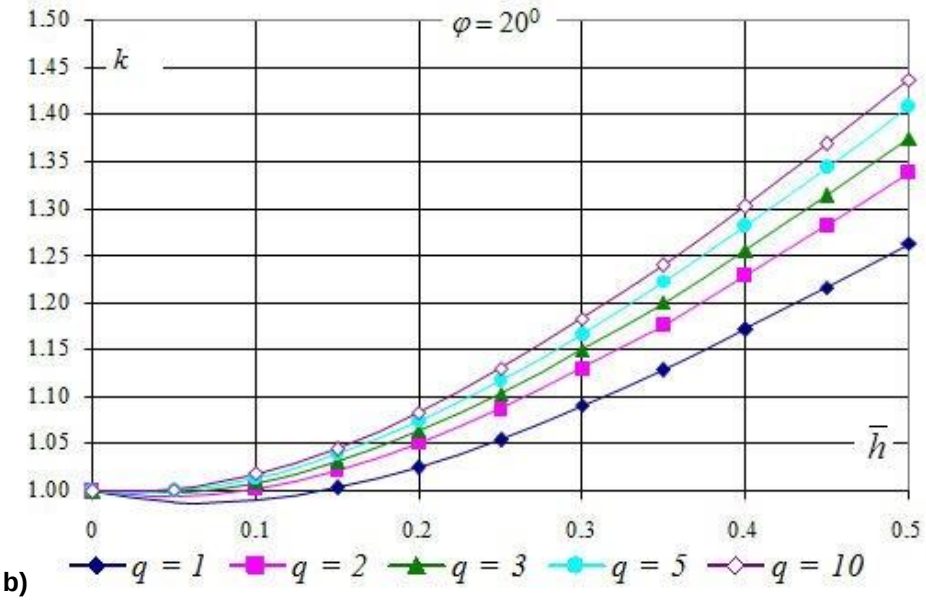

b)

Figure 7. Dependencies of coefficients *k* ($\bar{h}$, *q′*) for $\varphi = 10^0, 20^0$

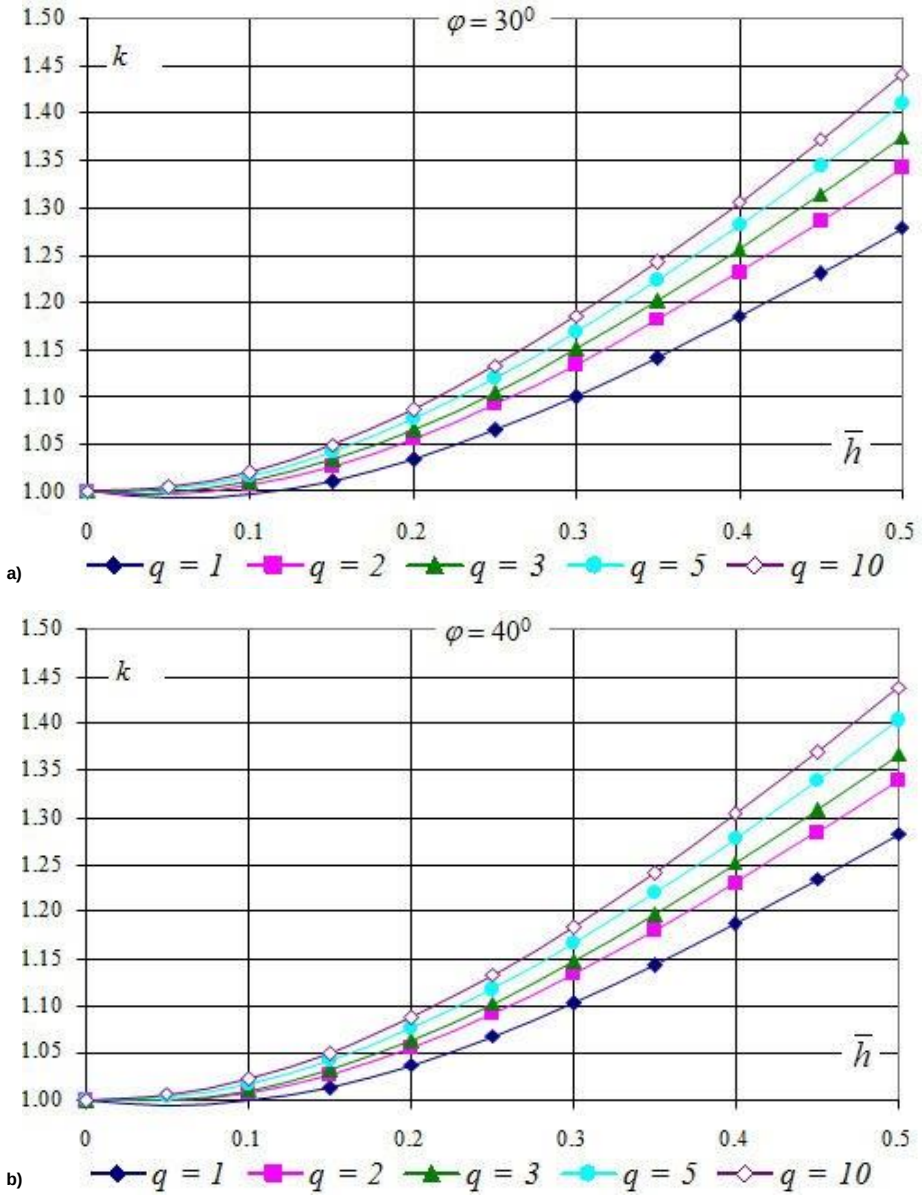

Figure 8. Dependencies of coefficients *k* ($\bar{h}$, *q′*) for *φ* = 30°, 40°

Thus, the ultimate pressure force on SSF may be evaluated by the following formulas:

– by coefficients *k* and values of the load-bearing capacity of flat foundation, *b* in width according to the Building Regulation [2]:

$$N_u = k \cdot b \cdot N_{u,\text{СП}} + (b - s) \cdot c \cdot \operatorname{ctg} \varphi;$$

– by coefficients *k* and values given in tables 1 – 4:

$$N_u = \gamma b^2 N'_u - s \cdot c \cdot \operatorname{ctg} \varphi$$

Here *s* – running meter area of SSF bed.

Conclusions

1. A new static solution to the Coulomb's wedge theory of load-bearing capacity of soil loaded with SSF indicating that taking into account a bent surface of the soil under the shell and the counterweight from strip foundations make it possible to reasonably increase the load-bearing capacity of soil.

2. It is stated that depending on the value of the bent surface height under the shell, within the gentleness criterion, the load-bearing capacity of soil can be increased up to 10 %. It is found out that the

load-bearing capacity of soil increases depending on the height of surface and counterweight pressure – q′.

References

1. Ter-Martirosyan Z.G., Pronozin Y.A., Kiselev N.Y. Shallow strip foundations joined by gently inclining envelopes on highly compressible soils. *Soil Mechanics and Foundation Engineering.* 2014. No. 4(51). Pp. 157–164.
2. *Svod pravil 22.13330.2011. Osnovaniya zdaniy i sooruzheniy. Aktualizirovannaya redaktsiya SNiP 2.02.01-83** [Building Regulation 22.13330.2011. Foundation beds in buildings and structures. Updated edition of building codes and regulations 2.02.01-83*]. Moscow, 2011. 161 p. (rus)
3. Korolev K.V. *Nesushchaya sposobnost osnovaniy v stabilizirovannom i nestabilizirovannom sostoyanii: dis. … dokt. tekhn. nauk* [Load-bearing capacity of stabilized and non-stabilized soils: dissertation….doctor of technical sciences]. Novosibirsk, 2014. 326 p. (rus)
4. Fedorovskii V.G. Limiting pressure on rows of strip plates and the "no-force-through" effect. *Soil Mechanics and Foundation Engineering.* 2006. No. 3(43). Pp. 85–91.
5. Yakimenko I.V., Bogomolov A.N., Bogomolova O.A. To the question of mutual influence of closely situated parallel undeepened ribbon foundations on the cohesive bases. *Proceedings of the Kazakhstan-Korean joint geotechnical seminar "Geotechnical infrastructure in megacities and new capitals".* Astana, 2010. Pp. 122–125.
6. Krabbenhoft S., Damkild L., Krabbenhoft K. Bearing capacity of strip footings in cohesionless soil subject to eccentric and inclined loads. *International Journal of Geomechanics.* 2014. No. 3(14). Article No. 04014003.
7. Islam M., Gnanendran C. Behaviour of two closely spaced strip footings placed on a stiff clay bed under cyclic loading. *Geotechnical Testing Journal.* 2013. No. 2(36). Article No. GTJ20120126
8. Kumar J., Bhoi M. Interference of two closely spaced strip footings on sand using model tests. *Journal of Geotechnical and Geoenvironmental Engineering.* 2009. Vol. 135. No. 4. Pp. 595–604.
9. Korolev K.V. Terminal (maximum) bearing capacity of the saturated bed of a strip foundation. *Soil Mechanics and Foundation Engineering.* 2013. Pp. 1–7.
10. Korolev K.V. Intermediate bearing capacity of saturated bed of strip foundation. *Soil Mechanics and Foundation Engineering.* 2014. No. 1(51). Pp. 1–8.
11. Korolev K.V., Karaulov A.M. Ob opredelenii predelnoy nagruzki v uprugoplasticheskikh raschetakh gruntovykh osnovaniy metodom konechnykh elementov [Determination of ultimate limit loading in elastic-plastic analyses of soil beds by finite element analysis]. *Sbornik trudov "Geotekhnika: aktualnyye teoreticheskiye i prakticheskiye problemy"* [Geotechnical engineering: theoretical and practical issues: Interuniversity themed collected papers]. Saint Petersburg: Saint Petersburg state university of architecture and civil engineering, 2007. Pp. 102–107. (rus)
12. Shashkin K.G., Shashkin V.A. Resheniye zadach predelnogo ravnovesiya s ispolzovaniyem metoda konechnykh elementov [Solution to the problems of coulomb's wedge theory by finite element analysis]. Zhilishchnoye stroitelstvo. 2013. No. 4. Pp. 47–50. (rus)
13. Ghosh P., Kumar S. Interference effect of two nearby strip footings on reinforced sand. *Contemporary Engineering Sciences.* 2009. Vol. 2. No. 12. Pp. 577–592.
14. Ghosh P. FLAC based numerical studies on dynamic interference of two nearby embedded machine foundations. *Geotechnical and Geological Engineering*. 2012. No. 5(30). Pp. 1161–1181.
15. Lee J., Eun J. Estimation of bearing capacity for multiple footings in sand. *Computer and Geotechnics Journal.* 2009. No. 6 (36). Pp. 1000–1008.

Литература

1. Ter-Martirosyan Z.G., Pronozin Y.A., Kiselev N.Y. Shallow strip foundations joined by gently inclining envelopes on highly compressible soils // Soil Mechanics and Foundation Engineering. 2014. № 4(51). Pp. 157–164.
2. Свод правил 22.13330.2011. Основания зданий и сооружений. Актуализированная редакция СНиП 2.02.01-83*. М.: 2011. 161 с.
3. Королев К.В. Несущая способность оснований в стабилизированном и нестабилизированном состоянии: дис. … докт. техн. наук. Новосибирск, 2014. 326 с.
4. Fedorovskii V.G. Limiting pressure on rows of strip plates and the "no-force-through" effect // Soil Mechanics and Foundation Engineering. 2006. № 3(43). Pp. 85–91.
5. Yakimenko I.V., Bogomolov A.N., Bogomolova O.A. To the question of mutual influence of closely situated parallel undeepened ribbon foundations on the cohesive bases // Proceedings of the Kazakhstan-Korean joint geotechnical seminar "Geotechnical infrastructure in megacities and new capitals". Astana, 2010. Pp. 122–125.
6. Krabbenhoft S., Damkild L., Krabbenhoft K. Bearing capacity of strip footings in cohesionless soil subject to eccentric and inclined loads // International Journal of Geomechanics. 2014. № 3(14). № статьи 04014003.
7. Islam M., Gnanendran C. Behaviour of two closely spaced strip footings placed on a stiff clay bed under cyclic loading // Geotechnical Testing Journal. 2013. № 2(36). № статьи GTJ201201268.
8. Kumar J., Bhoi M. Interference of two closely spaced strip footings on sand using model tests // Journal of Geotechnical and Geoenvironmental Engineering. 2009. Vol. 135. № 4. Pp. 595–604.
9. Korolev K.V Terminal (maximum) bearing capacity of the saturated bed of a strip foundation // Soil Mechanics and Foundation Engineering. 2013. Pp. 1–7.
10. Korolev K.V. Intermediate bearing capacity of saturated bed of strip foundation // Soil Mechanics and Foundation Engineering. 2014. № 1(51). Pp. 1–8.
11. Королев К.В., Караулов А.М. Об определении предельной нагрузки в упругопластических расчетах грунтовых оснований методом конечных элементов // Сборник трудов «Геотехника: актуальные теоретические и практические проблемы». СПб.: СПбГАСУ, 2007. С. 102–107.
12. Шашкин К.Г., Шашкин В.А. Решение задач предельного равновесия с использованием метода конечных элементов // Жилищное строительство. 2013. № 4. С. 47–50.
13. Ghosh P., Kumar S. Interference effect of two nearby strip footings on reinforced sand // Contemporary Engineering Sciences. 2009. Vol. 2. № 12. Pp. 577–592.
14. Ghosh P. FLAC based numerical studies on dynamic interference of two nearby embedded machine foundations // Geotechnical and Geological Engineering. 2012. № 5(30). Pp. 1161–1181.
15. Lee J., Eun J. Estimation of bearing capacity for multiple footings in sand // Computer and Geotechnics Journal. 2009. № 6 (36). Pp. 1000–1008.
16. Martin C.M., White D.J. Limit analysis of the undrained bearing capacity of offshore pipelines // Géotechnique. 2012. № 9(62). Pp. 847–863.
17. Martin C.M. Exact bearing capacity calculations using the method of characteristics // Proceedings of 11th International Conference on Computer Methods and Advances in Geomechanics. Turin, 2005. Vol. 4. Pp. 441–450.
18. Hazell E.C.J. Interaction of closely spaced strip footings //

Наумкина Ю.В., Пронозин Я.А., Епифанцева Л.Р. Несущая способность основания, нагруженного ленточно-оболочечными фундаментами // Инженерно-строительный журнал. 2016. № 6(66). С. 23–34.

16. Martin C.M., White D.J. Limit analysis of the undrained bearing capacity of offshore pipelines. *Géotechnique.* 2012. No. 9(62). Pp. 847–863.
17. Martin C.M. Exact bearing capacity calculations using the method of characteristics. *Proceedings of 11th International Conference on Computer Methods and Advances in Geomechanics.* Turin, 2005. Vol. 4. Pp. 441–450.
18. Hazell E.C.J. Interaction of closely spaced strip footings. *Final year project report, Department of Engineering Science*. University of Oxford. Oxford, 2004.
19. Martin C.M. Analysis of bearing capacity. *User guide for ABC: Technical Report OUEL 2261/03.* Department of Engineering Science. University of Oxford. Oxford, 2004.
20. Gerber A.D., Pronozin Ya.A., Yepifantseva L.R. Raschet osnovaniy lentochnykh fundamentov, obyedinennykh obolochkami ili membranami, po nesushchey sposobnosti [Analysis of load-bearing capacity of strip foundation beds combined with shells or membranes]. *Modern Problems of Science and Education].* 2014. No. 3. 78 p. (rus)
21. Korolev K.V. *Issledovaniye nesushchey sposobnosti osnovaniy blizko raspolozhennykh lentochnykh fundamentov melkogo zalozheniya: Avtoref. dis. ... kand. tekhn. nauk* [Investigation of bearing capacity grounds of closely spaced shallow strip foundations: Author. Dis. ... Cand. tehn. sciences]. Tomsk: TGASU, 2003. 25 p. (rus)
22. Korolev K.V. Canonical equations of the statics of a granular medium under the minor influence of the specific weight of the soil and solution of the prandtl problem. *Soil Mechanics and Foundation Engineering.* 2012. No. 5(49). Pp. 163–171.
23. Prandtl L. Über die Harte plastisher Korper. *Gottingen Nachrichten.* 1920. Pp. 340–350.

Final 2016 project report, Department of Engineering Science. Oxford: University of Oxford, 2004.
19. Martin C.M. Analysis of Bearing Capacity. User guide for ABC: Technical Report OUEL 2261/03. Department of Engineering Science. Oxford: University of Oxford, 2004.
20. Гербер А.Д., Пронозин Я.А., Епифанцева Л.Р. Расчет оснований ленточных фундаментов, объединенных оболочками или мембранами, по несущей способности // Современные проблемы науки и образования. 2014. № 3. 78 с.
21. Королев К.В. Исследование несущей способности оснований близко расположенных ленточных фундаментов мелкого заложения: Автореф. дис. ... канд. техн. наук. Томск: ТГАСУ, 2003. 25 с.
22. Korolev K.V. Canonical equations of the statics of a granular medium under the minor influence of the specific weight of the soil and solution of the prandtl problem // Soil Mechanics and Foundation Engineering. 2012. № 5(49). Pp. 163–171.
23. Prandtl L. Über die Harte plastisher Korper // Gottingen Nachrichten. 1920. Pp. 340–350.

Julija Naumkina,
+7(922)2676338; naujul@rambler.ru

Yakov Pronozin,
+7(922)2602083; geofond.tgasu@gmail.com

Larisa Epifantseva,
+7(922)2684509; epifanceva82@gmail.com

Юлия Владимировна Наумкина,
+7(922)2676338; эл. почта: naujul@rambler.ru

Яков Александрович Пронозин,
+7(922)2602083;
эл. почта: geofond.tgasu@gmail.com

Лариса Рафаиловна Епифанцева,
+7(922)2684509;
эл. почта: epifanceva82@gmail.com

© Naumkina J.V., Pronozin Y.A., Epifantseva L.R., 2016

Naumkina J.V., Pronozin Y.A., Epifantseva L.R. Load-bearing capacity of soil loaded with strip-shell foundations. *Magazine of Civil Engineering*. 2016. No. 6. Pp. 23–34. doi: 10.5862/MCE.66.3

doi: 10.5862/MCE.66.4

Distribution capacity of sandy soils reinforced with geosynthetics

Распределяющая способность песчаных грунтов, армированных геосинтетикой

A.S. Aleksandrov,
A.L. Kalinin,
M.V. Tsyguleva
Siberian State Automobile And Highway Academy, Omsk, Russia

Канд. техн. наук, доцент
А.С. Александров,
аспирант А.Л. Калинин,
преподаватель М.В. Цыгулева,
Сибирская государственная автомобильно-дорожная академия, г. Омск, Россия

Key words: stress dispersion angle; load distribution angle; geosynthetics; reinforcement of soil basements; distributing ability; colour strip analysis

Ключевые слова: рассеивания напряжений; угол распределения нагрузки; геосинтетика; армирование грунтовых оснований; распределяющая способность; метод цветных полосок

Abstract. A review of shear strength analysis methods for ground bases reinforced with geosynthetics is given in the article. An angle of stress dispersion has been found to be the parameter of soils and discrete materials which were calculated according to the experimental data. The analysis of mathematical models that connect the angle of stress dispersion with other soil parameters which are ascertained in the laboratory was performed. This analysis shows the absence of direct experimental methods for investigation of distribution capacity. For this reason indirect measurements are used to calculate the angle of stress dispersion. The direct method for measuring distribution capacity has been developed on the basis of a colour strip analysis. There are two variants. The first way deals with photo interpretation, the second one uses full-scale models for direct measurements. Statistical analysis shows that reinforcement of ground bases increases distribution capacity of the soil under the geosynthetics.

Аннотация. В статье выполнен обзор методов расчета грунтовых оснований, армированных геосинтетическими материалами по сопротивлению сдвигу. Установлено, что угол рассеивания напряжений является параметром грунтов и дискретных материалов, определяемым по данным эксперимента. Выполнен анализ математических моделей связывающих угол рассеивания напряжений с другими параметрами грунтов, которые определяются в лаборатории. На основе этого анализа показано, что прямые методы экспериментального исследования распределяющей способности отсутствуют. Поэтому угол рассеивания напряжений вычисляют по данным косвенных измерений. Применением метода цветных полосок разработан прямой метод исследования распределяющей способности. Предложено два способа измерения распределяющей способности грунта. Первый способ состоит в обработке фотоизображений, а второй – заключается в прямых измерениях, выполняемых на натурных моделях. Статистическая обработка результатов эксперимента показало, что армирование грунтовых оснований улучшает распределяющую способность грунта расположенного под геосинтетикой.

Introduction

A model of distribution capacity is based on the idea that load is distributed over the area which increases with depth [1]. Load in a ground elastic plastic half-space is distributed at the certain angle α_σ which is called angle of stress dispersion or angle of load distribution (Fig. 1).

Александров А.С., Калинин А.Л., Цыгулева М.В. Распределяющая способность песчаных грунтов, армированных геосинтетикой // Инженерно-строительный журнал. 2016. № 6(66). С. 35–48.

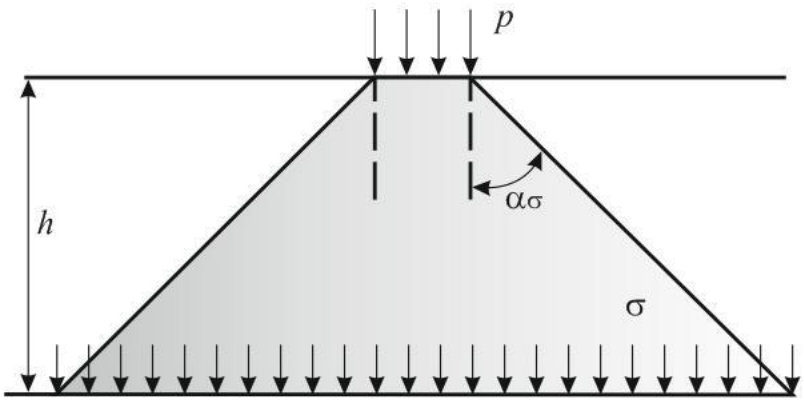

Figure 1. An original model of distribution capacity [1]

As it follows form the analysis of Figure 1, the pressure change with depth is determined by increasing the load distribution area. Consequently, vertical normal stress decreases and is calculated using the formula [1]

$$\sigma_z = p \cdot \left(1 + \frac{2 \cdot Z}{D_0} \cdot \mathrm{tg}\alpha_\sigma\right)^{-2}, \quad (1)$$

where p – pressure on the half-space surface, Pa; Z – depth plotted along the load symmetry axis from the surface to the point where the pressure is calculated, m; D_0 – diameter of a round plate under the load distributed on the half-space surface, m; α_σ – angle of stress dispersion, deg.

Since the directions of principal and coordinate axes coincide in the load symmetry axial section, formula (1) can be used to calculate the maximum principal stress in the ground half-space [2–6]. It is sufficient to substitute the dependent variable σ_z for the maximum principal stress σ_1.

For the calculations of stresses in a finite thickness layer to be done, Odermark's method can be used. It was offered in 1949 but nowadays it is often applied in order to solve a wide variety of road structural analysis problems [3–11]. Thus, a combination of the idea of relationship (1) with Odermark's method makes it possible to design road structures.

As for some foreign countries, a model of distribution capacity is used to compute the limiting pressures upon the ground base. While developing methods of limiting pressure calculation using the model of distribution capacity, dyadic and trinomial relationships are deduced. They are similar to the Prandtl-Reisner and Terzaghi formulae that have the parameter connected with an angle of stress dispersion [12]. Creation of geosynthetics and its application for soil reinforcement necessitated the analysis of such structures. For this purpose, methods of limiting pressure determination based on a model of distributing capacity were used [13]. According to such methods, structures with geosynthetics are supposed to have a larger angle of stress dispersion compared with unreinforced structures with the layers of the same material and thickness [14–19]. Besides, the method proposed in [20] allows deriving a formula for calculation of the first critical load applied to the road base of the particulate material or to the subgrade soil using the relationship (1). An important element of all described methods is experimental determination of an angle of stress dispersion.

Indirect methods of determining the angle of stress dispersion are currently known. This characteristic is calculated using some other parameters: angle of repose [1], undrained shear strength [19, 20], etc. B.S. Radovsky reports that Ye. Golovachev believed the angle of stress dispersion α_σ to be equal to the angle of repose $\beta_{от}$ [1]. This assumption can be written as

$$\alpha_\sigma = \beta_{от}. \quad (2)$$

The main problem of the relationship (2) is that the angle of repose can easily be calculated only for sandy loose soils. That is why equation (2) can not be used to find α_σ in clay and sandy compacted soils.

V.N. Gusev noticed that the angle of stress dispersion was influenced by consistency of the soil and he suggested that angle α_σ could be calculated by the formula

$$\alpha_\sigma = \alpha_{\sigma p} + s \cdot t, \quad (3)$$

where $\alpha_{\sigma p}$ – angle of load distribution (stress dispersion) in loose medium, deg; *s* – coefficient of medium material; *t* – shearing strength within the layer.

As for the relationship (3), it is rather difficult to calculate the angle of stress dispersion in loose medium $\alpha_{\sigma p}$. Thus, it makes sense to combine the ideas of Golovachev and Gusev and the angle α_σ can be calculated by the formula

$$\alpha_\sigma = \beta_1 + s \cdot t, \quad (4)$$

where β_1 – angle of repose of loose medium, deg.

The analysis of the relationship (4) shows that in order to calculate the angle of stress dispersion it is necessary to set up two experiments and to determine two parameters: angle β_1 and strength *t*. Besides, the coefficient *s* should also be determined as it is different for various soils.

Formulae connecting undrained shear strength with load parameters and angle of stress dispersion are presented in papers [20, 22, 23]. According to [20], undrained shear strength can be determined by the formula

$$c_u = P \cdot \left[2 \cdot \pi \cdot \left(\sqrt{\frac{\sqrt{2} \cdot P}{p_в}} + 2 \cdot h_0 \cdot \tan \alpha_\sigma \right) \cdot \left(\sqrt{\frac{P}{2 \cdot \sqrt{2} \cdot p_{tyre}}} + 2 \cdot h_0 \cdot \tan \alpha_\sigma \right) \right]^{-1}, \quad (5)$$

where *P* – load upon the ground base surface, N; p_{tyre} – tyre pressure, Pa; h_0 – total thickness of the road pavement, m.

As follows from the equation (5), the tangent of an angle of dispersion is determined from the quadratic formula, i.e.

$$\tan \alpha_{\sigma 1,2} = \frac{-b \pm \sqrt{b^2 - 16 \cdot h_0^2 \cdot c}}{8 \cdot h_0^2}; b = 2 \cdot h_0 \cdot \sqrt{\frac{P}{p_{tyre}}} \cdot \left(\frac{1}{\sqrt{2} \cdot \sqrt[4]{2}} + \sqrt[4]{2} \right);$$
$$c = P \cdot \left(\frac{1}{\sqrt{2} \cdot p_{tyre} - 2 \cdot \pi \cdot c_u} \right). \quad (6)$$

According to the results obtained in [22, 23], undrained shear strength is calculated from the formula which is similar to the relationship (4) and is written as

$$c_u = P \cdot \left[2 \cdot \pi \cdot \left(\sqrt{\frac{P}{p_{tyre}}} + 2 \cdot h_0 \cdot \tan \alpha_\sigma \right) \cdot \left(\sqrt{\frac{P}{2 \cdot p_{tyre}}} + 2 \cdot h_0 \cdot \tan \alpha_\sigma \right) \right]^{-1}. \quad (7)$$

Solving the equation (7) results in the following formulae

$$\tan \alpha_{\sigma 1,2} = \frac{-b \pm \sqrt{b^2 - 16 \cdot h_0^2 \cdot c}}{8 \cdot h_0^2}; \quad b = 2 \cdot h_0 \cdot \sqrt{\frac{P}{p_{tyre}}} \cdot \left(\sqrt{\frac{1}{2}} + 1 \right);$$
$$c = P \cdot \left(\frac{1}{\sqrt{2} \cdot p_{tyre} - 2 \cdot \pi \cdot c_u} \right). \quad (8)$$

J. Leng [16] suggests the formula similar to the relationships (6) and (8). It includes the amount of applied repeated loads in addition to the mentioned parameters and is written as

$$\tan\alpha_\sigma = \frac{\sqrt{\left(\sqrt{2}-1\right)^2 \cdot P_S/\left(2\cdot p_{tyre}\right)+2\cdot P_S/\left(\lambda\cdot\pi\cdot c_u\right)}}{6.5\cdot\log N/c_u^{0,63}} - \frac{\left(\sqrt{2}-1\right)\cdot P_S/\left(2\cdot p_{tyre}\right)}{6.5\cdot\log N/c_u^{0,63}}, \quad (9)$$

where P_S – design axial load; c_u – undrained strength; N – design number of loads.

Formulae (5)–(9) have the same parameters but the results of their calculations are different. Therefore after performing unconsolidated-undrained triaxial tests and determining the undrained shear strength using relationships (6), (8) and (9), the angle of stress dispersion will be different with the same load parameters.

A procedure for calculating the angle of stress dispersion based on the direct measurements of the diameter of pressure distribution upon the plate located at a certain distance from the ground model surface is presented in work [24]. The procedure presupposes making a ground model with a standard compaction measuring device, with a paper leaf at a certain distance from the surface. The model surface is exposed to the force action with a rigid circular die to form an indentation cup on the ground surface. Then the soil is removed from the upper part of the sample so that to clean the paper leaf which also has an indentation cup of a larger size. The difference in the diameters of the indentation cups determines the distribution capacity, with the angle of stress dispersion being determined by the right triangle trigonometry. This procedure allows calculating values of an angle of stress dispersion for sandy and clay soils [24], but it cannot be used to calculate the one in soils reinforced with geosynthetics. The importance of calculating the angle of stress dispersion in ground bases reinforced with geosynthetics comes from the analysis of papers [22, 25–29] where the data on the angles of stress dispersion are different as well as conclusions concerning the positive influence of the reinforcement on the value of the angle of stress dispersion. The analysis of determining the angle of stress dispersion in reinforced and unreinforced soils is performed in the work [25]. The results are presented in Table 1.

Table 1. Angle of stress dispersion in reinforced and unreinforced ground bases [25, p. 729]

Researcher and a quotation source	Value of the angle of stress dispersion α_σ	
	Unreinforced ground base	Reinforced ground base
E.J. Barenberg [26]	α_σ = arctan(0.3+5/h)	α_σ=arctan(0.6+5/h)
J.P. Giroud and L. Noiray [22]	$\alpha_\sigma = \pi/4-\varphi/2 = 45-\varphi/2$	α_σ = 26.6–35
Raumann G. [27]	α_σ = 28.8	α_σ = 33
J.B. Sellmeijer, C.J. Kenter and C. Van den Berg [28]	α_σ = 26.6–45	α_σ = 26.6–45
J.P. Love et al. [29]	–	α_σ = 26.6–31

Note: h – depth of inserting an interlayer; it is the distance from the layer surface to the reinforcement horizon and it is usually the depth of a crushed-stone level, cm; φ – angle of internal friction, deg.

In order to begin the analysis of the data given in Table 1, it is necessary to point out that the table shows the values of the angles of stress dispersion in a base course being placed on the reinforcing interlayer.

The diagram illustrating the effect of such reinforcement is shown in Figure 2. According to the figure, the angle of stress dispersion in the unreinforced structure $\alpha_{\sigma 0}$ is less than that in the reinforced structure $\alpha_{\sigma 1}$. This effect is observed in the material over the reinforcing grid (for example, a crushed-stone level).

The tabular analysis shows that the authors of the paper [28] did not obtain the increase of the angle of stress dispersion while reinforcing the ground base, i.e. there was no effect described in Figure 2.

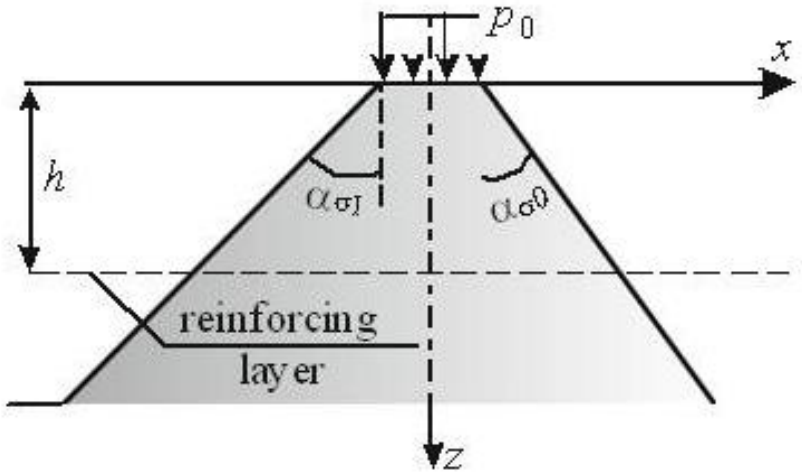

Figure 2. Diagram of different angles of stress dispersion in a reinforced and unreinforced layers

Some other researchers [22, 26, 27], on the contrary, provide values of angles of stress dispersion that proves the effect created. Since there is no single opinion about the effect of reinforcing shown in Figure 2, it can be assumed that the angle of stress dispersion increases in the material under the grid. There is a design diagram (Fig. 3) illustrating the reinforcement of a homogeneous ground base. A geogrid is placed within the layer of one and the same material, for example sand. According to this diagram, the angle of stress dispersion in the material under the grid increases in comparison with the analogous parameter of the same material over the grid.

Figure 3 introduces clarity into the traditional design diagram. Expediency of such a clarification should be proved experimentally. In this connection, it is necessary to calculate angles of stress dispersion in reinforced and unreinforced ground bases. Thus, a direct technique of measuring distribution capacity, that allows calculating angles of stress dispersion, is required. There are two reasons for it. First, it becomes possible to make a more precise calculation of angles of stress dispersion in reinforced and unreinforced ground bases if compared with the data in Table 1. Second, it is possible to explain the choice of a design diagram, for instance, Figure 2 or 3, or to suggest another design diagram being different from those presented in Figure 2 or 3.

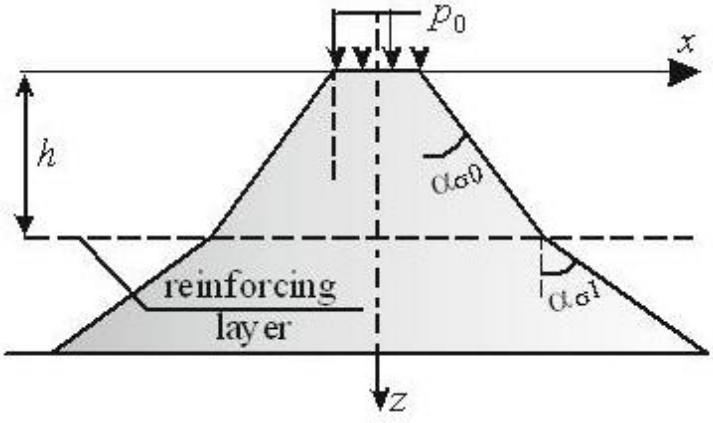

Figure 3. Diagram of different angles of stress dispersion in the material placed over and under the geogrid

Taking the foregoing into consideration, let us formulate the purpose and objectives of the research.

The purpose of this study is to investigate the distribution capacity of reinforced and unreinforced ground bases.

It can be done by achieving the following objectives:

1. Development of the direct method of measurement of reinforced and unreinforced ground bases distribution capacity, with the data being used to calculate an angle of stress dispersion.

2. Application of mathematical statistics methods for calculating average and design values of angles of stress dispersion in reinforced and unreinforced ground bases.

3. Application of fitting criteria for comparing samplings of angles of stress dispersion in reinforced and unreinforced ground bases and for validating one of the design diagrams (Fig. 2 and Fig. 3).

Methods

The authors made a colour strip analysis to measure distribution capacity. The method had been chosen due to its pictorial presentation and its application for detecting slide curves trajectories in ground bases in master's [30] and doctoral [31] theses. An illustration of area elements of sliding surface obtained with the colour strip analysis can be seen in Figure 4. Arrows are used to show the slide curves being aligned with the trajectory of stress dispersion presented in Figures 1–3. This coincidence being taken into account, an angle of stress dispersion can be calculated by the right triangle trigonometry presented in Figure 4 (b).

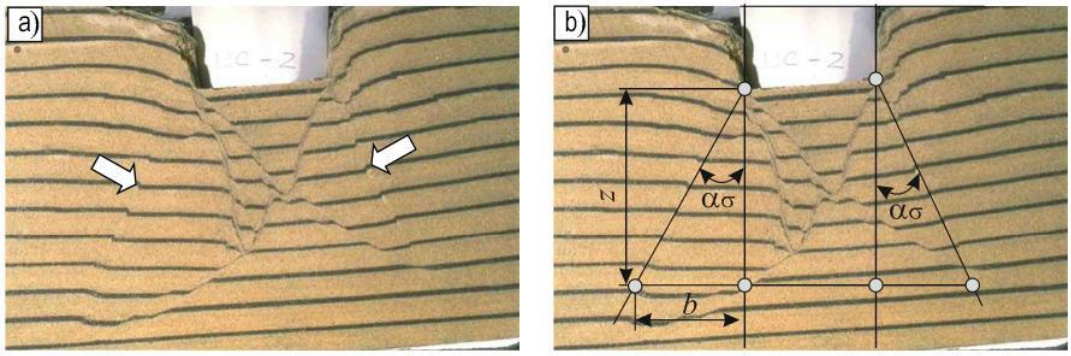

Figure 4. Sand base colour strip test:
a – general view of slide curves in a sand base [30];
b – chart for determining the angle of stress dispersion by the right triangle trigonometry

According to the analysis of Figure 4 (b) Kurdjumov method [32] can be used to calculate the angle of stress dispersion. The idea of this method is in soil photographing during the test, with the images being subsequently processed. It should be noted that the hypotenuse of the triangles passes through the points of colour strips breaks or next to them.

To perform the colour strip analysis models of reinforced and unreinforced ground bases were made, with fine sand being used as soil. Sand was compacted until the zero-air dry unit weight which was 98 % of the standard maximum dry density. It was necessary to determine the dry sand packed density to compact soil. A safety factor for compaction was calculated with the ratio of the required density to the dry sand packed density. The thickness of the sand layer to be obtained after leveling and, consequently, compacting was computed by multiplying of this safety factor and the layer thickness.

The model was made in layers. For the sand to be laid uniformly thread guide rails were used, with their height being equal to the thickness of the unconsolidated sand layer. The thread guide rails were arranged across an aquarium of the organic glass. Then the sand was laid between the thread guide rails and leveled with the bar moving along the rails. The sand layer having been leveled, the thread guide rails were carefully removed and some sand was added to fill the space.

The sand was compacted in two stages:

– at the beginning a roll-on of the layer was performed with a paint roller, the pressure from the hand gradually increasing while sand consolidating;

– to compact the sand finally a press with a rigid rectangular die put on the layer surface was used.

As for the criterion of the final compaction, it was a value of layer surface settling which was determined by the difference of the required thicknesses before and after compaction.

The model was made in a standard way, with layers of standard sand alternating with the coloured ones. Sand was coloured in green and blue. Different coloured stripes were arranged in alternation. For instance, the lower stripe was of green colour and the second one was blue. There were five layers of standard sand with four coloured stripes between them in the models.

A total of 15 models were manufactured. Five models are made without reinforcement, and 10 models produced by stacking two brands geosynthetics RD-60 75 × 75 and RD-60 100 × 100 into the model. Note that the reinforcing layer in road constructions carried out at the interface between the macadam and sand layers, in our models, this layer is laid in the sand. Laying geosynthetic reinforcement interlayer inside the sand is made to determine the scattering angles of stress above and below this layer. Laying geosynthetic materials performed on the surface of the third layer from the bottom of ordinary sand, and on top of it distributed sand, painted in green color. After laying and moistening colored sand his compaction was performed in the manner described above. At manufacturing the models applied criteria of geometric and the power of similarity. This allowed to define size of the stamp, the thickness of the sand layer. Table 2 shows the performance of physical and mechanical properties of the sand used in the model and compacted to the compaction factor of 0.98.

Table 2 Indicators of physical and mechanical properties of fine sand in the models of subgrade

№ sample	Indicators of physical properties, established by Russian standard GOST 5180-84 [24]				The mechanical properties and σ_3 at CN test without measuring the pore pressure		
	W, %	W/W_{opt}	ρ_d,t/m^3	$k=\rho_d/\rho_{dmax}$	σ_3, kPa	c, kPa	φ,^{o}
1	2	3	4	5	6	7	8
1 (kN)	9.33	0.94	1.85	0.98	50	3.3	36
2 (kN)					100		
3 (kN)					150		

Note: W – sand humidity; W_{opt} – optimum humidity; ρ_d – density of dry soil; *k* – compression ratio; ρ_{dmax} – maximum soil density in the standard device packing; σ_3 – the minimum principal stress in the device of triaxial compression when performing consolidated undrained test; c и φ – grip and angle of internal friction.

The essence of experimental method is reduced to the indentation the stamp into the surface of model and its deformation jointly with colored stripes. To transfer the load used the press GEOTECHAI-7000 LA 10 provided with the software package. For all models, the deformation rate was the same 3 mm/s. Pore pressure was not measured. During the test, we observe the change of location of the strips of colored sand. The load was applied so that the top 3 bands of colored sand receive noticeable deformation, and the fourth lower strip is not deformed. This allowed us to minimize the impact of the hard base on the deformation of sand in the model. With such character of the deformation color bars in reinforced models was possible to measure scattering angle in the upper part of the model, that is, over the reinforcing layer as well as the bottom of the model under geosynthetics. This allowed to draw a conclusion about the quantitative influence geosynthetic material on distributing ability of the sand. Then each model photographed for later processing photos with the help of computer programs to determine the scattering angles.

Computer programs were used for processing of photo images in order to perform linear measurements with an accuracy of up to 1 micron. In processing the results of the experiment in photographs set the location of the edges of the stamp and his axis of symmetry, which are shown by vertical lines I and II (Fig. 5).

Next determine the location of the lower border of the stamp, which is shown by the line III (Fig. 5). After this define position of start point uplift of sand on the surface of the color stripe, which corresponds to the intersection of the horizontal straight lines IV and V with vertical lines VI and VII (Fig. 5). The location of this point was fixed on picture by cross. Next perform location determination of point of an alleged gap of color strips. For this analyzed photographs test of works [30, 31], from which it follows that the most likely points of discontinuity of the color stripe are the point located in the middle of the deformed curved line segment, depicted vertical lines I and VI of, I and VII. At the Figure 5 these points signed C, D and E, F. To points C and D from the points corresponding the edges of the stamp – A and B held connecting them straight segments AC and BD, which indicate the locations the line of the stress distribution from the bottom of the stamp to the second color stripes, wherein in the models groups 1 and 3 are laid reinforcement geosynthetics. From the points C and D to the points E and F conducted segments CE and DF. These segments show the line of stress distribution between the second and third colored stripes.

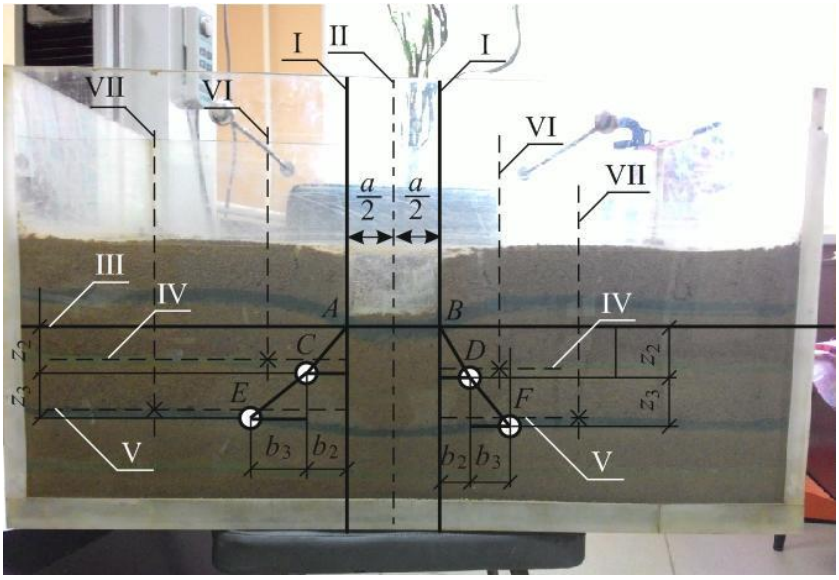

Figure 5. Scheme to the image processing model No. 11, belonging to the reinforced model sand base of group 3

Similar photos processing was made for the reinforced models. In Figure 5 there is an illustration of the processed pictures model No. 11, which analysis showed that the angles of scatter stress of the reinforcing mesh and underneath it are different. This fact confirmed the validity of the application to the calculation of reinforced soil bases the calculation scheme shown in Figure 3.

When processing the results of the test models of group 2, i.e. models of unreinforced sand foundation, it became clear that the segments AC and CE, as well as BD and DF are collinear or substantially coincide with it. It means in the unreinforced model stress distribution is limited to one line.

To determine scattering angles of the stress it is necessary to measure the length of the opposite and adjacent sides of a right triangle. In Figure 5 length of the opposite cathetus specified of length of b_2 and b_3, and the length of the adjacent side – z_2 and z_3. As the tangent of the angle in a right triangle is equal to ratio of the length of the opposite cathetus to the adjacent cathetus length, the scattering angles of the stress can be determined by the formulae:

$$\alpha = \text{arctg}\frac{b_2}{z_2}; \qquad \alpha = \text{arctg}\frac{b_3}{z_3}. \tag{10}$$

Thus, for each colored band it is possible to determine two values of scattering angles of stress located on different sides of the stamp left and right respectively. This allowed for the reinforced models sandy grounds to form two sample scattering angles of stress.

The first sample contains 10 data points of scattering angles of stress α_{j1} characterizing distributing ability of sand over the reinforcing layer.

The second sample also includes 10 data points α_{j2} scattering angles stress, but characterize the ability to distributing sand under the reinforcing layer.

One sample of 20 private scattering angles of stress α_j is formed for unreinforced models.

Besides the processing of facsimiles direct measurements of all necessary sizes, illustrated in Figure 5, are used. In this case, all the lines which we are interested in were restored directly to the full-scale models and fixed by twine.

The initial position of the colored strips and the surface of the sand model were fixed before the test by applying labels to the ends of the aquarium. After the test the model, each label was used to secure the edges of the twine. Thus, the horizontal lines were restored. Restoration of vertical lines was performed with a plumb. Horizontal and vertical lines as well as the hypotenuse of right-angled triangles, which form together with the vertical cathetus, scattering angles stress, shown in Figure 6, was recovered in such manner.

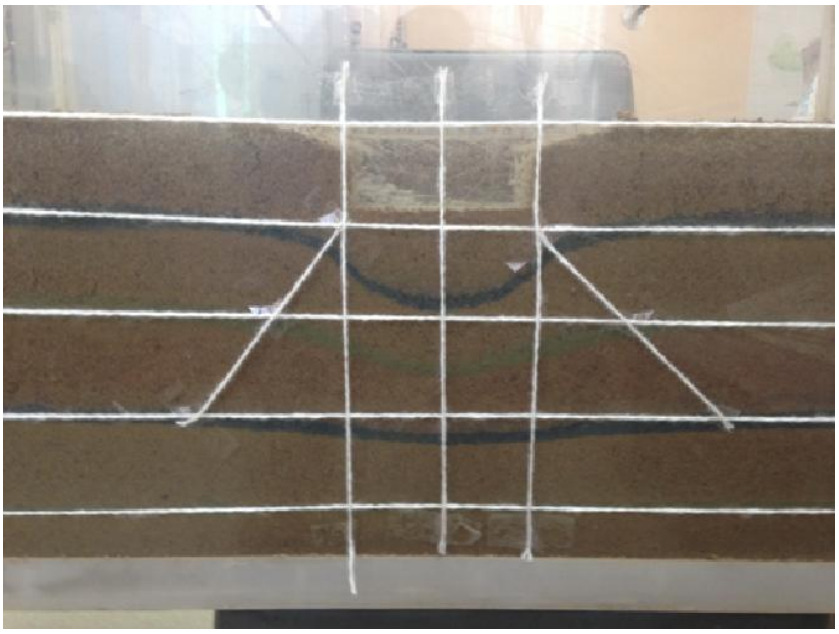

Figure 6. Recovered area stress distribution in the model No. 7, belonging unreinforced models of sand base of 2 group

Results and Discussion

Direct measurements of the size we are interesred in was made by a metal line, which has a certificate of calibration. The measurement accuracy is 1 mm. Methods of calculating the scattering angles of stress analogous to the method applied in the processing of photographs. Despite the similarity of methods of measurement accuracy linear dimensions are different. Therefore, particular values of scattering angles, calculated from the results of direct measurements performed on a full-scale model, also grouped in five sample. At the first statistical processing of the data tested the possibility of combining the respective sample (samples 1 and 6, 2 and 7, 3 and 8, 4 and 9, 5 and 10) in a general population. For this purpose the Student's *t*-test and Fisher's *F*-test, following the standard procedure, were used.

Verifiable conditions of criteria have form:

$$t < t_{\alpha}; \qquad F < F_{\alpha}, \tag{11}$$

where t_{α} – critical value of the Student distribution, also known as the coefficient of the normalized deviations accepted under bilateral confidence level of 0.95; F_{α} – the critical value of *F*-distribution.

The *t* and *F* criterion show that each pair of sample belongs to single corresponding general aggregate. Thus conclusion about the applicability of any developed by us techniques of measurement the linear size by means of which stress is calculated scattering angle can be done. For example, Table 3 shows the results of verification execution of the criteria (11) for sample No. 1 and No. 6, in which are grouped scattering angles stress in the upper part of the model group 1, in which the sand reinforced by mesh RD-60 75 × 75. Table 4 shows the results of verification execution of the criteria (11) for sample No. 2 and No. 7, in which are grouped the scattering angles stress in the bottom of the model group 1, in which the sand reinforced mesh by RD-60 75 × 75.

Table 3. Results of testing sample No. 1 and No. 6 on the appurtenance for one of the general population

Statistical characterization		Sample No. 1	Sample No. 6
Private values scattering angles of stress, °	1	39.41	40.40
	2	40.11	39.51
	3	39.85	39.74
	4	39.63	39.62
	5	38.70	38.69
	6	39.06	38.03
	7	38.80	39.43
	8	39.40	39.60
	9	39.76	39.78
	10	39.40	40.08
Mathematical expectation (middle sample), °		39.412	39.488
Root mean square deviation, °		0.45	0.46
Dispersion, grade ^{2}		0.21	0.68
Statistics t		0.28	
The critical value of the Student's distribution t_α		2.26	
Statistics F		2.23	
The critical value of the distribution of R. Fischer F_α		3.18	
Checking conditions	$t<t_\alpha$	Performed as 0.28<2.26	
	$F<F_\alpha$	Performed as 2.23<3.18	
Conclusion: As a result of the implementation of both conditions criteria Student and Fisher sample No. 1 and No. 6 belong to the same general population			

Table 4. Results of testing sample No. 2 and No. 7 on the appurtenance for one of the general population

Statistical characterization		Sample No. 2	Sample No. 7
Private values scattering angles of stress, °	11	44.76	43.06
	12	44.59	44.39
	13	43.83	43.59
	14	43.66	43.59
	15	43.39	42.70
	16	42.41	43.57
	17	42.00	42.61
	18	43.12	43.04
	19	42.36	42.44
	20	41.99	41.75
Mathematical expectation (middle sample), °		43.211	43.074
Root mean square deviation, °		1.01	0.75
Dispersion, grade ^{2}		1.03	0.56
Statistics t		0.33	
The critical value of the Student's distribution t_α		2.26	
Statistics F		1.84	
The critical value of the distribution of R. Fischer F_α		3.18	
Checking conditions	$t<t_\alpha$	Performed as 0.33<2.26	
	$F<F_\alpha$	Performed as 1.84<3.18	
Conclusion: As a result of the implementation of both conditions criteria Student and Fisher sample No. 2 and No. 7 belong to the same general population			

As the criteria (11) are satisfied, each pair of checked samples can be combined into one new sample for which to perform further statistical processing. Combining samples will increase the number of

outcomes (partial values of scattering angles stress) in each new sample, whereby the quality of data will increase. After combining the samples of their total number was equal to 5. Samples 1 and 2 contain 20 particular values scattering angles stress in models of grounds reinforced with a mesh RD-60 75 × 75. The sample No. 1 contains scattering angles stresses on this grid, and the sample No. 2 shows the scattering angles stress under the grid. Sample No. 3 includes scattering angles of stress of unreinforced models. Sample 4 is similar to the sample 1, the sample 5 – sample 2, but samples No. 4 and No. 5 contains scattering angles of models of reinforced mesh RD-60 100 × 100.

New samples were tested for the presence of blunders, using as a criterion exceptions private values fulfillment of the condition Russian Standard GOST 20522-2012, then determined the estimated value of the scattering angles stress. In addition, the samples No. 1, No. 2, No. 3, No. 4 were verified to belong to the same general population. As a result, it was found that these samples are not subject to the unification. It follows therefrom that the factor of reinforcement of foundation soil is significant and results in increased scattering angles under the grid.

It was found that under the reinforcing mesh RD-60 100 × 100 scattering angle of stress increases by 2.9 %, while under the net of the RD-60 75 × 75 – increased by 9.1 %. This experimental fact suggests dependence on the effectiveness of the reinforcement from the grid cell size, made from one and the same material and having the same tensile strength.

To assess the reliability of the calculation scheme shown in Figure 2, it was performed statistical processing of private value of scattering angle of stress in sandy layers above the reinforcing grid and scattering angle of stress at the top of the unreinforced sand model. Performing of such statistical processing demanded the formation of four samples, each containing 20 private scattering angles of stress. The essence of the statistical processing involves estimating the possibility of combining the four samples in a general totality. Student's and Fisher's criteria, which we applied above, allow you to compare only two samples, for the assessment of belonging to the one general population three or more samples of these criteria are unfit. As far as number of private scattering angle of stress is identical in all four samples, rank criterion of Wilcoxon or rank criterion Kruskal–Wallis can be use.

In accordance with mathematical statistics literature data, Wilcoxon criterion is a nonparametric alternative to the Student criterion, which operates by comparing the total dispersion of two independent samples. Kruskal–Wallis criterion is a nonparametric alternative to the Fisher test. Kruskal–Wallis criterion is based on an assessment of the differences between the *c* medians ($c > 2$), and is a generalization of the Wilcoxon rank criterion. Therefore, we applied the criterion of Kruskal–Wallis test, which showed that the compound samples impossible. It follows that the reinforcement of the subgrade leads to a change in the scattering angle stress over the grid.

Thus, reinforcement of ground facilities leads to increased scattering angle of stress under a grid and some decrease this angle in the material located above the grid. This conclusion is confirmed by experiment refutes the calculation scheme shown in Figure 2 and confirms the circuit illustrated in Figure 3.

Table 5. Comparison of the results of determining the dispersion angle of the stress with those of other authors

Researcher and a quotation source	**Expected value α_σ**		**The discrepancy results, %**	
	Unreinforced ground base	Reinforced ground base	Unreinforced ground base	Reinforced ground base
According to the proposed method	39.45	43.14	–	–
J.P. Giroud and L. Noiray [19]	30	32.8	24	24
Raumann G. [24]	28.8	33	27	24
J.B. Sellmeijer, C.J. Kenter and C. Van den Berg [25]	35.5	42.5	10	1.5
J.P. Love et al. [26]	–	28.8	–	33.2

Analysis of the data Table 5 shows that in most cases the difference of the results is more than 20 %. This indicates that the application of the proposed methodology will improve the accuracy of the determination of this parameter of material.

Furthermore, the results publication can be applied to calculate the principal stresses. In order to do this the method proposed in [33] was used. The method lies in the fact that the minimum principal stress is defined as the percentage of the maximum principal stress. The formula has the form:

$$\sigma_2 = \sigma_3 = \alpha \cdot \xi \cdot \sigma_1, \quad (12)$$

where α – coefficient, which is a function of depth; ξ – lateral pressure coefficient.

The maximum principal stress can be represented by multiplication the pressure and the function reduce of its depth K. Applying this rule to the formula (1), for the cross section along the symmetry axis load we obtain:

$$\sigma_1 = \sigma_z = p \cdot K, \qquad K = \left(1 + \frac{2 \cdot Z}{D_0} \cdot \mathrm{tg}\alpha_\sigma\right)^{-2}. \quad (13)$$

Function of depth α determined by the formula [33]:

$$\alpha = 1 - \sqrt{1 - K^2}. \quad (14)$$

Substituting addictive (13) and (14) into the formula (12) allows getting model for determining the minimum principal stress:

$$\sigma_2 = \sigma_3 = p \cdot \xi \cdot \left(1 + \frac{2 \cdot Z}{D_0} \cdot \mathrm{tg}\alpha_\sigma\right)^{-2} \cdot \left(1 - \sqrt{1 - K^2}\right). \quad (15)$$

Thus, formulas (1) and (15) allow to calculate the main stresses for condition $\sigma_1 \geq \sigma_2 = \sigma_3$, which occurs in section along the symmetry axis of the load, distributed over the circular area. Therefore, it becomes possible to calculate the equivalent stresses on the various conditions of plasticity, including multi-surface modern conditions. Furthermore, according calculated to the relation (1) and (15) the principal stresses can be applied to calculate the residual strain on various mathematical models plastic deformation when subjected to repeated loads.

Conclusions

In conclusion, we can draw several inferences:

1. A method was developed direct measurement the distributing ability of reinforced and non-reinforced soil bases, based on the method of color stripe.

2. Calculation of scattering angle stress can be done one of two ways:

- processing pictures with deformed colored stripes in accordance with the data in Figure 5.
- restoration of essential lines, characterize the distributing ability on natural models, by performing the operation illustrated in Figure 6.

3. Statistical processing showed that the factor of the reinforcement of the sandy foundation is significant, that is affecting the value of the scattering angle stress in the materials located above the grid, as well as under it.

4. Under the Reinforcing Netting made of the same material, scattering angle of stress is increased by an amount depending on the cell size. It is found that the smaller the cell size, the greater the value of scattering angle of stress under the reinforcing grid.

References

1. Radovskiy B.S. Pervyye predstavleniya o prochnosti i raschete dorozhnykh odezhd: dorozhnyye odezhdy do XX veka [First perceptions about the strength and calculation of road pavements: pavement until the twentieth century]. *Dorozhnaya tekhnika.* 2012. Pp. 120–133. (rus)
2. Dolgikh G.V. *Raschet nezhestkikh dorozhnykh odezhd po kriteriyu bezopasnykh davleniy na grunty zemlyanogo polotna: diss…cand.tech.nauk.* [Calculation of nonrigid road pavements on the criterion of safe pressures in the soil subgrade. PhD Thesis]. Omsk: SibADI, 2014. 237 p. (rus)

Литература

1. Радовский Б.С. Первые представления о прочности и расчете дорожных одежд: дорожные одежды до XX века // Дорожная техника. 2012. С. 120–133.
2. Долгих Г.В. Расчет нежестких дорожных одежд по критерию безопасных давлений на грунты земляного полотна: дис. … канд. техн. наук. Омск: СибАДИ, 2014. 237 с.
3. Taha El. Modelisation des deformation permanentes des graves non traitees. Application au calcul de l'ornierage des chaussees souples. PhD Thesis. Universite de Limoges, 2005. 173 p.

Aleksandrov A.S., Kalinin A.L., Tsyguleva M.V. Distribution capacity of sandy soils reinforced with geosynthetics. *Magazine of Civil Engineering*. 2016. No. 6. Pp. 35–48. doi: 10.5862/MCE.66.4

3. Taha El. Modelisation des deformation permanentes des graves non traitees. Application au calcul de l'ornierage des chaussees souples. PhD Thesis. Universite de Limoges, 2005. 173 p.
4. Dolgikh G.V. Eksperimentalnaya otsenka raspredelyayushchey sposobnosti glinistykh gruntov [Experimental estimation of distribution of the clay soils]. *Vserossiyskaya 65-ya nauchno-tekhnicheskaya konferentsiya FGBOU VPO «SibADI» [Proceedings of 65th scientific technical conference in SibADI].* Omsk: FGBOU VPO SibADI, 2011. Pp. 48–54. (rus)
5. Aleksandrov A.S., Aleksandrova N.P., Dolgikh G.V. Modifitsirovannyye modeli dlya rascheta glavnykh napryazheniy v dorozhnykh konstruktsiyakh iz diskretnykh materialov [Modified model for calculation of the principal stresses in road constructions of discrete materials]. *Stroitelnyye materialy.* 2012. No. 10. Pp. 14–17. (rus)
6. Aleksandrova N.P., Semenova T.V., Dolgikh G.V. Sovershenstvovaniye modeley rascheta glavnykh napryazhe-niy i deviatora v grunte zemlyanogo polotna [Development of models to calculate the principal stresses and deviator in the soil subgrade]. *Vestnik SibADI.* 2014. No. 2(36). Pp. 49–54. (rus)
7. Odemark N. Investigations as to the elastic properties of soils and design of pavements according to the theory of elasticity. *Medclelande.* 1949. Vol. 77. Pp. 43–52.
8. Lee Y.-H. Study of backcalculated pavement layer moduli from the LTPP database. *Journal of Science and Engineering.* 2010. Vol. 13. No. 2. Pp. 145–156.
9. Fi I., Szentpéteri I. A mechanistic-empirical approach for asphalt overlay design of asphalt pavement structures. *Civil Engineering*. 2014. Vol. 58/1. Pp. 55–62.
10. Horak E., Hefer A., Maina J. Determination of pavement number for flexible pavements using fwd deflection bowl information. *Proceedings of the 34th Southern African Transport Conference (SATC 2015).* 2015. Pp. 187–200.
11. Burd H.J., Frydman S. Bearing capacity of plane-strain footings on layered soils. *Canadian Geotechnical Journal.* 1997. Vol. 34. Pp. 241–253.
12. Meyer N., Elias J.M. Design methods for roads reinforced with multifunctional geogrid composites for sub-base stabilization. *German Conference on Geosynthetics.* Munich: Technical University Munich, 1999. Pp. 1–8.
13. Benjamin C.V.S., Bueno B., Zornberg J.G. Field monitoring evaluation of geotextile-reinforced soil retaining walls. *Geosynthetics International Journal.* 2007. Vol. 14. No. 2. Pp. 100–118.
14. Bueno B.S., Costanzia M.A., Zornberg J.G. Conventional and accelerated creep tests on nonwoven needle-punched geotextiles. *Geosynthetics International.* 2005. Vol. 12. No. 6. Pp. 276–287.
15. Hu Y.C., Zhang Y.M. Analysis of load-settlement relationship for unpaved road reinforced with geogrid. *First International Symposium on Geotechnical Safety & Risk.* 2007. Pp. 609–615.
16. Leng J. *Characteristics and behavior of geogrid-reinforced aggregate under cyclic load.* PhD Thesis. Raleigh, 2002. 152 p.
17. Mounes S.M. An overview on the use of geosynthetics in pavement structures. *Scientific Research and Essays*. 2011. No. 6(11). Pp. 2234–2241.
18. Zornberg J.G., Gupta R. Geosynthetics in pavements: North American contributions. *9th International Conference on Geosynthetics.* Guaruja, Brazil, 2010. Pp. 379–398.
19. Badanin A.N., Bugrov A.K., Krotov A.V. Obosnovaniye pervoy kriticheskoy nagruzki na zernistuyu sredu supeschanogo osnovaniya [The determination of the first critical load on particulate medium of sandy loam foundation]. *Magazine of Civil Engineering*. 2012. No. 9(35). Pp. 29–34. (rus)
20. Koerner R.M. *Designing with geosynthetics. Fifth edition*. Upper Saddle River. New Jersey, 2005. 796 p.
4. Долгих Г.В. Экспериментальная оценка распределяющей способности глинистых грунтов // Всероссийская 65-я научно-техническая конференция ФГБОУ ВПО «СибАДИ». Омск: ФГБОУ ВПО «СибАДИ», 2011. С. 48–54.
5. Александров А.С., Александрова Н.П., Долгих Г.В. Модифицированные модели для расчета главных напряжений в дорожных конструкциях из дискретных материалов // Строительные материалы. 2012. № 10. С. 14–17.
6. Александрова Н.П., Семенова Т.В., Долгих Г.В. Совершенствование моделей расчета главных напряже-ний и девиатора в грунте земляного полотна // Вестник СибАДИ. 2014. № 2(36) С. 49–54.
7. Odemark N. Investigations as to the elastic properties of soils and design of pavements according to the theory of elasticity // Medclelande. 1949. Vol. 77. Pp. 43–52.
8. Lee Y.-H. Study of backcalculated pavement layer moduli from the LTPP database // Journal of Science and Engineering. 2010. Vol. 13. № 2. Pp. 145–156.
9. Fi I., Szentpéteri I. A mechanistic-empirical approach for asphalt overlay design of asphalt pavement structures // Civil Engineering. 2014. Vol. 58/1. Pp. 55–62.
10. Horak E., Hefer A., Maina J. Determination of pavement number for flexible pavements using fwd deflection bowl information // Proceedings of the 34th Southern African Transport Conference (SATC 2015). 2015. Pp. 187–200.
11. Burd H.J., Frydman S. Bearing capacity of plane-strain footings on layered soils // Canadian Geotechnical Journal. 1997. Vol. 34. Pp. 241–253.
12. Meyer N., Elias J.M. Design methods for roads reinforced with multifunctional geogrid composites for sub-base stabilization // German Conference on Geosynthetics. Munich: Technical University Munich, 1999. Pp. 1–8.
13. Benjamin C.V.S., Bueno B., Zornberg J.G. Field monitoring evaluation of geotextile-reinforced soil retaining walls // Geosynthetics International Journal. 2007. Vol. 14. № 2. Pp. 100–118.
14. Bueno B.S., Costanzia M.A., Zornberg J.G. Conventional and accelerated creep tests on nonwoven needle-punched geotextiles // Geosynthetics International. 2005. Vol. 12. № 6. Pp. 276–287.
15. Hu Y.C., Zhang Y.M. Analysis of load-settlement relationship for unpaved road reinforced with geogrid // First International Symposium on Geotechnical Safety & Risk. 2007. Pp. 609–615.
16. Leng J. Characteristics and behavior of geogrid-reinforced aggregate under cyclic Load. PhD Thesis. Raleigh, 2002. 152 p.
17. Mounes S.M. An overview on the use of geosynthetics in pavement structures // Scientific Research and Essays. 2011. № 6(11). Pp. 2234–2241.
18. Zornberg J.G., Gupta R. Geosynthetics in pavements: North American contributions // 9th International Conference on Geosynthetics. Guaruja, Brazil, 2010. Pp. 379–398.
19. Баданин А.Н., Бугров А.К., Кротов А.В. Обоснование первой критической нагрузки на зернистую среду супесчаного основания // Инженерно-строительный журнал. 2012. № 9(35). С. 29–34.
20. Koerner R.M. Designing with geosynthetics. Fifth edition., New Jersey: Upper Saddle River, 2005. 796 p.
21. Клейн Г.К. Строительная механика сыпучих тел М.: Стройиздат, 1977. 256 с.
22. Giroud J.P., Noiray L. Geotextile-reinforced unpaved road design // Journal of Geotechncial Engineering, ASEC. 1981. Vol. 107. Pp. 1233–1254.
23. Giroud J.P., Ah-Line C., Bonaparte R. Design of unpaved roads and trafficked areas with geogrids // Proceedings of the symposium on polymer grid reinforcement in civil engineering. London, 1984. Pp. 116–127.
24. Александров А.С., Александрова Н.П., Кузин Н.В.,

Александров А.С., Калинин А.Л., Цыгулева М.В. Распределяющая способность песчаных грунтов, армированных геосинтетикой // Инженерно-строительный журнал. 2016. № 6(66). С. 35–48.

21. Kleyn G.K. Stroitelnaya mekhanika sypuchikh tel [Structural theory of granular materials]. Moscow: Stroyizdat, 1977. 256 p.
22. Giroud J.P., Noiray L. Geotextile-reinforced unpaved road design. *Journal of Geotechncial Engineering, ASEC*. 1981. Vol. 107. Pp. 1233–1254.
23. Giroud J.P., Ah-Line C., Bonaparte R. Design of unpaved roads and trafficked areas with geogrids. *Proceedings of the symposium on polymer grid reinforcement in civil engineering.* London, 1984. Pp. 116–127.
24. Aleksandrov A.S., Aleksandrova N.P., Kuzin N.V., Dolgikh G.V. Issledovaniye vertikalnykh napryazheniy v zemlyanom polotne s uchetom raspredelyayushchey sposobnosti gruntov [Study of vertical stresses in the subgrade with account of the distribution capacity of soils]. *Transportnoye stroitelstvo.* 2010. No. 8. Pp. 18–21. (rus)
25. Espinoza R.D., Bray J.D. An integrated approach to evaluating single-layer reinforced soils. *Geosynthetics International.* 1995. Vol. 2. No. 4. Pp. 723–739.
26. Barenberg E.J. *Design procedures for soil-fabric-aggregate systems with Mirafi 500X fabric.* PhD Thesis. Department of Civil Engineering. University of Illinois, USA. 1980. 26 p.
27. Raumann G. Geotextiles in unpaved roads: design considerations. *Proceedings of the second international conference on geotextiles.* Las Vegas, 1982. Vol. 2. Pp. 417–422.
28. Sellmeijer J.B., Kenter C.J., Van den Berg C. Calculation method for fabric reinforced road. *Proceedings of the second international conference on geotextiles.* Las Vegas, 1982. Vol. 2. Pp. 393–398.
29. Love J.P. Analytical and model studies of reinforcement of a layer of granular fill on soft clay subgrade. *Canadian Geotechnical Journal.* 1987. Vol. 24. No. 4. Pp. 611–622.
30. Melnikov A.V. *Issledovaniye prochnosti i deformiruyemosti slabykh gruntov osnovaniy, usilennykh ar-mirovaniyem: diss…magistra tekniki I tiknologii stroitel'stva* [Investigation of the strength and deformability of weak Foundation soils, reinforced with reinforcement. Thesis MS]. Penzenskiy gosudarstvennyy universitet arkhitektury i stroitelstva. Penza, 2012. 216 p. (rus)
31. Korolev K.V. Nesushchaya sposobnost osnovaniy v stabilizirovannom i nestabilizirovannom sostoyanii. Dokt.Diss [Bearing capacity of foundations in stabilized and unstabilized condition. Doct.Diss]. Novosibirsk, 2014. 325 p. (rus)
32. Khristov Kh. Sankt-Peterburg, 1889 g.: pervoye fotograficheskoye issledovaniye protsessa razrusheniya grunta pod fundamentom [Saint Petersburg, 1889: the first photographic survey of the ground failure process under foundation]. *Rekonstruktsiya gorodov i geotekhnicheskoye stroitelstvo.* 2003. No. 7. Pp. 187–192. (rus)

Долгих Г.В. Исследование вертикальных напряже-ний в земляном полотне с учетом распределяющей способности грунтов // Транспортное строительство. 2010. № 8. С. 18–21.
25. Espinoza R.D., Bray J.D. An integrated approach to evaluating single-layer reinforced soils // Geosynthetics inter-nationals. 1995. Vol. 2. № 4. Pp. 723–739.
26. Barenberg E.J. Design procedures for soil-fabric-aggregate systems with Mirafi 500X fabric. PhD Thesis. Department of Civil Engineering. University of Illinois, USA. 1980. 26 p.
27. Raumann G. Geotextiles in unpaved roads: design considerations // Proceedings of the second international conference on geotextiles. Las Vegas, 1982. Vol. 2. Pp. 417–422.
28. Sellmeijer J.B., Kenter C.J., Van den Berg C. Calculation method for fabric reinforced road // Proceedings of the second international conference on geotextiles. Las Vegas, 1982. Vol. 2. Pp. 393–398.
29. Love J.P. Analytical and model studies of reinforcement of a layer of granular fill on soft clay subgrade // Canadian Geotechnical Journal. 1987. Vol. 24. № 4. Pp. 611–622.
30. Мельников А.В. Исследование прочности и деформируемости слабых грунтов оснований, усиленных ар-мированием: дис. … магистра техники и технологии строительства / Пензенский государственный университет архитектуры и строительства. Пенза, 2012. 216 с.
31. Королев К.В. Несущая способность оснований в стабилизированном и нестабилизированном состоянии: дис. … д-ра техн. наук. Новосибирск, 2014. 325 с.
32. Христов Х. Санкт-Петербург, 1889 г.: первое фотографическое исследование процесса разрушения грунта под фундаментом // Реконструкция городов и геотехническое строительство. 2003. № 7. С. 187–192.

Anatoliy Aleksandrov,
+7(913)6164212; Aleksandrov00@mail.ru

Alexsandr Kalinin,
+7(965)9858572; a1exsandr55ne@mail.ru

Margarita Tsyguleva,
+7(381)2651563; m.v.tsyguleva@gmail.com

Анатолий Сергеевич Александров,
+7(913)6164212;
эл. почта: Aleksandrov00@mail.ru

Александр Львович Калинин,
+7(965)9858572;
эл. почта: a1exsandr55ne@mail.ru

Маргарита Викторовна Цыгулева,
+7(381)2651563;
эл. почта: m.v.tsyguleva@gmail.com

© Aleksandrov A.S., Kalinin A.L., Tsyguleva M.V., 2016

Aleksandrov A.S., Kalinin A.L., Tsyguleva M.V. Distribution capacity of sandy soils reinforced with geosynthetics. *Magazine of Civil Engineering*. 2016. No. 6. Pp. 35–48. doi: 10.5862/MCE.66.4

doi: 10.5862/MCE.66.5

Laboratory and numerical study of waves in the port area

Лабораторные и численные исследования волн в акватории порта

I.G. Kantardgi,
National Research Moscow State University of Civil Engineering, Moscow, Russia
M.J. Zheleznyak,
Institute of Environmental Radioactivity, Fukushima University, Fukushima, Japan

Д-р техн. наук, профессор И.Г. Кантаржи,
Национальный исследовательский Московский государственный строительный университет, г. Москва, Россия
канд. физ.-мат. наук, профессор М.И. Железняк,
Институт радиологии окружающей среды, Университет Фукусима, г. Фукусима, Япония

Key words: port area waves; experiments and numerical modelling; method of comparison; standing waves

Ключевые слова: волны в акватории порта; эксперименты и численное моделирование; метод сопоставления; стоячие волны

Abstract. Parameters of waves in water area of the projected port are normally obtained using physical and numerical modelling. Physical modelling allows defininig structural details of the port's facilities and provides with information for the appropriate selection of a numerical model. The problems created by this approach are shown in the case study of the projected port in Vostok (East) Bay, the Sea of Japan. The experimental study of waves propagation in the port water area was carried out in the wave basin. The port area was reproduced at a scale of 1:50, and the modelling was conducted under the Froude number similarity. Experimental results are provided for the study of wave propagation in the port model from the effects of the waves of 5 % exceedance probability. To confirm the results of the laboratory experiments, four relevant mathematical models were used, one of them is the ARTEMIS model which is based on gentle slopes equations. The heights of numerically modeled waves in the control points were compared with the waves measured with sensors-wave gauges. The calculated values at the control point and minimum and maximum values in a circular neighborhood with the radius of 30 m (1/4 of the average wavelength of 120 m) were compared with the results of the experiments. The proposed approach allows comparing the results of physical modelling with the results of numerical modelling and selecting the appropriate numerical model based on the results of the comparison.

Аннотация. Параметры волн в акватории порта обычно получают путем физического и численного моделирования. Физическое моделирование позволяет определить конструктивные детали портовых сооружений и предоставляет информацию для выбора соответствующей численной модели. Проблемы, с которыми этот подход связан, показаны в исследовании проектируемого порта в бухте Восток, Японское море. Экспериментальное исследование распространения волн в акватории порта были проведены в волновом бассейне. Район порта был воспроизведен в масштабе 1:50, и моделирование проводилось по параметру подобия Фруда. Результаты эксперимента используются для изучения распространения волн в численной модели порта от воздействия волны 5% обеспеченности. Чтобы подтвердить результаты лабораторных экспериментов, были использованы четыре соответствующие математические модели, одна из них ARTEMIS, основанная на уравнениях пологих склонов. Высоты волн численно моделируются и сравниваются с измерениями в контрольных точках датчиками волн. Рассчитанные значения в контрольной точке и минимальное и максимальное значения в круговой окрестности контрольной точки с радиусом 30 м (1/4 средней длины волны 120 м) сопоставлялись с результатами измерений. Предлагаемый подход позволяет сравнивать результаты физического моделирования с результатами численного моделирования и выбирать на основе результатов сравнения подходящую численную модель.

Кантаржи И.Г., Железняк М.И. Лабораторные и численные исследования волн в акватории порта // Инженерно-строительный журнал. 2016. № 6(66). С. 49–59.

Introduction

If the definition of calculated waves approaching the projected port facilities is subject to numerical simulation with verification by natural data, the impact of the waves on the port facilities is determined by numerical and physical modelling methods. Then, to verify the received data by physical modelling of the interaction of waves with models of constructions. That meets the requirements of the relevant regulatory documents [1, 2].

This approach has been adopted in most of the world's major centers of the world leading research port facilities [3–8]. When comparing the results of physical and numerical simulation of waves, it has solved the task of choosing the numerical model of wave propagation around port facilities [4, 5]. Furthermore, this model is used to compare different design options. A typical task of the research of interaction of waves with port structures is the task of determining the waves on a protected water area of the port [9].

However, the analysis of published papers on numerical and physical modelling of wave propagation in the port water area shows that these works do not pay attention to detailed methodology of comparing the obtained wave heights, measured using the physical models and numerical modelling [3, 7].

For example, [7] shows only the results of numerical research. However, the problem of standing waves or crowding in the water is discussed in this work. However, the authors' experience shows that in a head-to-head comparison of the heights of waves generated by numerical and physical modelling, problems that require examination arise [9].

The task is considered by the example of the research using the methods of numerical and physical modelling of waves interaction with the projected port of Eastern petrochemical company.

The projected marine terminal is to be designed for shipping of finished/refined products and for receiving crude oil. Mooring facilities are located in Vostok Bay, the Sea of Japan. Vostok Bay is a part of the southeast side of Peter the Great Bay and intrudes the land for approximately 7.3 km. The distance between its capes is about 5.8 km and the area of the water table is 38 sq. km with the length of the shoreline of about 29 km. The open part of Vostok Bay faces the south-southwest direction.

The moorings disposition inside of the bay allows for designing the protection structures against the waves approaching only from the south and west. The layout of the breakwater and the moorings is shown in Figure 1.

The projected marine terminal is designed for procuring of a new refinery with the capacity of 30 million tons per year. The refinery is not built yet and the time of the construction is not predetermined yet.

To select an adequate mathematical model of wave propagation in the port water area, a standard approach is used to compare the results of numerical simulation of wave fields with measurements at certain points of the physical model. In this case, possible formation of partially standing waves in the port water area (physical model) can lead to difficulties in this comparison. A similar problem arose during the present study.

Laboratory and numerical studies of waves at the port water area were conducted to verify the effectiveness of the breakwater in providing of acceptable parameters of waves at the moorings, like in other authors' papers [10–12]. The aim of this paper is to discuss the technology of comparing the results of numerical and physical modelling of wave fields inside the port water area and to investigate this technology for the example of the designed port.

The actual normative methods [13–15] are available for the problem's solutions with serious limitations [16].

Numerical and experimental study

To study waves propagation, the physical model of the water area of the port was built in the wave basin of Moscow State Civil Engineering University (MSCEU). The study program was developed to investigate the distribution of 5 % exceedance South and Southwest waves at the port water area and their impact on the eastern and western sides of the breakwater.

The scale of the model of 1:50 was determined according to the water basin size of 27 x 27 m, actual size of the port water area, distance from the wave generator to the entrance to the port, depth of

the basin, prevailing wave direction, and the correspondence of wave processes in nature and in the model as per Froude's similarity criteria.

Physical modelling was conducted in a usual way for such tasks, by the criterion of Froude $\mathrm{Fr} = \mathrm{h}/\mathrm{gT}^2$ in the conditions of auto modelling under Reynolds parameter. In accordance with the criterion of modelling individual elements, the weight of protective mounts on the model was defined as $m_n = m_m\lambda^3$, where m_n is the mass of a single element in natural conditions, m_m is the mass of the element in the model, the λ is the linear scale of modelling.

Four series of experiments were conducted to study South and Southwest waves impact on the eastern and western sides of the breakwater.

At the eastern side of the breakwater, the experiments were conducted for South waves with the parameters of T = 12.3 s and $h_{5\%}$ = 5 m and for Southwest waves with the parameters of T = 10.4 s and $h_{5\%}$ = 5 m. The modelling parameters were estimated as T = 1.74 s, $h_{5\%}$ = 10 cm, and T = 1.5 s, $h_{5\%}$ = 10.0 cm, respectively.

At the western side of the breakwater, the experiments were conducted for South waves with the parameters of T = 12.3 s, $h_{5\%}$ = 8.5 m, and for Southwest waves with the parameters of T = 10.4 s, $h_{5\%}$ = 7.2 m. The modelling parameters were estimated as T = 1.74 s, $h_{5\%}$ = 17 cm and T = 1.47 s, $h_{5\%}$ = 14.4 cm, respectively.

The description of the study and the results of the physical and numerical experiments related to South waves with diffraction on the western side of the breakwater is provided below.

The locations of wave sensors and the wave generator in the wave basin are shown in Figure 2. Different numerical models are used to calculate shallow waves and waves at the water area of water ports. The spectral model SWAN [17, 18] is used worldwide, and it is open-source software.

The model is based on the wave action density balance equation (or conservation of energy under no ambient currents condition) with the source and sink terms. The model can be used in Cartesian or spherical coordinates depending on the scale of applications. Diffraction processes are described approximately and cannot provide a detailed wave field solution for wave interactions with hydrotechnical structures.

Different mathematical models were used to obtain the calculated field waves and comparisons with the results of physical modelling of waves in the port water area: SWAN, SWAN 123 (spectral version), WaveWatch III, and ARTEMIS. And to get the final results, the model SWAN (waves on the way to port installations) and the model ARTEMIS (waves in the port water area) were used.

The results of physical modelling were compared with the results of numerical modelling conducted using the ARTEMIS software [19]. Software ARTEMIS is based on the gentle slope hydrodynamic equations [20, 21]. The software solves the waves transformation in coastal zones including the processes of refraction-diffraction, bottom friction energy dissipation and breaking of waves. The finite element numerical method is utilized to solve the elliptic equations. ARTEMIS is successfully used for similar studies [3]. It is open source software and can be found at http://www.opentelemac.org/ [22].

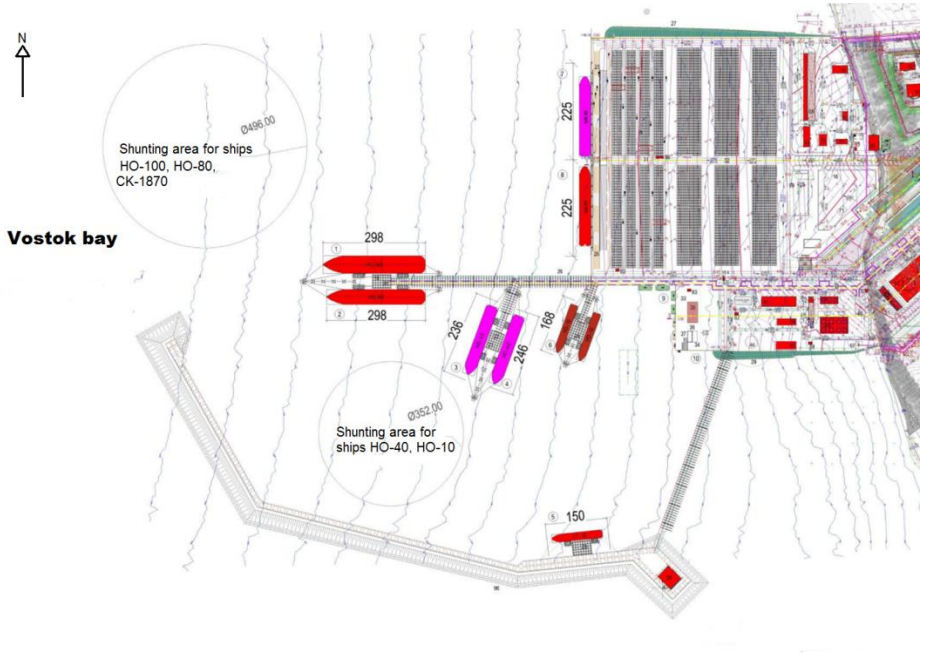

Figure 1. Marine Terminal Layout. Dimensions are in meters

The bathymetric map of the Sea of Japan, Peter the Great Bay, and Vostok Bay, with the scale of 1:25000 obtained by the echo-sounder survey was digitized and used for numerical modelling. The port's structures were included into the digitized map.

Waves interaction with different types of structures was considered by introducing the reflection coefficients along the structures' boundaries. The reflection coefficient of kr = 0.9 was used for vertical structures and for the side slopes of the wave canal. The reflection coefficient of 0.5 was used for the slopes of the structures protected by an armor berm.

Two types of the breakwater were considered. The main type was a wave impermeable structure with a revetment slope. The alternative type was a structure with a wave permeable central part that allows some waves to get to the water area of the port (Figure 4).

The revetment slope was designed with three layers of protection: the bottom layer made of stones with weights from 50 to 150 kg was overlayed by the layer made of stones from 500 to 1500 kg, and the top layer was made of shaped concrete units (hexabits) with weight of 10 tones.

To obtain the reflection coefficients, the laboratory experiments of incoming and passing waves were conducted in a wave flume and wave's parameters were recorded. Scale modelling in the flume was selected as 1:25. The example of the setup of a pier with piles and a surge plate (wave deflector to reduce wave overtopping) in the wave flume is presented in Figure 4. The reflection coefficient for impermeable structure breakwater (Figure 3) was obtained as 0.5, the reflection coefficient for wave permeable breakwater with a surge plate (Figure 4) was obtained as 0.65.

To absorb the waves at the wavemarker's back side for both wave flume and in the basin, the permeable slope construction with metal shavings was used (Figure 5). Methodical experiments show that this design provides a coefficient of wave reflection no higher than 2 %.

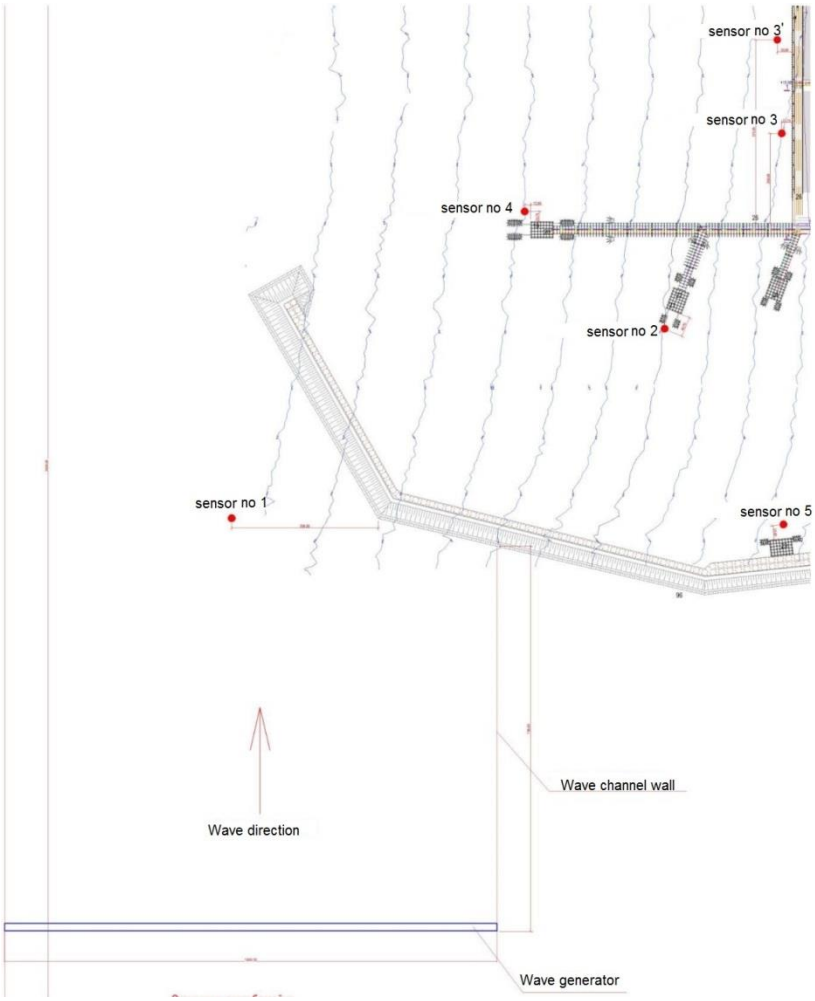

Figure 2. Marine terminal model layout with the locations of wave sensors and the wave generator. South waves impact on the western side of the breakwater study

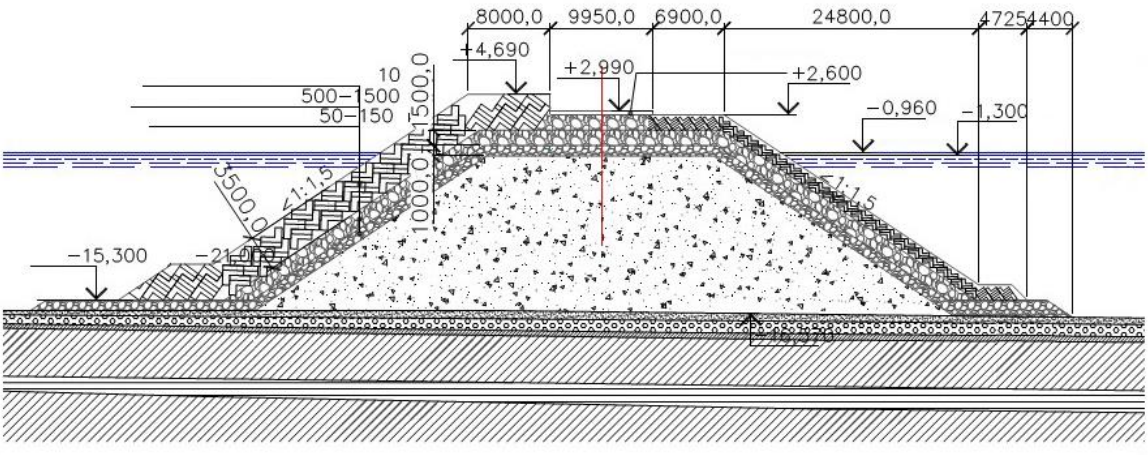

**Figure 3. Cross section of the protected breakwater, slope type.
Horizontal sizes are in millimeters, vertical levels are shown in meters, Baltic System**

The bathymetry of the calculation domain for the study of the western side of the breakwater and South waves is shown in Figure 6.

ARTEMIS numerical grids were built in accordance with the numerical modelling requirements. It means that there should be no less than grid's 7 nodes for the wave length. The grids were built for the monochromatic wave with the period of 7 secs and for the number of nodes of 10. The mesh sizes changed from 2 m for shallow water to 8 m for deep water. The sizes of grids were as following: for the

study of the eastern side of the breakwater and South waves the number of nodes was 87959 and the number of elements was 174018; for the study of the eastern side of the breakwater and Southwest waves the number of nodes was 88969 and the number of elements was 175945; for the study of the western side of the breakwater and South waves the number of nodes was 81581 and the number of elements was 161487; for the study of the western side of the breakwater and Southwest waves the number of nodes was 51317 and the number of elements was 101413.

The bathymetry of the calculation domain to study the western side of the breakwater and South waves is shown in Figure 6.

The waves' parameters generated by the wave generator in physical modelling for South waves were T = 1.74 s and $h_{5\%}$ = 17.0 cm at the sensor's location 1 (entrance to the port). The corresponding parameters in the numerical modelling were T = 12.3 s, $h_{5\%}$ = 8.5 m, and the values were assigned to the wave generating boundary (Figure 6). The location of the wave-generating boundary in the numerical model corresponds to the location of the wave generator in the physical model.

The results of the numerical modelling of the wave fields are presented in Figures 7 and 8.

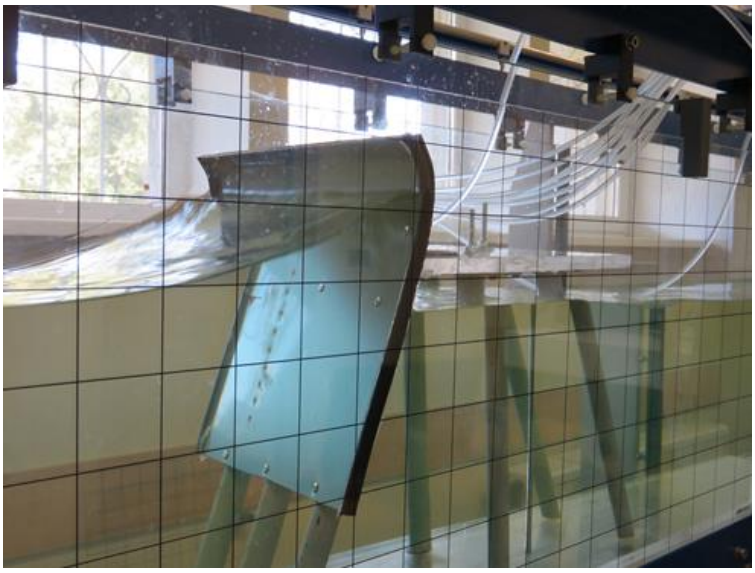

Figure 4. Experiment setup for estimating reflection coefficients of complex structures

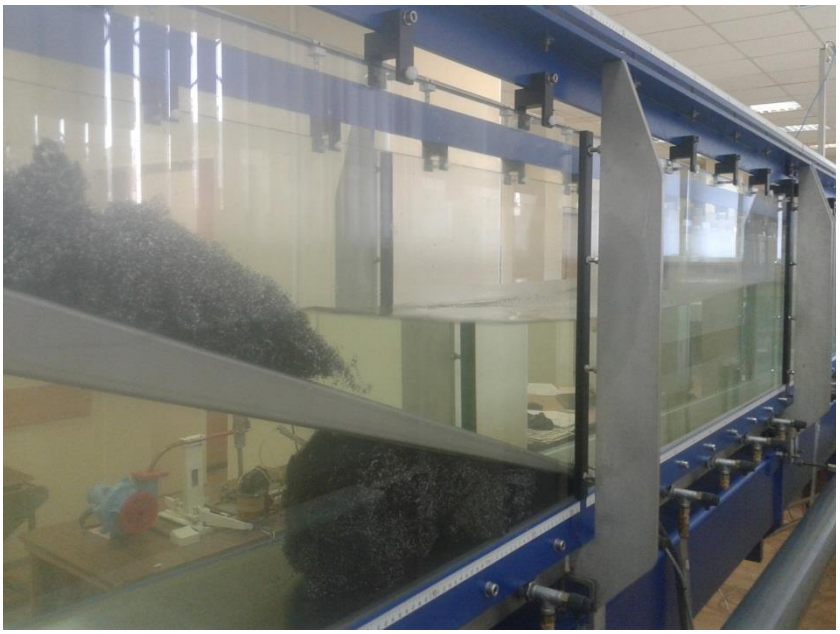

Figure 5. Wave absorber in the wave flume

Results and Discussion

General pictures of the wave fields recorded during physical modelling are similar to the obtained result with numerical modelling. The numerical modelling exhibits the same diffraction and turn of the wave front at the breakwater head and propagation of the wave further to the diffraction area of the port (Figure 7). The general view of the wave field of the physical model is shown in Figure 9.

The waves' heights obtained during physical modelling and converted to natural values are summarized in Table 1. The results of numerical modelling are also presented in Table 1.

The calculated waves' heights at the sensor locations 1, 3', and 4 are similar to the measured ones, but at the sensor locations 2, 3, and 5 they are somewhat different from the measured ones. Nevertheless, all obtained results fall to the interval from the minimum to maximum calculated values, inside of 30 m radius with centers at the sensor locations.

Table 1. Wave heights obtained by the ARTEMIS model and recorded during physical modelling for the study of the South waves impact on the western side of the breakwater. The min and max values of the calculated heights are the calculated values inside of the circle with the radius of 30 m with the center at the sensor location.

Control location	Measured wave height, m	Water depth (physical model), m	Calculated wave height, m			Water depth (numerical model), m
			Control point	min	max	
1	8.5	22	8.21	7.00	10.02	20.59
2	1.01	15	0.45	0.02	1.67	14.99
3	0.74	13	2.32	0.21	4.45	13.00
3'	0.94	13.5	0.99	0.23	3.9	13.47
4	1.61	18	2.12	1.28	2.78	18.00
5	0.62	11.5	0.37	0.22	0.69	11.39

The graphical representation of the calculated and measured values is shown in Figure 10.

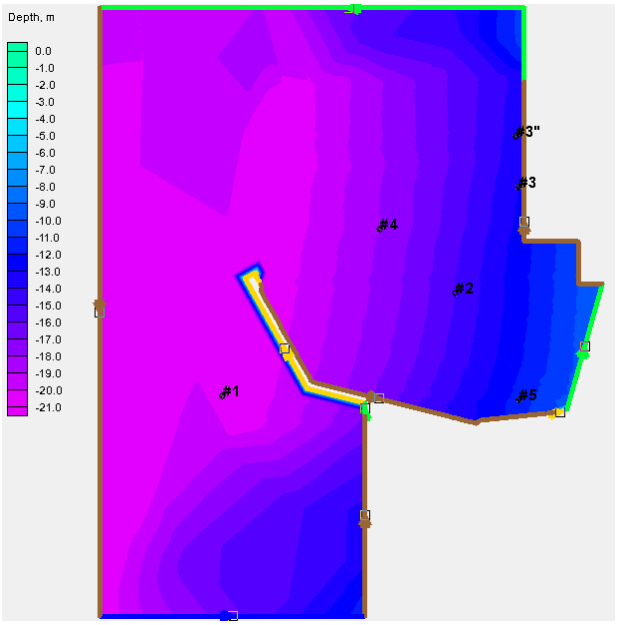

Figure 6. Modelling domain of the study of the South Waves impact on the western side of the breakwater. The wave-generating boundary is in blue. Free boundaries are in green. Other boundaries are reflecting boundaries with kr = 0.9 (brown), kr = 0.5 (yellow). The control locations 1, 2, 3, 3', 4, and 5 correspond to the locations of the wave sensors during physical modelling

One of the reasons for the difference between the wave heights, measured and calculated, can be that the wave field for the monochromatic wave is significantly inhomogeneous and shows changes in a series of maximums and minimums. As a result of frequent waves' reflections and interferences, the partial standing waves occur at the port water area. Thus, significant changes in the wave heights at the control location can be observed. Correspondingly, in spite of the similarity of the wave fields of physical and numerical modelling, a small offset of the minimums and maximums can lead to a significantly different result at the control location. However, within the definite distance from the control locations, the calculated heights close to the measured ones can be found. Therefore, to compare the results, the calculated values within the radius of 30 m or a ¼ of the average wave length of 120 m were considered and are shown in Table 1. The results of the measured values reside in the minimum maximum interval for all control locations. The same method of comparing the calculated and measured results was applied to the other three studies, and the same trend was observed.

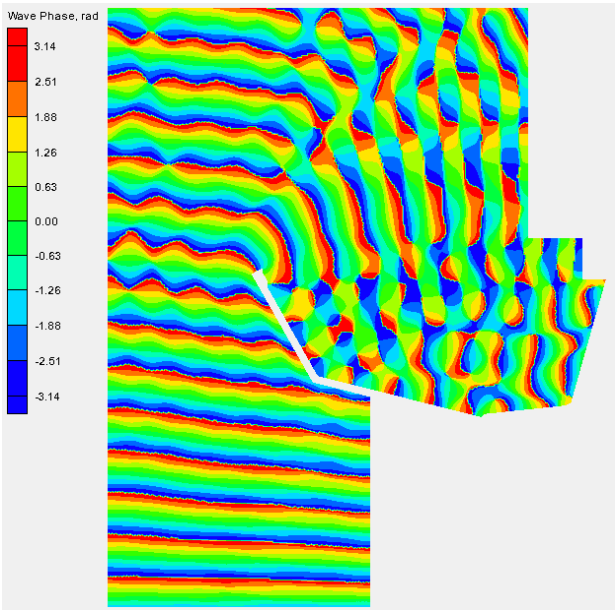

Figure 7. Calculated waves phases for the physical model of the port water area for the study of the South Waves impact on the western side of the breakwater

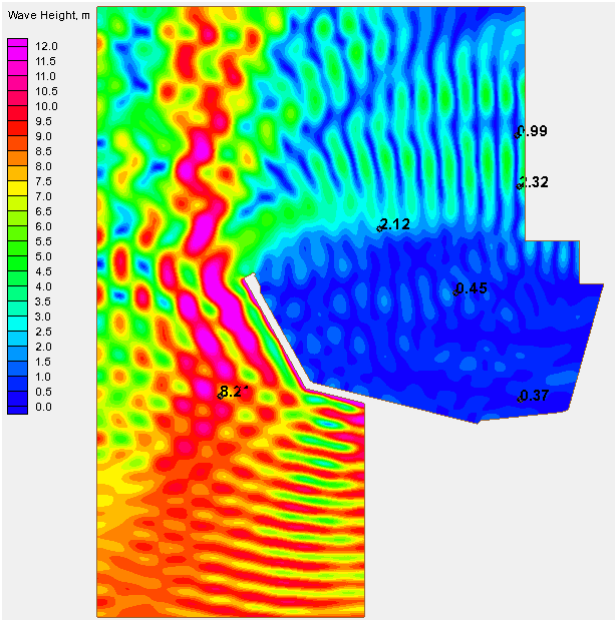

Figure 8. Calculated wave heights for the physical model of the port water area for the study of the South Waves impact on the western side of the breakwater. Wave heights are shown in colors and in numbers at the control locations

Figure 9. General view of the wave field generated by South Waves during physical modelling

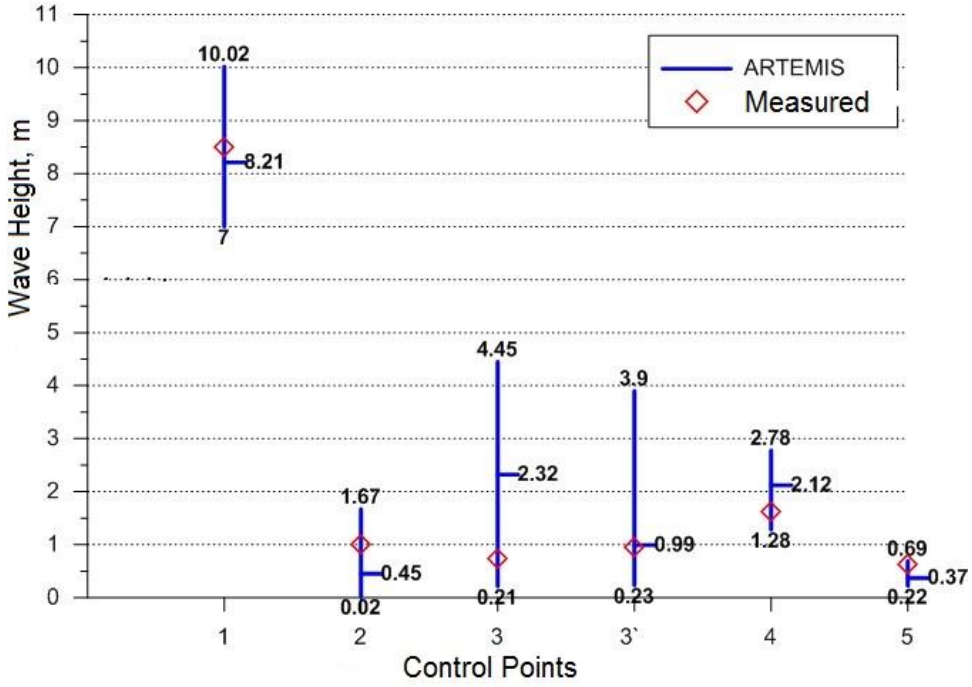

Figure 10. Measured and calculated wave heights. Study of the South Waves impact on the western side of the breakwater

In published works of other authors, a detailed comparison of wave fields on the water area of the port derived from physical and numerical modelling was not touched upon.

Conclusions

When comparing the results of physical and numerical modelling of the wave field at the port water area, the phenomenon of forming partial standing waves with different intensities at different locations should be considered. In the case of the partial standing wave occurrence, the calculated and measured heights of waves at the corresponding locations can be significantly different. It is recommended to compare the calculated results with the measured results within the radius of a ¼ of the average wave length from the location where the waves were measured. The calculated maximum and minimum wave

heights within the radius and the calculated wave height at the control location should be used to compare with the measured result at the control location.

The approach to comparing the results has been used to study waves at the water area of the projected oil-tanker port at Vostok Bay, the Sea of Japan. The approach also allows determining the use of the numerical model of wave diffraction.

The obtained research results allowed choosing the numerical model used to study options for the design of protective structures of the projected port.

References

1. Kantarzhi I.G., Kuznetsov K.I. Naturnyye izmereniya volneniya pri opredelenii nagruzok na morskiye gidrotekhnicheskiye sooruzheniya [In site measurement of waves for determination of loads onto sea hydraulic structures]. *Magazine of Civil Engineering.* 2014. No. 4(48). Pp. 49–62. (rus)
2. Kantarzhi I.G. Fizicheskoye i chislennoye modelirovaniye voln u portovykh gidrotekhnicheskikh sooruzheniy. Beregovaya zona – vzglyad v budushcheye [Physical and numerical modelling of waves and port structures. Coastal area – looking into the future]. *Materialy XXV mezhdunarodnoy beregovoy konferentsii* [Proceeding of international coastal conference]. 2014, Sochi: Izd-vo GEOS, 2014. Vol. 2. Pp. 128–131. (rus)
3. Kofoed-Hansen H., Sloth P., Sørensen O.R., Fuchs J Combined numerical and physical modelling of seiching in exposed new marina. *Proceedings of 27th international conference of coastal engineering.* 2000. Pp. 3600–3614.
4. Smit P., Stelling G., Zijlema M. Assessment of non-hydrostatic wave-flow model SWASH for directionally spread waves propagating through a barred basin. *Proceedings of ACOMEN 2011*. 2011. Pp. 1–10.
5. Rijnsdorp D.P., Smit P.B., Zijlema M. Non-hydrostatic modelling of infragravity waves using SWASH. *Proceedings of 33rd Conference on Coastal Engineering.* 2012. Pp. 1287–1299.
6. Zijlema M., Stelling G., Smit P. SWASH: An operational public domain code for simulating wave fields and rapidly varied flows in coastal waters. *Coastal Engineering*. 2011. № 10(58). Pp. 992–1012.
7. Divinskiy B.V., Kosyan R.D., Kuklev S.V. Parametry vetrovogo volneniya na zashchishchennykh akvatoriyakh [Wind waves parameters in protected water bodies]. Fundamentalnaya i prikladnaya gidrofizika [Fundemental and applied hydrophysics]. 2010. No. 4(10). Pp. 5–16. (rus)
8. Divinskiy B.V., Kosyan R.D., Podymov I.S., Pushkarev O.V. Ekstremalnoye volneniye v severo-vostochnoy chasti Chernogo morya v fevrale 2003 g. [Extreme waves in North-East part of the Black Sea in Feb/2003]. *Oceanology*. 2004. Vol. 43. No. 6. Pp. 2–15. (rus)
9. Kantarzhi I., Zuev N., Shunko N., Zeleznyak M., Dikiy P., Sorokin M. Numerical and physical modelling of the waves inside the new marina in Gelendjik (Black Sea). Application of physical modelling to port and coastal protection. *Proceedings of 5th international conference Coastlab.* Varna, 2014. Vol. 2. Pp. 253–262.
10. Dikiy P.V., Dzyuba N.N., Zheleznyak M.I., Sorokin M.V. Modelirovaniye volnovogo rezhima poberezhya Imeretinskoy nizmennosti [Modelling of the wave regime of Imeretinka coast]. *International Journal for Computational Civil and Structural Engineering.* 2011. No. 2(7). Pp. 54–63. (rus)
11. Kantardgi I., Zheleznyak M., Demchenko R., Dykyi P., Kivva S., Kolomiets P., Sorokin M. Modelling of nonlinear hydrodynamics of the coastal areas of the Black Sea by the chain of the proprietary and open source models. Proceedings of EGU. Vienna, 2014. Pp. 113–119.

Литература

1. Кантаржи И.Г., Кузнецов К.И. Натурные измерения волнения при определении нагрузок на морские гидротехнические сооружения // Инженерно-строительный журнал. № 4(48). 2014. С. 49–62.
2. Кантаржи И.Г. Физическое и численное моделирование волн у портовых гидротехнических сооружений. Береговая зона – взгляд в будущее // Материалы XXV международной береговой конференции. Сочи: Изд-во ГЕОС, 2014. Т. 2. С. 128–131.
3. Kofoed-Hansen H., Sloth P., Sørensen O.R., Fuchs J. Combined numerical and physical modelling of seiching in exposed new marina // Proceedings of 27th international conference of coastal engineering. 2000. Pp. 3600–3614.
4. Smit P., Stelling G., Zijlema M. Assessment of non-hydrostatic wave-flow model SWASH for directionally spread waves propagating through a barred basin // Proceedings of ACOMEN 2011. 2011. Pp. 1–10.
5. Rijnsdorp D.P., Smit P.B., Zijlema M. Non-hydrostatic modelling of infragravity waves using SWASH // Proceedings of 33rd Conference on Coastal Engineering. 2012. Pp. 1287–1299.
6. Zijlema M., Stelling G., Smit P. SWASH: An operational public domain code for simulating wave fields and rapidly varied flows in coastal waters // Coastal Engineering. 2011. № 10(58). Pp. 992–1012.
7. Дивинский Б.В., Косьян Р.Д., Куклев С.В. Параметры ветрового волнения на защищенных акваториях // Фундаментальная и прикладная гидрофизика. 2010. № 4(10). С. 5–16.
8. Дивинский Б.В., Косьян Р.Д., Подымов И.С., Пушкарев О.В. Экстремальное волнение в северо-восточной части Черного моря в феврале 2003 г. // Океанология. 2004. Т. 43. № 6.С. 2–15.
9. Kantarzhi I., Zuev N., Shunko N., Zeleznyak M., Dikiy P., Sorokin M. Numerical and physical modelling of the waves inside the new marina in Gelendjik (Black Sea). Application of physical modelling to port and coastal protection // Proceedings of 5th international conference Coastlab. Varna, 2014. Vol. 2. Pp. 253–262.
10. Дикий П.В., Дзюба Н.Н., Железняк М.И., Сорокин М.В. Моделирование волнового режима побережья Имеретинской низменности // International Journal for Computational Civil and Structural Engineering. 2011. № 2(7). С. 54–63.
11. Kantardgi I., Zheleznyak M., Demchenko R., Dykyi P., Kivva S., Kolomiets P., Sorokin M. Modelling of nonlinear hydrodynamics of the coastal areas of the Black Sea by the chain of the proprietary and open source models // Proceedings of EGU. Vienna, 2014. Pp. 113–119.
12. Кантаржи И.Г. Уточнение расчетных элементов волн и льда для определения нагрузок на морские гидротехнические сооружения на основе натурных наблюдений // Гидротехническое строительство. 2014. № 1. С. 21–33.
13. Руководство по определению нагрузок и воздействий на гидротехнические сооружения (волновых, ледовых и от судов). Л: ВНИИГ имени Б.Е. Веденеева, 1977.

Kantardgi I.G.,Zheleznyak M.J. Laboratory and numerical study of waves in the port area. *Magazine of Civil Engineering*. 2016. No. 6. Pp. 49–59. doi: 10.5862/MCE.66.5

12. Kantarzhi I.G. Utochneniye raschetnykh elementov voln i lda dlya opredeleniya nagruzok na morskiye gidrotekhnicheskiye sooruzheniya na osnove naturnykh nablyudeniy [Development of design parameters of waves to define the design loads onto sea hydraulic strucutures on the basr of in field observations]. *Gidrotekhnicheskoye stroitelstvo* [Hydraulic structures]. 2014. No. 1. Pp. 21–33. (rus)
13. *Rukovodstvo po opredeleniyu nagruzok i vozdeystviy na gidrotekhnicheskiye sooruzheniya (volnovykh, ledovykh i ot sudov)* [Manual on determination of loads and impacts onto the hydraulic structures (of waves, ice, and boats)]. Leningrad: VNIIG imeni B.Ye. Vedeneyeva, 1977. 254 p. (rus)
14. *SP 38.13330.2012. Nagruzki i vozdeystviya na gidrotekhnicheskiye sooruzheniya (volnovyye, ledovyye i ot sudov)* [Loads and impacts on hydrotekhnical structures (of waves, ice and boats)]. Moscow. Minregion Rossii, 2011. 116 p. (rus)
15. *RD 31.33.02-81. Metodicheskiye ukazaniya po opredeleniyu vetrovykh i volnovykh usloviy pri proyektirovanii morskikh portov* [Manual on wind and wave conditions in design of the sea ports]. Moscow: SoyuzmorNIIproyekt. 1981. 91 p. (rus)
16. Galenin B.G., Duginov B.A., Krivickij S.V., Krylov Ju.M., Podmogil'nyj I.A., Poljakov Ju.P., Popkov R.A., Strekalov S.S. *Veter, volny i morskiye porty* [Wind, waves and sea ports]. Leningrad. Gidrometeoizdat, 1986. 264 p. (rus)
17. Holthuijsen L.H. *Waves in oceanic and coastal waters.* Cambridge University Press. Cambrige, 2007. 236 p.
18. Booij N., Haagsma I.J., Holthuijsen L., Kieftenburg A., Ris R., van der Westhuysen A., Zijlema M. *SWAN Cycle III version 40.51. User manual.* The Netherlands, 2009. 67 p.
19. Hasselmann K., Barnett T.P., Bouws E., Walden H. Measurements of wind-wave growth and swell decay during the Joint North Sea Wave Project (JONSWAP). *Ergnzungsheft zur Deutschen Hydrographischen Zeitschrift Reihe*. 1973. No. 12. 95 p.
20. Aelbrecht D. ARTEMIS 3.0: A finite element model for predicting wave agitation in coastal areas and harbours including dissipation. *Computer modelling of seas and coastal regions III.* Boston, 1997. Pp. 343–352.
21. Berkhoff J.C. Computation of combined refraction-diffraction. *13th Coastal Engineering Conference.* New York, 1972. Vol. 1. Pp. 471–490.
22. Berkhoff J. C. *Mathematical models for simple harmonic linear water waves: wave diffraction and refraction.* Delft: Hydraulic Laboratory, 1976. 102 p.
23. Hervouet J. M. TELEMAC, a hydroinformatic system. *La Houille Blanche.* 1999. No. 3–4. Pp. 21-28.

254 С.
14. СП 38.13330.2012. Нагрузки и воздействия на гидротехнические сооружения (волновые, ледовые и от судов)». Актуализированная редакция СНиП 2.06.04-82*. М.: Минрегион России, 2011. 116 с.
15. РД 31.33.02-81. Методические указания по определению ветровых и волновых условий при проектировании морских портов. М.: СоюзморНИИпроект, 1981. 91 с.
16. Галенин Б.Г., Дугинов Б.А., Кривицкий С.В., Крылов Ю.М., Подмогильный И.А., Поляков Ю.П., Попков Р.А., Стрекалов С.С. Ветер, волны и морские порты. Л.: Гидрометеоиздат, 1986. 264 с.
17. Holthuijsen L.H. Waves in oceanic and coastal waters. Cambrige: Cambridge University Press, 2007. 236 p.
18. Booij N., Haagsma I.J., Holthuijsen L., Kieftenburg A., Ris R., van der Westhuysen A., Zijlema M. SWAN Cycle III version 40.51. User manual. The Netherlands, 2009. 67 p.
19. Hasselmann K., Barnett T.P., Bouws E., Walden H. Measurements of wind-wave growth and swell decay during the Joint North Sea Wave Project (JONSWAP) // Ergnzungsheft zur Deutschen Hydrographischen Zeitschrift Reihe. 1973. № 12. 95 p.
20. Aelbrecht D. ARTEMIS 3.0: A finite element model for predicting wave agitation in coastal areas and harbours including dissipation // Computer modelling of seas and coastal regions III. Boston, 1997. Pp. 343–352.
21. Berkhoff J.C. Computation of combined refraction-diffraction // 13th Coastal Engineering Conference. New York, 1972. Vol. 1. Pp. 471–490.
22. Berkhoff J. C. Mathematical models for simple harmonic linear water waves: wave diffraction and refraction. Delft: Hydraulic Laboratory, 1976. 102 p.
23. Hervouet J. M. TELEMAC, a hydroinformatic system // La Houille Blanche. 1999. № 3–4. Pp. 21-28.

Izmail Kantardgi,
+7(903)5337830; kantardgi@yandex.ru

Mark Zheleznyak,
+818058441091; zheleznyak.m@gmail.com

Измаил Григорьевич Кантаржи,
+7(903)5337830;
эл. почта: kantardgi@yandex.ru

Марк Иосифович Железняк,
+818058441091;
эл. почта: zheleznyak.m@gmail.com

© Kantardji I.G., Zheleznyak M.I., 2016

Кантаржи И.Г., Железняк М.И. Лабораторные и численные исследования волн в акватории порта // Инженерно-строительный журнал. 2016. № 6(66). С. 49–59.

doi: 10.5862/MCE.66.6

Method of thermotechnical uniformity coefficient evaluation by analyzing thermograms

Метод оценки коэффициента теплотехнической однородности из анализа термограмм

G.P. Vasilyev,
V.A. Lichman,
I.A. Yurchenko,
M.V. Kolesova,
JSC "INSOLAR-INVEST", Moscow, Russia

д-р техн. наук, научный руководитель Г.П. Васильев,
канд. физ.-мат. наук, старший научный сотрудник В.А. Личман,
ведущий инженер И.А. Юрченко,
ведущий инженер-эколог М.В. Колесова,
ОАО "ИНСОЛАР-ИНВЕСТ", г. Москва, Россия

Key words: energy efficiency; the coefficient of thermotechnical uniformity; specific geometrical parameter; thermal resistance; temperature field; temperature; heating; thermogram; building; construction

Ключевые слова: энергоэффективность; коэффициент теплотехнической однородности; геометрический параметр; сопротивление теплопередаче; ограждающая конструкция здания; температурное поле; теплота; термограмма; здание; строительство

Abstract. One of the primary problems solved for increasing energy efficiency of a building is increasing of the insulating properties of the building envelope. The paper describes the method for determining the coefficient of thermotechnical uniformity by analyzing a thermogram of parts of a building envelope. The method is based on obtaining temperature distribution matrix on the surface of a building envelope fragment by thermography. Two methods for assessing the coefficient of thermotechnical uniformity are proposed. One method for determining the coefficient of thermotechnical uniformity is based on obtaining mean temperature values by numerically processing thermograms, another on numerical integration along the contour lines of temperature curves.

Аннотация. Одной из приоритетных задач, решаемой при повышении энергетической эффективности зданий, является повышение теплозащитных свойств их наружных ограждающих конструкций. В данной работе изложен метод оценки величины коэффициента теплотехнической однородности из анализа термограмм наружных ограждающих частей зданий. Метод основан на получении путем термографирования матрицы распределения температуры на поверхности фрагмента ограждающей конструкции. Предложены два способа оценки величины коэффициента теплотехнической однородности. Один способ оценки величины коэффициента теплотехнической однородности основан на получении усредненных значениях температур путем числовой обработки термограмм, другой – на численном интегрировании вдоль контуров линий температурных кривых.

Introduction

In Russian Civil Engineering, a dimensionless thermal uniformity coefficient r of the building envelope or its fragment is widely used. This coefficient is determined as $r = R_0^{rel}/R_0^r$, where R_0^{rel} – conventional thermal resistance of a multilayer building envelope having uniformal layers, that is calculated from $R_0^{rel} = R_{si} + \sum d_k/\lambda_k + R_{se}$ (R_{si} , R_{se} – thermal resistances of the internal and the external building envelope layers, $m^2 \cdot K/W$; λ_k – thermal conductivity coefficient of the k-th uniformal layer, $W/(m \cdot K)$; d_k – thickness of the layer, m); R_0^r – reduced thermal resistance of a non-uniformal building envelope, calculated from $R_0^r = (t_{int} - t_{ext}) \cdot A/Q$, where t_{int}, t_{ext} – internal and external air temperatures, ℃; A – surface area of a non-uniformal building envelope or its fragment, m^2; Q – total heat flux through this surface, W. The value of the total heat flux Q through the non-uniformal building envelope, containing “thermal bridges” (thermal conductive insertions, gaps, corners, etc.) is determined

Vasilyev G.P., Lichman V.A., Yurchenko I.A., Kolesova M.V. Method of evaluation of thermotechnical uniformity coefficient by analyzing thermograms. *Magazine of Civil Engineering*. 2016. No. 6. Pp. 60–67. doi: 10.5862/MCE.66.6

from numerical computer aided calculation of thermal fields or experimentally. Knowing the value of thermal uniformity coefficient the designer is able to perform quick evaluation of R_0^r .

Non-uniformal segments of the building envelope (so called "thermal bridges" – joints, dowels, thermal inserts, etc.) take a considerable area of the building envelope that is why they have a considerable impact on insulating properties and durability of the construction [1–3]. Looking for engineering solutions for increasing thermal uniformity of the building envelope is one of the relevant tasks solved by the modern thermal engineering. Both simplified and detailed calculation methods for determining heat transfer (thermal resistance) coefficients of building envelope are well developed and available today [4–6].

Surface thermography is performed according to Russian standards. However, the obtained thermograms due to random impacts of side effects are qualitative. The procedure for thermogram procession has several parameters, providing for alterations in temperature and color match. The core parameters are surface radiation coefficient of the construction – a measure of radiation, emitted by the object, compared to the ideal black body and apparent reflected temperature – a parameter, used to compensate radiation of other bodies [7, 8].

Thermographic analysis is a useful tool for evaluating energy performance a building. It also may be used to verify the presence of air seepage, moisture or water leaks. It is difficult to understand in details all the parameters that influence the thermal scene, that's why infrared thermography is not commonly used for quantitative diagnosis [9, 10].

Most studies involving infrared thermography in building monitoring leads to qualitative results. The technology of infrared cameras has advanced and thermal maps generated by the latest models offer a lot of information in terms of image definition. Better quality of the IR sensors makes the information more accurate. The software for image processing has advanced the most, in terms of graphics management of the pictures: a single shooting makes it possible to make many more evaluations, changing the parameters, to locate homogeneous areas and make very precise calculation of the average values of temperatures. A complete methodology based on the infrared thermovision technique has been developed to reach quantitative data of thermal transmittances of building envelopes [11].

In practice [12] analysis of infrared thermography measurements on a multi-layered wall is a handy tool for thermal monitoring of the walls of a building with tenants. Estimating unknown parameters in the modeling in order to determine the thermal resistance of the wall. Identification is achieved by solving the corresponding inverse problem formulated in the least-squares sense.

In [13] a study is presented to calculate the U-value in building envelopes starting from IR thermography. The absolute deviation between the notional and the measured U-values for IR thermography is found to be at an acceptable level, being in the range of 10 % – 20 %.

The objective of the study presented by [14] is to calculate the sensible heat flux from the exterior surface of buildings using time sequential thermography, based upon an appropriate simplification of the building model. The authors analyzed the thermograms, dividing them into zones by constructing polygons and according to temperature, shape, material and position.

The authors of [15] wished to define a methodology to determine the level of thermal insulation in old buildings through spot measurements of thermal resistance and planar infrared thermography. Currently, the available approaches to evaluate the U-value in existing buildings are: non-destructive methods using heat flux sensors or infrared thermography or destructive methods.

The authors of [16] presented a method to calculate the U-value with IR. To validate their method, they compared IR results with measurements using a heat flux apparatus to obtain the wall heat fluxes and surface temperatures, and U-values were calculated using Fourier's law, taking into account radiation and convection phenomena.

The proposed method is based on the fact that the temperature distribution field, obtained by the thermography, may be corrected ("calibrated") using the values of temperatures, measured by sensors, placed in several specified points. Thus, a qualitative thermogram is transformed into a numerical array of quantative data on temperature distribution across the outer surface of the building envelope.

Methods

Determining the coefficient of thermotechnical uniformity for a fragment of the building envelope

Stage one is selecting (using thermography) of thermally uniformal sections of the building envelope (the reference areas). Next, via contact method, temperature is measured in the selected points of the internal surface of the uniformal fragments of the building envelope, using temperature sensors.

Thermograms are processed using specialized software provided by the thermovisors manufacturers (for example ThermaCAM, FLIR systems). Using the parameters specified above thermograms is calibrated according to the temperature measured by the sensors in the selected points. In this way we achieve equality of temperatures measured by the sensors and obtained from thermography. Then thermograms are digitized and processed using a software tool created in MATLAB. [17–20].

For each building envelope fragment, three types of elements are selected: surface, linear and point. Surface elements are "smooth" parts of the building envelope fragment, having uniform heat flow density. Linear elements – panel joints, window and door esconsons – elements that have one dimension significantly smaller than the other one and insignificant compared to the examined element of the building envelope. Point elements – metallic panel connections, dowels, pins etc. – are elements, with insignificant dimensions of their projection on the surface of the fragment of the building envelope. The coefficient of thermotechnical uniformity of the building envelope fragment containing linear and point thermal non-uniformities is determined from the equation:

$$r = \frac{1}{1+R_0\cdot\left(\sum\frac{L_j}{A}\cdot\Psi_j+\sum\frac{N_k}{A}\cdot\chi_k\right)}, \quad (1)$$

where R_0,· m^2K/W – conditional thermal resistance of the building envelope fragment;

$\Psi_j = \Delta Q_j/(t_{int}-t_{ext})$ – specific heat loss through the j-th linear thermal non-uniformity, $W/(m\cdot K)$ (linear heat transfer coefficient);

ΔQ_j – additional heat loss through linear thermal non-uniformity, W/K;

t_{int}, t_{ext} – the temperature of the internal and external air respectively, $^{\circ}C$;

L_j/A – ratio of the total length L_j, m of the j-th linear element to the total area of the fragment A,· m^2 ;

χ_k – specific heat loss through the k-th point thermal non-uniformity, W/K (point or volumetric heat transfer coefficient);

$n_k = N_k/A$ – the ratio of average number of point elements N_k to the total area of the fragment A,· m^2.

The first method for assessing the coefficient of thermotechnical uniformity value is based on the average temperature values, obtained by numerical procession of the thermograms:

$$r = \frac{1}{1+\left(\sum\frac{L_j}{A}\cdot b_j^{mean}\cdot\Delta_j+\sum\frac{N_k}{A}\cdot A_k^{mean}\cdot\Delta_k\right)}, \quad (2)$$

where,

$$\Delta_k = \frac{\tau_k^{mean}-\tau_0^{mean}}{\tau_0^{mean}-t_{ext}}, \quad (3)$$

τ_k^{mean} – average temperature of the surface of the building envelope fragment, determined from the thermogram analysis, $^{\circ}C$;

τ_0^{mean} – average temperature of the uniformal part (reference area) of the external surface of the building envelope, $^{\circ}C$;

b_j^{mean} – average width of a linear thermal non-uniformity of the j – kind of the external surface of the building envelope, m;

A_k^{mean} – average area, with a point thermal non-uniformity of the k – kind, m^2.

Vasilyev G.P., Lichman V.A., Yurchenko I.A., Kolesova M.V. Method of evaluation of thermotechnical uniformity coefficient by analyzing thermograms. *Magazine of Civil Engineering*. 2016. No. 6. Pp. 60–67. doi: 10.5862/MCE.66.6

The second method for determining the coefficient of thermotechnical uniformity is based on numerical integration along the contour lines of temperature curves.

The value of $\Psi,\cdot W/(m\cdot K)$ in the equation (1) is determined from the ratio

$$\Psi = \frac{q^L - q_0.d}{(t_{int} - t_{ext})}, \quad (4)$$

where $q^L - q_0.d,\cdot W/m$ – additional heat loss through linear thermal non-uniformity; $q^L = \int_0^d q(x)dx \approx \sum_{i=1}^n q_i \cdot x_i,\cdot \frac{W}{m}$ – numerical integral of heat flow density along the line, having length of d,m, perpendicular to the linear non-uniformity; $q_0,\cdot W/m$ – value of the heat flow density through the uniformal reference area.

Value of specific heat loss through the point non-uniformity $\chi,\cdot W/m$ in the equation (1), may be calculated by integrating the volume along the temperature curve contour, obtained from a thermogram:

$$\chi = \frac{\Delta Q}{\Delta t} = \frac{\pi\cdot\int_0^{qmax} f^2(q)dq}{(t_{int} - t_{ext})} = \frac{\pi\cdot\sum x_i^2 q_i}{(t_{int} - t_{ext})}, \quad (5)$$

where $q_i = \alpha_{ext}(\tau_{ext,i} - t_{ext}),\cdot W/m^2$ – value of the heat flow density through the external surface of the building envelope fragment; $\tau_{ext,i}$ – the temperature in the i-th point of the external surface of the fragment ℃, determined from thermograms as well as by direct measurements in several reference points; $\alpha_{ext},\cdot W/(m^2K)$ – surface coefficient of heat transfer, determined from measurements.

The coefficient of thermotechnical uniformity of the entire building envelope sample is calculated as the weighted average of the fragments:

$$r = \sum A_i r_i / \sum A_i, \quad (6)$$

If beside the temperature sensors a calorimeter for measuring the heat flow is placed in the reference points of the building envelope, it gives an opportunity to determine the surface coefficient of heat transfer of the internal surface allowing determining the value of the thermal resistance of the building envelope fragment.

Results and Discussion.

Let us evaluate the coefficient of thermotechnical uniformity of a panel based on the thermograms shown on Figure 1.

The area of opaque part of the panel equals $A = 5.6\cdot 2.8 - 1.2 = 14.5\cdot m^2$; $b_1^{mean} = 1.1\cdot m$; $L_1 = 5.6\cdot m$; specific geometric parameter is $L_1/A = 0.38\cdot m^{-1}$; average temperatures, obtained from analysis of several dozens of similar areas from different thermograms of the same building: $\tau_1^{mean} = -6.5\cdot$ ℃; $\tau_0^{mean} = -7.2\cdot$ ℃; average external air temperature is $t_{ext} = -7.6\cdot$ ℃. The coefficient of thermotechnical uniformity of the panels of the examined building equals: $r = \frac{1}{1+\left(\frac{5.6}{14.5}\right)\cdot 1.1\cdot\frac{(-6.5+7.2)}{(-7.2+7.6)}} = 0.57$

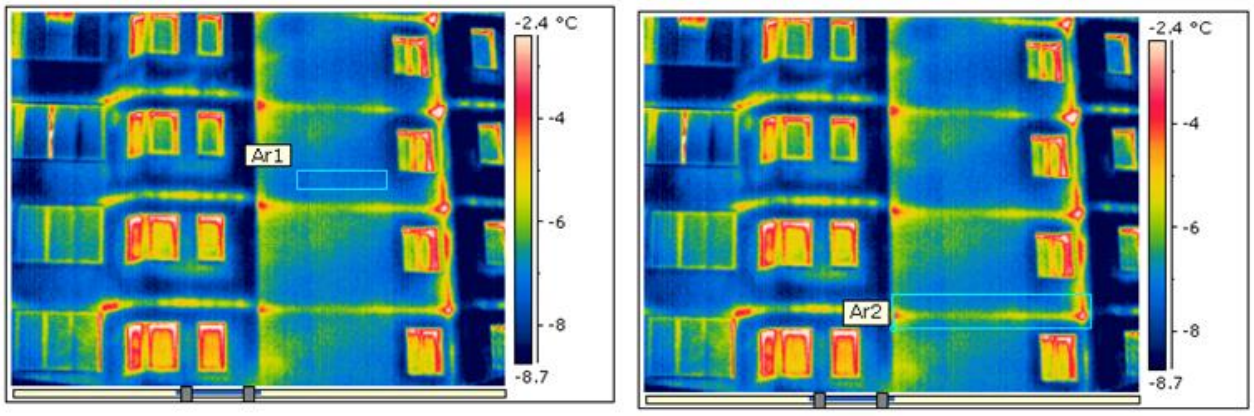

Figure 1. Results of processing data from thermograms of a panel building, obtained under field conditions

Васильев Г.П., Личман В.А., Юрченко И.А., Колесова М.В. Кантаржи И.Г., Железняк М.И. Метод оценки коэффициента теплотехнической однородности из анализа термограмм // Инженерно-строительный журнал. 2016. № 6(66). С. 60–67.

Let us evaluate the coefficient of thermotechnical uniformity of a balcony based on the thermograms shown on Figure 2. Geometrical parameters of the balcony are $A = 3.1 \cdot 2.8 - 2.5 = 6.2 \cdot m^2$; $b_1^{mean} = 0.3 \cdot m$; $L_1 = 3.1 \cdot m$; specific geometrical parameter is $L_1/A = 0{,}50 \cdot m^{-1}$. Average temperatures, obtained from the thermogram analysis for this building are: $\tau_1^{mean} = -6.9 \cdot ℃$; $\tau_0^{mean} = -8.4 \cdot ℃$; average external air temperature is $t_{ext} = -8.8 \cdot ℃$; the coefficient of thermotechnical uniformity equals: $r = \frac{1}{1+\left(\frac{3.1}{6.2}\right)\cdot 0.3 \cdot \frac{(-6.9+8.4)}{(-8.4+8.8)}} = 0.64$

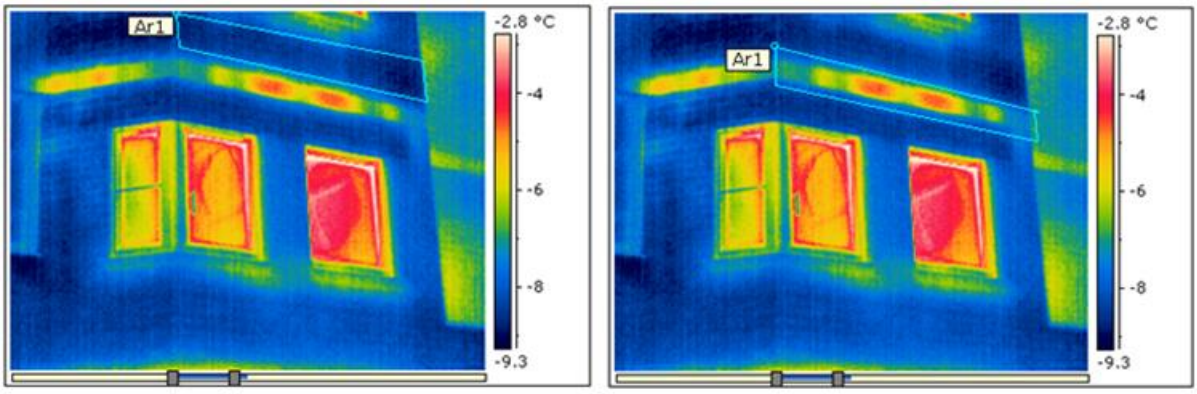

Figure 2. Results of processing data from thermograms of a panel building

Let us evaluate the coefficient of thermotechnical uniformity of the place where the window unit fits the panel (Figure 3). Geometrical parameters are $b_1^{mean} = 0.2 \cdot m$; $L_1 = 4.4 \cdot m$; $A = 3 \cdot 2.5 - 1.2 = 6.3 \cdot m^2$; specific geometrical parameter is $L_1/A = 0.69 \cdot m^{-1}$; average external air temperature is $t_{ext} = -6.4 \cdot ℃$; average temperatures obtained from thermogram analysis are $\tau_1^{mean} = -2.8 \cdot ℃$; $\tau_0^{mean} = -6.0 \cdot ℃$. The coefficient of thermotechnical uniformity equals: $r = \frac{1}{1+\left(\frac{4.4}{6.3}\right)\cdot 0.1 \cdot \frac{(-2.8+6.0)}{(-6.0+6.4)}} = 0.69$

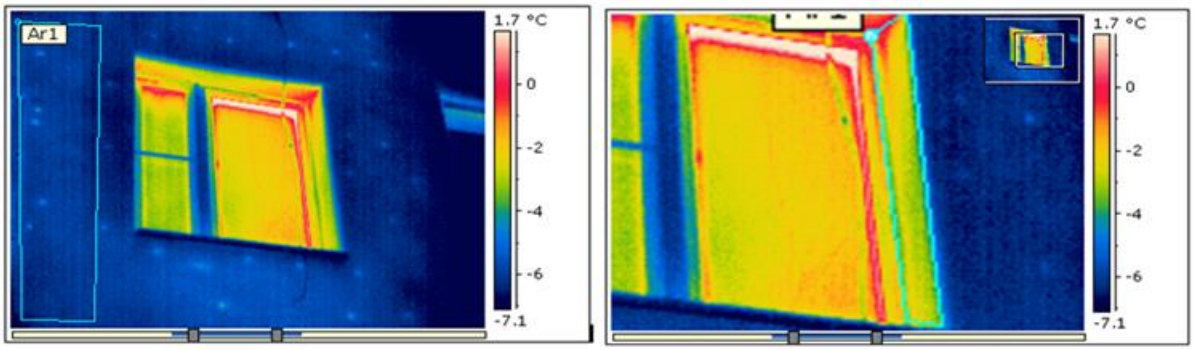

Figure 3. Results of processing data from thermograms of a panel building

Let us evaluate the coefficient of thermotechnical uniformity caused by metallic pins (Figure 4). Average number of pins within $1 \cdot m^2$ is 5; the area of the point thermal non-uniformity is $A_k^{mean} = 7.85 \cdot 10^{-3}$; average external air temperature is $t_{ext} = -9.9 \cdot ℃$; average temperature in the vicinity of a point thermal non-uniformity caused by a metal pin is $\tau_1^{mean} = -7.3 \cdot ℃$; average temperature of the reference area is $\tau_0^{mean} = -9.6 \cdot ℃$. The coefficient of thermotechnical uniformity of a fragment of a building envelope, containing metal pins equals: $r = \frac{1}{1+5 \cdot 7.85 \cdot 10^{-3} \cdot \frac{(-7.3+9.6)}{(-9.6+9.9)}} = 0.76$

Vasilyev G.P., Lichman V.A., Yurchenko I.A., Kolesova M.V. Method of evaluation of thermotechnical uniformity coefficient by analyzing thermograms. *Magazine of Civil Engineering*. 2016. No. 6. Pp. 60–67. doi: 10.5862/MCE.66.6

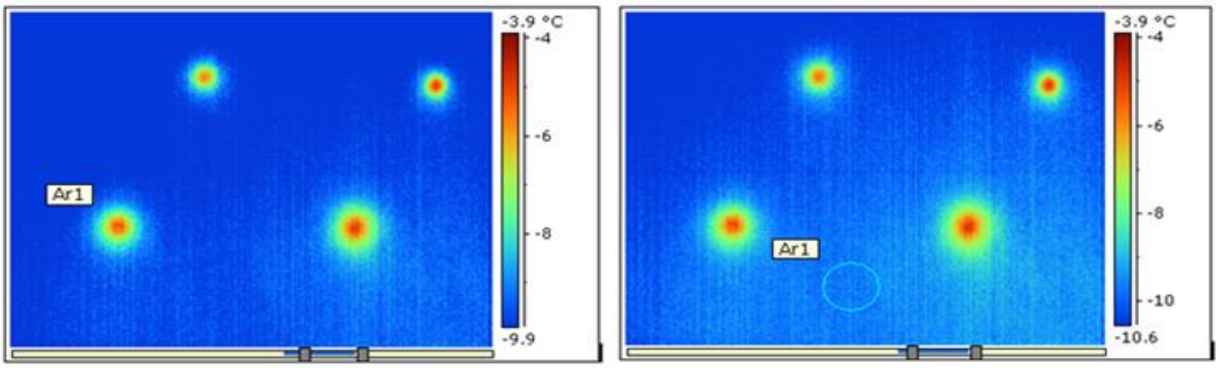

Figure 4. Results of processing data from thermograms of a panel building

Figure 5 contains thermograms showing linear thermal non-uniformity caused by the gaps between mineral wool panels and point thermal non-uniformity, caused by the metal pins. Values the coefficient of thermotechnical uniformity calculated using equations (5), (4) and (1) equal $r = 0.94$ (for gaps between panels) and $r = 0.81$ for metal pins.

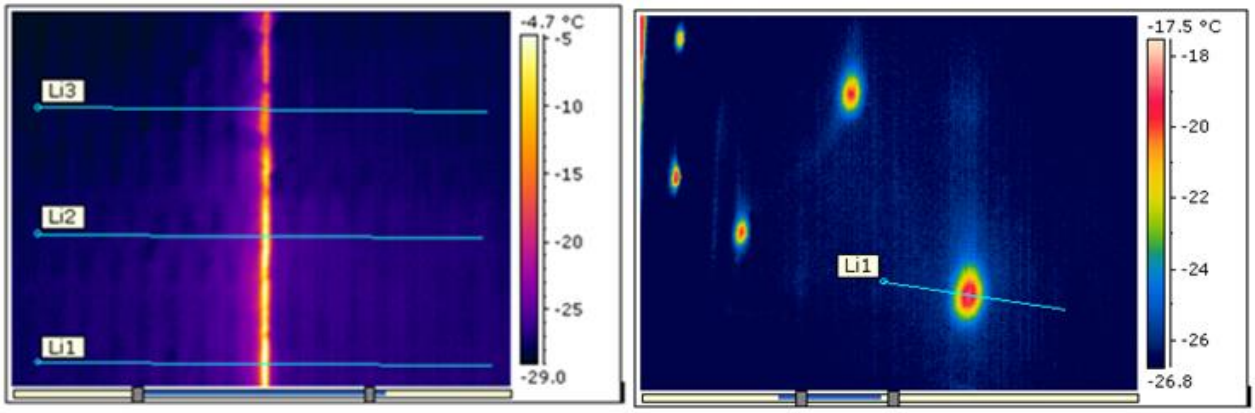

Figure 5. Thermograms, showing linear (left) and point (right) thermal non-uniformities of the external surface of samples tested in a climatic chamber

Conclusion

The proposed method is an efficient way to assess the thermal insulation quality of a tenanted building. It allows to:

- assess the thermotechnical uniformity coefficient of a fragment of building envelope under the field conditions;

- locate under the field conditions flawed elements having thermotechnical uniformity coefficient significantly lower than the average value for similar constructions which in turn provides an opportunity to study the insulation quality of said fragments.

The paper presents analytical equations allowing to evaluate the value of the coefficient of thermotechnical uniformity by analyzing thermograms.

A more detailed analysis of design decisions may be carried out based on this method to further improve them and reduce the impact of heat conductive elements on the overall performance of the fragment.

Several examples of processing thermograms obtained in the field conditions using the abovementioned equations are shown.

The described method of determining the coefficient of thermotechnical uniformity and thermal resistance of building envelope fragments tested in a climatic chamber may be used in addition to methods, described in Russian standards, allowing to reduce the testing time. The method is based on combining measuring of the temperature of the uniform building envelope fragments with analyzing temperature fields obtained by thermography.

Васильев Г.П., Личман В.А., Юрченко И.А., Колесова М.В. Кантаржи И.Г., Железняк М.И. Метод оценки коэффициента теплотехнической однородности из анализа термограмм // Инженерно-строительный журнал. 2016. № 6(66). С. 60–67.

The coefficient of thermotechnical uniformity is determined by dividing the difference between the internal air temperature and mean temperature of a uniform building envelope fragment by the difference between the internal air temperature and mean temperature of a non-uniform building envelope fragment.

If in addition to the temperature the heat flow density is measured in the chosen spots, it is possible to calculate the surface coefficient of heat transfer for the interior surface. This allows evaluating thermal resistance of the fragment, based on the thermogram.

A software piece for data analysis was developed to determine the value the coefficient of thermotechnical uniformity and thermal resistance of a building envelope fragment based on temperature fields, obtained from thermograms.

Acknowledgement

The Research was conducted by JSC "INSOLAR-INVEST" with the financial support of the Ministry of Education and Science of Russia. Unique identifier of the project RFMEFI57614X0034.

References

1. Gorshkov A., Vatin N., Nemova D., Tarasova D. The brickwork joints effect on the thermotechnical uniformity of the exterior walls from gas-concrete blocks. *Applied Mechanics and Materials.* 2015. No. 725–726. Pp. 3–8.
2. Vatin N.I., Gorshkov A.S., Nemova D.V., Staritcyna A.A., Tarasova D.S. The energy-efficient heat insulation thickness for systems of hinged ventilation facades. *Advanced Materials Research.* 2014. No. 941–944. Pp. 905–920.
3. Grinfeldi G.I., Gorshkov A.S., Vatin N.I. Tests results strength and thermophysical properties of aerated concrete block wall samples with the use of polyurethane adhesive. *Advanced Materials Research.* 2014. No. 941–944. Pp. 786–799.
4. Theodosiou T.G., Papadopoulos A.M. The impact of thermal bridges on the energy demand of buildings with double brick wall constructions. *Energy and Buildings.* 2008. No. 40 Pp. 2083–2089.
5. Renon O. Thermal bridge modeling In energy plus. *Building Energy Simulation User News*. 2002. Vol. 23. No. 4.
6. Vatin N., Gorshkov A., Rymkevich P., Nemova D., Tarasova D. Nonstationary thermal conductionthrough the building envelope. *Applied Mechanics and Materials.* 2014. No. 670–671. Pp. 365–369.
7. Vatin N., Gamayunova O. Energy efficiency and energy audit: the experience of the Russian Federation and the republic of Belarus. *Advanced Materials Research*. 2015. Vol. 1065–1069. Pp. 2159–2162.
8. Balaras C. A., Argiriou A. A., Infrared thermography for building diagnostics. *Energy and Buildings.* 2002. Vol. 34. No. 2. Pp. 171–183.
9. Ocaña S.M., Guerrero I.C., Requena I.G. Thermographic survey of two rural buildings in Spain. *Energy and Buildings.* 2004. Vol. 36. Pp. 515–523.
10. Bareira E., de Freitas V.P. Evaluation of building materials using infrared thermography. *Construction and Building Materials.* 2007. Vol. 21. Pp. 218–224.
11. Albatici R., Tonelli A.M. Infrared thermovision technique for the assessment of thermal transmittance value of opaque building elements on site. *Energy and Buildings.* 2010. Vol. 42. Pp. 2177–2183.
12. Monchau J., Ibos L., Feuillet V. Diagnosis of insulated building walls using passive infrared thermography and numerical simulations. *7th European Workshop on Structural Health Monitoring.* Nantes, France, 2014.
13. Datcu S., Ibos L., Candau Y., Matteï S. Contribution to improvement of building wall surface temperature measurements by infrared thermography. *Infrared Physics and Technology.* 2005. Vol. 46. No. 6 Pp. 451–467.
14. Fokaides P., Kalogirou S. Application of infrared thermography for the determination of the overall heat

Литература

1. Gorshkov A., Vatin N., Nemova D., Tarasova D. The brickwork joints effect on the thermotechnical uniformity of the exterior walls from gas-concrete blocks // Applied Mechanics and Materials. 2015. № 725–726. Pp. 3–8.
2. Vatin N.I., Gorshkov A.S., Nemova D.V., Staritcyna A.A., Tarasova D.S. The energy-efficient heat insulation thickness for systems of hinged ventilation facades // Advanced Materials Research. 2014. № 941–944. Pp. 905–920.
3. Grinfeldi G.I., Gorshkov A.S., Vatin N.I. Tests results strength and thermophysical properties of aerated concrete block wall samples with the use of polyurethane adhesive // Advanced Materials Research. 2014. № 941–944. Pp. 786–799.
4. Theodosiou T.G., Papadopoulos A.M. The impact of thermal bridges on the energy demand of buildings with double brick wall constructions // Energy and Buildings. 2008. № 40 Pp. 2083–2089.
5. Renon O. Thermal bridge modeling in energy plus // Building Energy Simulation User News. 2002. Vol. 23. № 4.
6. Vatin N., Gorshkov A., Rymkevich P., Nemova D., Tarasova D. Nonstationary thermal conductionthrough the building envelope // Applied Mechanics and Materials. 2014. № 670–671. Pp. 365–369.
7. Vatin N., Gamayunova O. Energy efficiency and energy audit: the experience of the Russian Federation and the republic of Belarus // Advanced Materials Research. 2015. Vols. 1065–1069. Pp. 2159–2162.
8. Balaras C.A., Argiriou A.A. Infrared thermography for building diagnostics // Energy and Buildings. 2002. Vol. 34. № 2. Pp. 171–183.
9. Ocaña S.M., Guerrero I.C., Requena I.G. Thermographic survey of two rural buildings in Spain // Energy and Buildings. 2004. Vol. 36. Pp. 515–523.
10. Bareira E., de Freitas V.P. Evaluation of building materials using infrared thermography // Construction and Building Materials. 2007. Vol. 21. Pp. 218–224.
11. Albatici R., Tonelli A.M. Infrared thermovision technique for the assessment of thermal transmittance value of opaque building elements on site // Energy and Buildings. 2010. Vol. 42. Pp. 2177–2183.
12. Monchau J., Ibos L., Feuillet V. Diagnosis of insulated building walls using passive infrared thermography and numerical simulations // 7th European Workshop on Structural Health Monitoring. Nantes, France, 2014.
13. Datcu S., Ibos L., Candau Y., Matteï S. Contribution to improvement of building wall surface temperature measurements by infrared thermography // Infrared Physics and Technology. 2005. Vol. 46. № 6. Pp. 451–467.
14. Fokaides P., Kalogirou S. Application of infrared

Vasilyev G.P., Lichman V.A., Yurchenko I.A., Kolesova M.V. Method of evaluation of thermotechnical uniformity coefficient by analyzing thermograms. *Magazine of Civil Engineering*. 2016. No. 6. Pp. 60–67. doi: 10.5862/MCE.66.6

transfer coefficient (U-Value) in building envelopes. *Appl. Energy*. 2011. Vol. 88. Pp. 4358–4365.
15. Dall'O', Sarto L., Galante A., Pasetti G, Comparison between predicted and actual energy performance for winter heating in high-performance residential buildings in the Lombardy region (Italy). *Energy Building.* 2012. Vol. 47. Pp. 247–253.
16. Simões I., Simões N., Tadeu A. Laboratory assessment of thermal transmittance of homogeneous building elements using infrared thermography. [Electronic resourse]. System requirements: AdobeAcrobatReader. URL: http://dx.doi.org/10.21611/qirt.2014.081 (date of application: 03.10.2016).
17. Vasilyev G.P., Lichman V.A., Peskov N.V., Brodach M.M., Tabunshchikov Y.A., Kolesova M.V. Simulation of heat and moisture transfer in a multiplex structure. *Energy & Buildings*. 2015. Vol. 86. Pp. 803–807.
18. Vasilyev G.P., Leskov V.A., Gornov V.F., Kolesova M.V., Lichman V.A. Study of heat engineering homogeneity fragments of enclosing structures in the climatic chamber. *MATEC Web of Conferences.* 2016. Vol. 40. No. of publication 05003
19. Vasilyev G.P., Gornov V.F., Lichman V.A., Yurchenko I.A., A Method of assessing energy consumption of buildings during commissioning. *ARPN Journal of Engineering and Applied Sciences.* 2015. Vol. 10. No. 15. Pp. 6509–6512.
20. Vasilyev G.P., Leskov V.A., Gornov V.F., Lichman V.A, Kolesova M.V., Dmitriev A.N. Definition of the heat resistance of three-layer ferroconcrete panel. *MATEC Web of Conferences.* 2016. No. 40. No. of publication 05004

thermography for the determination of the overall heat transfer coefficient (U-Value) in building envelopes // Appl. Energy. 2011. Vol. 88. Pp. 4358–4365.
15. Dall'O', Sarto L., Galante A., Pasetti G. Comparison between predicted and actual energy performance for winter heating in high-performance residential buildings in the Lombardy region (Italy) // Energy Building. 2012. Vol. 47. Pp. 247–253.
16. Simões I., Simões N., Tadeu A. Laboratory assessment of thermal transmittance of homogeneous building elements using infrared thermography [Электронный ресурс]. Систем.требования: AdobeAcrobatReader. URL: http://dx.doi.org/10.21611/qirt.2014.081 (дата обращения: 03.10.2016).
17. Vasilyev G.P., Lichman V.A., Peskov N.V., Brodach M.M., Tabunshchikov Y.A., Kolesova M.V. Simulation of heat and moisture transfer in a multiplex structure // Energy & Buildings. 2015. Vol. 86. Pp. 803–807.
18. Vasilyev G.P., Leskov V.A., Gornov V.F., Kolesova M.V., Lichman V.A. Study of heat engineering homogeneity fragments of enclosing structures in the climatic chamber // MATEC Web of Conferences. 2016. Vol. 40. № публикации 05003
19. Vasilyev G.P., Gornov V.F., Lichman V.A., Yurchenko I.A., A Method of assessing energy consumption of buildings during commissioning // ARPN Journal of Engineering and Applied Sciences. 2015. Vol. 10. № 15. Pp. 6509–6512.
20. Vasilyev G.P., Leskov V.A., Gornov V.F., Lichman V.A, Kolesova M.V., Dmitriev A.N. Definition of the heat resistance of three-layer ferroconcrete panel // MATEC Web of Conferences. 2016. № 40. № публикации 05004

Gregory Vasilyev,
+74991440667; gpvassiliev@mail.ru

Vladimir Lichman,
+74991440667; valitsch@mail.ru

Igor Yurchenko,
+74991440667; iyurchenko@insolar.ru

Marina Kolesova,
+74991440667; eco-insolar@mail.ru

Григорий Петрович Васильев,
+74991440667; эл. почта: gpvassiliev@mail.ru

Владимир Александрович Личман,
+74991440667; эл. почта: valitsch@mail.ru

Игорь Андреевич Юрченко,
+74991440667; эл. почта:
iyurchenko@insolar.ru

Марина Владимировна Колесова,
+74991440667; эл. почта: eco-insolar@mail.ru

© Vasilyev G.P., Lichman V.A., Yurchenko I.A., Kolesova M.V., 2016

Васильев Г.П., Личман В.А., Юрченко И.А., Колесова М.В. Кантаржи И.Г., Железняк М.И. Метод оценки коэффициента теплотехнической однородности из анализа термограмм // Инженерно-строительный журнал. 2016. № 6(66). С. 60–67.

Требования к материалам, представляемым к публикации

Материалы принимаются только через систему электронной редакции журналов СПбГПУ. Авторам необходимо зарегистрироваться в системе (http://journals.spbstu.ru/) и подать статью через нее, предварительно ознакомившись с нижеприведенными требованиями и условиями опубликования. Публикация в журнале бесплатна для авторов.

Этические нормы и авторские права

Подавая статью в журнал, автор соглашается на условия лицензионного договора, в частности, на то, что все статьи без исключения публикуются в открытом доступе на сайте журнала и в Научной электронной библиотеке России. Также автор подтверждает, что статья является оригинальной, ранее не опубликованной, содержит только проверенные и точные данные; любые данные, полученные не автором, имеют соответствующие ссылки на источник.

Тематика и язык статей

В «Инженерно-строительном журнале» публикуются оригинальные, ранее не опубликованные статьи, содержащие полученные авторами новые научные результаты, по тематике «Строительство». Принимаются статьи только на английском языке. Метаданные (аннотация, ключевые слова, список литературы) подаются на двух языках.

№	Дата выхода	Срок подачи материалов
1(69)	17.02.2017	30.12.2016
2(70)	31.03.2017	20.02.2017
3(71)	12.05.2017	03.04.2017
4(72)	23.06.2017	10.05.2017

Структура и содержание статей

Структура статьи должна соответствовать стандарту IMRAD (Introduction, Methods, Results, and Discussion). Введение должно включать обзор литературы по теме, дискуссия (и/или заключение – Conclusions) – нумерованные выводы.

Технические требования к статьям

Статьи подаются в формате docx (MS Word 2007–2013). Файл статьи, подаваемый через электронную редакцию, должен содержать только сам текст, без названия, списка литературы, фамилий и данных авторов. Все эти поля заполняются отдельно при подаче через электронную редакцию.

Рекомендуемый объем статей: от 15000 до 30000 знаков с пробелами. Таблицы выполняются средствами Word (не рисунками) и располагаются внутри текста статьи. Иллюстрации должны быть дополнительно представлены в отдельных графических файлах (один рисунок – один файл). Допустимые форматы: JPEG, TIFF, BMP. В текстовый файл иллюстрации также должны быть включены. Все обозначения на рисунках должны быть на латинице.

Список литературы на русском языке должен быть оформлен в соответствии с ГОСТ 7.0.5-2008. Цитируемая литература приводится общим списком в конце статьи в порядке упоминания. Порядковый номер в тексте заключается в квадратные скобки. Текст статьи должен содержать ссылки на все источники из списка литературы. Также к статье прилагается список литературы на латинице, оформленный в соответствии с инструкцией по транслитерации списка литературы, размещенной на сайте издания.

Аннотация к статье

В журнал подается расширенная аннотация на двух языках: русском и английском. Аннотация должна повторять структуру статьи: описание объекта исследования, методы исследования, основные научные результаты . Аннотация должна содержать от 100 до 250 слов.

Подробные требования к статьям см. на сайте журнала:
http://www.engstroy.spbstu.ru/autors.html

Федеральное государственное автономное образовательное учреждение высшего образования
Санкт-Петербургский политехнический университет Петра Великого

ПОЛИТЕХ
Санкт-Петербургский политехнический университет Петра Великого

Инженерно-строительный институт
Центр дополнительных профессиональных программ

195251, г. Санкт-Петербург, Политехническая ул., 29,
тел/факс: 552-94-60, www.stroikursi.spbstu.ru,
stroikursi@mail.ru

Приглашает специалистов проектных и строительных организаций,
не имеющих базового профильного высшего образования
на курсы профессиональной переподготовки (от 500 часов)
по направлению «Строительство» по программам:

П-01 «Промышленное и гражданское строительство»

Программа включает учебные разделы:

- ***Основы строительного дела***
- ***Инженерное оборудование зданий и сооружений***
- ***Технология и контроль качества строительства***
- ***Основы проектирования зданий и сооружений***
- ***Автоматизация проектных работ с использованием AutoCAD***
- ***Автоматизация сметного дела в строительстве***
- ***Управление строительной организацией***
- ***Управление инвестиционно-строительными проектами. Выполнение функций технического заказчика***

П-02 «Экономика и управление в строительстве»

Программа включает учебные разделы:

- ***Основы строительного дела***
- ***Инженерное оборудование зданий и сооружений***
- ***Технология и контроль качества строительства***
- ***Управление инвестиционно-строительными проектами. Выполнение функций технического заказчика и генерального подрядчика***
- ***Управление строительной организацией***
- ***Экономика и ценообразование в строительстве***
- ***Управление строительной организацией***
- ***Организация, управление и планирование в строительстве***
- ***Автоматизация сметного дела в строительстве***

П-03 «Инженерные системы зданий и сооружений»

Программа включает учебные разделы:

- ***Основы механики жидкости и газа***
- ***Инженерное оборудование зданий и сооружений***
- ***Проектирование, монтаж и эксплуатация систем вентиляции и кондиционирования***
- ***Проектирование, монтаж и эксплуатация систем отопления и теплоснабжения***
- ***Проектирование, монтаж и эксплуатация систем водоснабжения и водоотведения***
- ***Автоматизация проектных работ с использованием AutoCAD***
- ***Электроснабжение и электрооборудование объектов***

П-04 «Проектирование и конструирование зданий и сооружений»

Программа включает учебные разделы:

- ***Основы сопротивления материалов и механики стержневых систем***
- ***Проектирование и расчет оснований и фундаментов зданий и сооружений***
- ***Проектирование и расчет железобетонных конструкций***
- ***Проектирование и расчет металлических конструкций***
- ***Проектирование зданий и сооружений с использованием AutoCAD***
- ***Расчет строительных конструкций с использованием SCAD Office***

П-05 «Контроль качества строительства»

Программа включает учебные разделы:

- ***Основы строительного дела***
- ***Инженерное оборудование зданий и сооружений***
- ***Технология и контроль качества строительства***
- ***Проектирование и расчет железобетонных конструкций***
- ***Проектирование и расчет металлических конструкций***
- ***Обследование строительных конструкций зданий и сооружений***
- ***Выполнение функций технического заказчика и генерального подрядчика***

По окончании курса слушателю выдается диплом о профессиональной переподготовке установленного образца, дающий право на ведение профессиональной деятельности